BERICHTE
aus dem Fachbereich Geowissenschaften
der Universität Bremen

No. 200

Al-Rousan, S.

OCEAN AND CLIMATE HISTORY RECORDED IN STABLE ISOTOPES OF CORALS AND FORAMINIFERS FROM THE NORTHERN GULF OF AQABA

Berichte, Fachbereich Geowissenschaften, Universität Bremen, No. 200,
116 pages, Bremen 2002

ISSN 0931-0800

The "Berichte aus dem Fachbereich Geowissenschaften" are produced at irregular intervals by the Department of Geosciences, Bremen University.

They serve for the publication of experimental works, Ph.D.-theses and scientific contributions made by members of the department.

Reports can be ordered from:

Gisela Boelen

Sonderforschungsbereich 261

Universität Bremen

Postfach 330 440

D 28334 BREMEN

Phone: (49) 421 218-4124

Fax: (49) 421 218-3116

e-mail: boelen@uni-bremen.de

Citation:

Al-Rousan, S.

Ocean and climate history recorded in stable isotopes of corals and foraminifers from the northern Gulf of Aqaba.

Berichte, Fachbereich Geowissenschaften, Universität Bremen, No. 200, 116 pages, Bremen, 2002.

ISSN 0931-0800

BERICHTE
aus dem Fachbereich Geowissenschaften
der Universität Bremen

No. 200

Al-Rousan, S.

OCEAN AND CLIMATE HISTORY RECORDED IN STABLE ISOTOPES OF CORALS AND FORAMINIFERS FROM THE NORTHERN GULF OF AQABA

Berichte, Fachbereich Geowissenschaften, Universität Bremen, No. 200,
116 pages, Bremen 2002

ISSN 0931-0800

OCEAN AND CLIMATE HISTORY RECORDED IN STABLE ISOTOPES OF CORALS AND FORAMINIFERS FROM THE NORTHEN GULF OF AQABA

Dissertation

Zur Erlangung des Grades
Doktor der Naturwissenschaften
(Dr. rer. nat.)

am
Fachbereich Geowissenschaften (FB5)
der Universität Bremen

vorgelegt von

Saber Al-Rousan

Bremen, 2002

Tag des Kolloquiums:

25. Juni 2002

Gutachter:

Professor Dr. Gerold Wefer

Professor Dr. Rüdiger Henrich

Prüfer:

Prof. Dr. Venugopalan Ittekkot

Dr. Jürgen Pätzold

Abstract

Long, high-resolution paleoclimatic records are required to extend the short climatic instrumental data in order to understand the global climate system and its variations. In tropical and sub-tropical regions, stable isotope records derived from massive corals can provide such information both for the last several centuries (from living corals) and for well-dated windows of the more distant past (from well-preserved fossil corals). The data obtained from coral proxy are in some cases equivalent in quality and resolution to those derived from instrumental data. However, it is subjected to some limitations that may affect the reliability of the proxy particularly on the sub-annual time scale. In this thesis we investegated some of these limitations from *Porites* corals from the northern Gulf of Aqaba in order to improve the accuracy of records obtained from this proxy.

Stable oxygen isotope composition were analysed in the skeletons of two coral colonies (*Porites* cf. *lutea and Porites* cf. *nodifera*) from the northern Gulf of Aqaba. The records were used to evaluate the effect of some biological factors such as extension rate, density, calcification rate and species differences that may affect the environmental signals obtained from this proxy. Results demonstrate that a large majority of the seasonal variations in coral oxygen isotope from the area can be explained by seawater temperature variations, and only a small fraction can be attributed to $\delta^{18}O$ variations of surface water. However, it seems to be that the interannual salinity variations are responsible for decreasing the correlation between coral $\delta^{18}O$ and seawater temperature at the annual time scale. Coral $\delta^{18}O$ was also found to be growth dependent, the relation between the two variables can be explained by a simple exponential model, in which the inverse function extends over extension rates 1-5 mm/yr. For more rapidly growing corals and portions of coral colonies, the relation is constant and the extension rate did not appear to have any significant effect on coral $\delta^{18}O$. Furthermore, the offset in $\delta^{18}O$ profiles cannot be always explained as a function of extension and/or calcification rate and may result from coral species differences.

High-resolution coral $\delta^{18}O$ records (weekly/biweekly) from the northern Gulf of Aqaba were also calibrated against high-resolution *in situ* monitoring of seawater temperature, salinity and isotopic composition over 14 month period from different water depths. The records were obtained to assess the ability of *Porites* corals to accurately record environmental variations, and to constrain the environmental sources of isotopic variations. Results show that high-resolution coral $\delta^{18}O$ records from all depths were able to capture fine details of the weekly

temperature records and resolved more that 95% of the weekly temperature variations. However, attenuation and amplification of the corals seasonal amplitudes were recorded in deep slow growing corals due to changes or interruption in coral growth rates on the annual time scales. The study shows also no evidence for smoothing and distortion of the environmental signals obtained from corals due to calcification throughout the thickness of the tissue layer as suggested by earlier studies. The emperical relation between coral $\delta^{18}O$ and seawater temperature and $\delta^{18}O$ composition based on corals from different depths from this study and the relation between coral $\delta^{18}O$ and extension rate as well as that between seawater salinity and $\delta^{18}O$ achieved from both studies can be applied to evaluate and correct past and future coral $\delta^{18}O$ chronologies obtained from modern and fossil corals from the region.

The stable carbon isotope ($\delta^{13}C$) records of the planktonic foraminifera *Globigerinoides sacculifer* and *Globigerinoides ruber* from the northern Gulf of Aqaba have been used to trace modern climate variability influenced by human activities. The study was conducted on three multicorers extends almost 1000 years B.P. with high temporal resolution up to 10 years. The records documents changes in the seawater dissolve inorganic carbon variability, indicated by a gradual decrease of the $\delta^{13}C_{DIC}$ of approximately 0.63‰ in the last 200 years as a result of increasing input of the ^{13}C depleted CO_2 into the atmosphere. Whereas values older than 1750 did not show such trend back to 1000 A.D. Furthermore, variations in carbon isotope of the organic matter ($\delta^{13}C_{org}$) show a trend toward lighter values closely follow those of the foraminifera and support the interpretation. The variations in CO_2 concentration calculated from $\delta^{13}C_{org}$ values, representing the pre-industrial and industrial conditions in the Gulf of Aqaba are estimated to be from 287 to 363 ppm. These values are within the range estimated for CO_2 concentrations from ice cores during the last two centuries. Moreover, a comparison of the carbon isotope measurements of the northern Gulf of Aqaba seawater obtained in 1999 with measurements recorded in 1979 shows a decrease of $\delta^{13}C_{DIC}$ values of about 0.44‰ during the last 20 years with annual decrease of about 0.021‰. The results from this study reveal that $\delta^{13}C$ of planktonic foraminifers combined with organic matter $\delta^{13}C$ from marine sediments allow good indicators to reconstruct past changes in atmospheric CO_2 concentrations from the northern Gulf of Aqaba.

Acknowledgments

I would like to express my deep gratitude for my advisor Prof. Dr. Gerold Wefer for giving me the opportunity to carry out this PhD work and for his continuous support throughout my study. Special thanks are also due to Prof. Dr. Rüdiger Henrich for being a referee to this thesis.

I am grateful to my co-advisor Dr. Jürgen Pätzold for his encouragements, sincere criticism advice, critical reading and fruitful discussions, without his support this work would not have been possible. I wish to thank also my second co-advisor Dr. Salim Al-Moughrabi for his support, comments and dive during the collection of samples.

I thank the staff of the Marine Science Station in Aqaba for their general help and support. Special thanks are due to the diving staff Ahmed Al-Qatawneh, Omar Al-Momany, Tariq Al-Salamn, Abdullah Al-Momany and Yousef Ahmed for helping in coral and water samples collection. I wish also to thank Khaled Al-Trabeen, Ali Hammad, and Khaled Al-Sokhny for their assistant in the field and lab work during sample collection.

I would like to thank my PhD colleagues Mohammed Rasheed, Fuad Al-Horani, Riyad Manasreh, Blel Azouzi, and Mohammed Salem for their support, encouragement and friendship that helped me to complete this thesis.

Many thanks are due to Dr. Thomas Felis, Dr. Henning Kuhnert for the comfortable atmosphere in our lab, and for their constructive comments, stimulating discussions and ideas, which greatly improve the thesis. Thanks also due to Dr.Yaser Moustfa who was my office mate for one year for his support and general help during my first time in Germany. Dr. Helge Arz is deeply thanked for his valuable comments and assistance in sediment sampling work. Marine Geology group deserve a great acknowledge for the friendly atmosphere which accounted for a productive working climate. I wish to thank Dr. Monika Segl and her team for performing the stable isotope analyses; many thanks are also due to Hella Buschhoff and Ursula Röhl for their great assistance during my laboratory work.

Last, but certainly not least, I owe special thanks to my beloved parents, brothers and sister for their help, patience and moral support during my education way and my stay in Germany.

This research is part of the Red Sea Program (RSP II) on marine sciences funded by the German Federal Ministry for Education, Science, Research and Technology (BMBF). The thesis is partly supported by a grant from the University of Bremen.

Table of contents
Abstract
Acknowledgments

1. General introduction

1.1. Sources of paleoclimatic information

To understand recent and future climatic changes, whether as a consequence of human activities or of natural variability, it is necessary to document how climates have varied in the past, i.e., the space-and time-scales of natural climate variability. Some measure of this natural variability were deduced from instrumental observations, which are poor before the age of satellite remote sensing, and are restricted to the last 150 year.

Long high-quality records are needed to extend the instrumental records and therefore, to provide more complete picture of natural climate changes over decades, multidecads or even centuries time scales, and to understand how human activities may already have altered the climate locally, regionally and perhaps globally.

Reliable global records of high-resolution paleoclimatic data have been obtained from natural archives or proxies which are climate-dependent, and which incorporate into their structure a measure of this dependency (Bradley, 1999). For example, short-term climatic changes have been investigated from various isotopic and other chemical compounds present in ice cores (e.g., Friedli et al., 1986; Francey et al., 1999), tree rings (e.g., Cook, 1995; Feng, 1999), varved sediments (e.g., von Rad et al., 1999; Hughen et al., 1996), pollen series (e.g., Shulmeister and Lees, 1995) and other investigations have provided an excellent record to study the continental climate variability over the recent centuries.

Records from long-lived corals have showed the presence of decadal patterns of ENSO-like variability from the tropical Pacific that is unrecognisable from existing instrumental data (e.g., Carriquiry et al., 1994; 1998; Wellington and Dunbar, 1995). Similarly, long term variations in the stable carbon isotopic composition of the seawater dissolved inorganic carbon ($\delta^{13}C_{DIC}$) due to human activity have been detected from shallow dwelling corals and sponges (e.g., Nozaki et al., 1978; Druffel and Benavides, 1986; Böhm et al., 1996).

As paleoclimate reconstructions from these proxies offer the only source of information on long-term climatic variability, calibrations of these proxy records are needed for all further studies. Calibration involves using modern climatic records and proxy materials to understand how, and to what extent proxy materials are climate-dependent.

1.2. Corals as environmental proxies

Massive hermatypic coral skeletons have been proven to provide high quality recorders of climatic and environmental changes from tropical and subtropical oceans on a seasonal to century time-scales (e.g., Pätzold, 1984; 1986; McConnaughey, 1989; Aharon, 1991; Dunbar et al., 1994; Crowley et al., 1997; Kuhnert et al., 2000; Felis et al., 2000), which are in some cases equivalent in quality and resolution to those derived from instrumental data.

The term "coral" is generally applied to members of the order Scleractinia, which have hard calcareous skeletons (Veron, 1993). The aragonitic coral skeleton is covered by thin living tissue layer formed by the polyps, which lives symbiotically with unicellular algae (zooxanthellae). These are known as the hermatypic corals and belong to the subgroup reef builders. The basic unit of the skeleton is considered to be the sclerodermite, a group of fiber, which fan out from a point called the center of calcification. Sclerodermites often grow vertically to produce atrabecula in which the fibers radiate outward and upward from a central axis (Barnes and Lough, 1989).

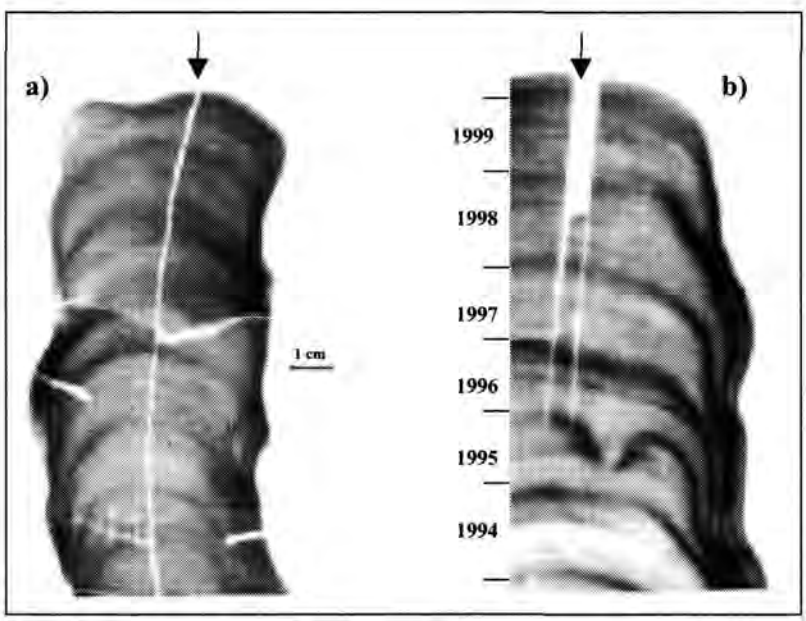

Figure 1.1. X-radiograph positive prints of *Porites* coral slabs (Aq19) with age interpretation. The skeletal density banding pattern of alternating high and low density sub-bands can be clearly seen. The isotopic sampling profiles obtained using the drilling procedure (a) and grinding procedure (b) are indicated by the arrows.

Most of the reef corals live at depths less than 20 m and grow continuously at rates of 6-20 mm/year, with most species producing annual density bands (much like tree rings) that provide time markers for the development of long chronologies (Knutson et al., 1972; Scoffin et al., 1989). The bands are of annual periodicity and composed of alternating high density (HD) and low density (LD) sub-bands (Figure 1.1). During growth, corals incorporate trace

elements and stable isotopes from the surrounding seawater, which can be used for paleoenvironmental studies.

High-resolution trace elements and stable isotopes coral records were used to study some climatic events like El Niño (Cole and Fairbanks, 1990; Cole et al., 1993; Shen et al., 1992; Felis et al., 2000), and to reconstruct climatic and environmental parameters such as sea surface temperatures, salinities, rainfall, nutrient and river inputs (e.g. Swart, 1983; Isdale, 1984; Shen et al., 1987; McConnaughey, 1989; Lea et al., 1989; Cole and Fairbanks, 1990). Also it has been used to study some environmental changes caused by human activities, such as industrial and sewage pollutions (Schneider and Smith, 1982; Dodge et al., 1984; Shen et al., 1987; Shen and Boyle, 1988), nuclear testing (Knuston et al., 1972) and anthropogenic CO_2 increase (Nozaki et al., 1978; Aharon, 1991). Thus, coral records can be used to assess long-term climate trends as well as the range of natural variability in the tropical-subtropical environment.

1.2.1. Stable oxygen isotopes in corals

Oxygen isotopic composition of the aragonite skeletons has been considered to be the most commonly used parameter in coral paleoceanographic studies, because these measurements are readily developed in quantity and are relatively straightforward to interpret (NOAA 1993). Coral stable oxygen isotopes ($\delta^{18}O$) reflect a combination of local sea surface temperatures and oxygen isotope composition of the ambient seawaters in which they grew (Epstein et al., 1953; Fairbanks and Dodge, 1979; Swart et al., 1983; Aharon, 1991; Wefer and Berger, 1991).

Coral $\delta^{18}O$ as a function of temperature has been derived from the widely famous paleotemperature equation by Epstein et al. (1953). The equation describes the relation between seawater temperature, $\delta^{18}O$ of biogenic carbonate and seawater $\delta^{18}O$ as follows:

$$T = 16.5 - 4.3\,(\delta^{18}O_C - \delta^{18}O_W) + 0.14\,(\delta^{18}O_C - \delta^{18}O_W)^2$$

where T is temperature in °C, $\delta^{18}O_C$ is the carbonate stable oxygen composition and $\delta^{18}O_W$ is that of seawater. Based on this equation, the $\delta^{18}O$ of biogenic carbonate decreases by ~ 0.22‰ for each 1°C increase in seawater temperature. However Grossman and Ku (1986) found this gradient to be about 0.23‰/1°C for aragonite. Recently, Gagan et al. (1994) suggested a temperature dependence of 0.18‰/1°C for *Porites* corals at a weekly resolution

from Great Barier Reef, where as Quinn et al. (1998) suggested 0.172‰/1°C for a New Calidonia *Porites* coral on a monthly scale.

Coral $\delta^{18}O$ has been also used to reconstruct variations in $\delta^{18}O$ of seawater (e.g., Dunbar and Wellington, 1981; Cole and Fairbanks, 1990), which often related to water salinities and varies as a function of precipitation, evaporation and runoff (hydrological balance). Offset below values predicted from equilibrium precipitation may be caused by vital effect, that appears to be constant within a given coral genus (Weber and Woodhead, 1972) and along rapidly growing portions (Pätzold, 1984; McConnaughey, 1989). Changes in growth rate were also found to have an impact on the fractionation of stable isotopes, and may change the absolute isotopic value (e.g., Land et al., 1975; Weil et al., 1981; Pätzold, 1986; McConnaughey, 1989; Leder et al., 1996; Allison et al., 1996).

1.2.2. Stable carbon isotopes in corals

Contrary to $\delta^{18}O$, the $\delta^{13}C$ signals in coral skeletons is often difficult to interpret, because of the complicated interactions of environmental influences with physiological processes that involves strong isotopic fractionation (Weber and Woodhead, 1970; Goreau, 1977; Swart, 1983).

Variations of coral $\delta^{13}C$ on the annual time scale is mainly controlled by the photosynthetic activity of the coral endosymbiotic algae, which preferentially take up ^{12}C from dissolved inorganic carbon (DIC) in seawater, so lighter rates of photosynthesis lead to DIC becoming enriched in ^{13}C, which in turn affects the $\delta^{13}C$ of skeleton carbonate (Goreau, 1977; Erez, 1978; Swart, 1983; McConnaughey, 1989).

However, in certain environments, coral $\delta^{13}C$ were used to derive some climatic information, because it shows strong correlations to specific environmental variables. The correlation between $\delta^{13}C$ and light intensity was interpreted as a result of insolation (cloudiness) variability (e.g., Weil et al., 1981; Pätzold, 1984; McConnaughey, 1989; Winter et al., 1991), or water column transparency (e.g., Wellington and Dunbar, 1995). Furthermore, carbon stable isotope from coral skeleton was linked to nutrient or food availability in some environments (Felis et al., 1998; Grottoli-Everett and Wellington, 1999), and to seawater dissolved inorganic carbon (DIC) variability in others (Nozaki et al., 1978).

1.3. Planktonic foraminifera as environmental proxies

Planktonic foraminifera are small unicellular animals (Protozoa) that inhabit all oceans from the tropic to the polar seas. They live in the upper parts of the world oceans, and build a calcite shell that consists of small chambers, which serve as their skeleton (Figure 1.2). Their distribution and abundance is influenced by biotic parameters such as temperature, salinity, light, oxygen and nutrient concentrations (Hemleben et al., 1989).

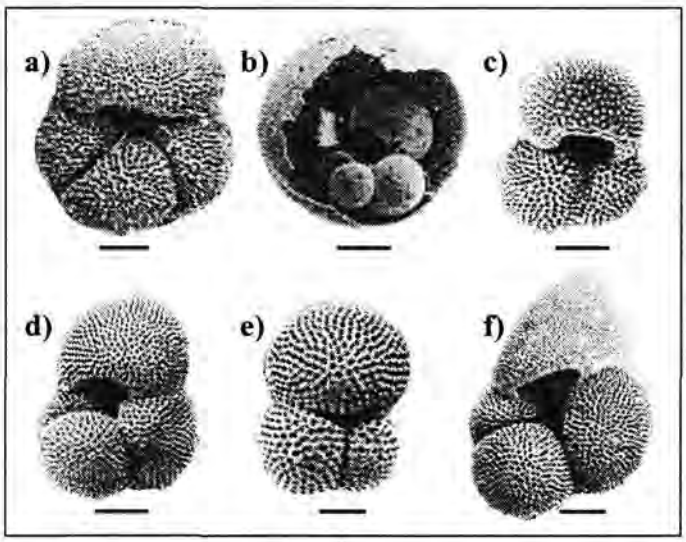

Figure 1.2. Examples of some planktonic foraminifera species (Hemleben et al., 1989). a) *Globigerinoides conglobatus*. Scale = 200μm, b) *Orbulina universa*. Scale = 200μm, c) *Globigerinoides ruber*. Scale = 100μm, d-f) *Globigerinoides sacculifer* with different growth types. Scale = 200μm.

The shells of the planktonic foraminifera are major components in the pelagic sediments. Their stable isotope and trace element chronologies as well as their faunal assemblages composition are considered as a primary tool for paleoceanographic and paleoclimatic reconstructions (Vincent and Berger, 1981; Hemleben et al., 1989; Wefer et al., 1999), due to their high relative abundance and good preservation potential (Seibold and Berger, 1993).

1.3.1. Stable oxygen isotopes

Stable oxygen isotopic composition of foraminifera shells is considered as the most widely applied method used in oceanography. It depends on the fact that carbonate precipitates from the same aqueous solution should have different ratios of ^{18}O to ^{16}O, depending on the temperature at which the precipitation occur (Urey, 1947; Emiliani, 1954). For that, several empirical studies have employed this fact to estimate past sea surface water temperatures from calcareous marine organisms (e.g., Epstein, 1953; Shackleton, 1974).

Epstein et al. (1953) have derived an empirical relationship to estimate paleotemperatures from calcareous mollusks. This was applied to planktonic foraminifera in deep-sea sediments by Emiliani (1954, 1955, 1966). The major assumption of this method that foraminifera skeletons are deposited in isotopic equilibrium and the fractionation is mainly controlled by temperature at the time of deposition. However, it was found that foraminifera display disequilibrium precipitation or vital effect, due to incorporation of metabolic CO_2 (e.g., Erez, 1978; Spero et al., 1991), which is different from one species to another (Grossman, 1987).

Furthermore, other factors may complicate this simple interpretation such as ice volume effect (Craig, 1965; Shackleton, 1967), variation of depth habitat of foraminifera (Emiliani, 1971) and dissolution of ocean basin carbonate (Berger, 1975; Duplessy et al., 1981).

The isotopic oxygen compositions in planktonic foraminifera has been also used to estimate paleosalinity changes (Duplessy et al., 1991; Rostek et al., 1993; Wolff et al., 1999) which varies as a respond to large scale dilution effect or local changes in precipitation/evaporation relationship.

1.3.2. Stable carbon isotope

Carbon isotope composition of planktonic foraminifera ($\delta^{13}C$) has been considered as the primary tool for the paleo-carbon isotope reconstructions of surface waters. The main factor effecting $\delta^{13}C$ ratio in planktonic foraminifera skeletons is the $\delta^{13}C$ of seawater dissolved inorganic carbon (DIC). However, physiological processes such as respiration and symbiotic photosynthesis (vital effect) can cause significant variations in $\delta^{13}C$ of foraminifera shell (Spero, 1992; Erez and Honjo, 1981). Whereas some species of planktonic foraminifera were used to infer the $\delta^{13}C$ values of the dissolved inorganic carbon in paleoceans, because they have $\delta^{13}C$ values, which are offset by nearly constant factor due to this effect (Shackleton and Vincent, 1978; Spero, 1992; Keir, 1995).

Variations of the carbon isotope composition of seawater ($\delta^{13}C_{\Sigma CO2}$) at the annual time scale are mainly related to nutrient cycle and biological productivity. It has been found that $\delta^{13}C_{\Sigma CO2}$ in the ocean is inversely correlated with the nutrient concentration of the ocean water (Brocker and Peng, 1982; Kroopinck, 1985). While at longer-term trends, it is related to changes in the carbon isotope composition of dissolved CO_2 in seawater due to the exchange with the atmosphere. For instance the $\delta^{13}C_{\Sigma CO2}$ of the ocean surface water has decreased during the past

two centuries due to the addition of isotopically light fossil fuel CO_2 to the atmosphere as recorded in ice cores (e.g., Friedli et al., 1986, Francy et al., 1999). The exchange between atmospheric and dissolved ocean CO_2 has lead to decrease in surface ocean $\delta^{13}C$ as deduced from shallow dwelling corals and sponges (e.g., Nozaki et al., 1978; Böhm et al., 1996).

1.4. Study area

1.4.1. Location

The Gulf of Aqaba (Figure 1.3) is the eastern segment of the V-shaped northern extension of the Red Sea and is located in the subtropical arid area between 28°29' –30° North and 34°30'-35° East. It is a partially enclosed water body with about 170 km long, 10-26 km wide and more than 1800 m deep (Klinker et al., 1978). The Gulf is separated from the Red Sea proper by a sill at the Straits of Tiran, which has a maximum depth of about 250 m, so that restricted water exchange through the sill allows the Gulf to maintain water masses distinct from those in the Red Sea (Wolf-Vecht, 1992).

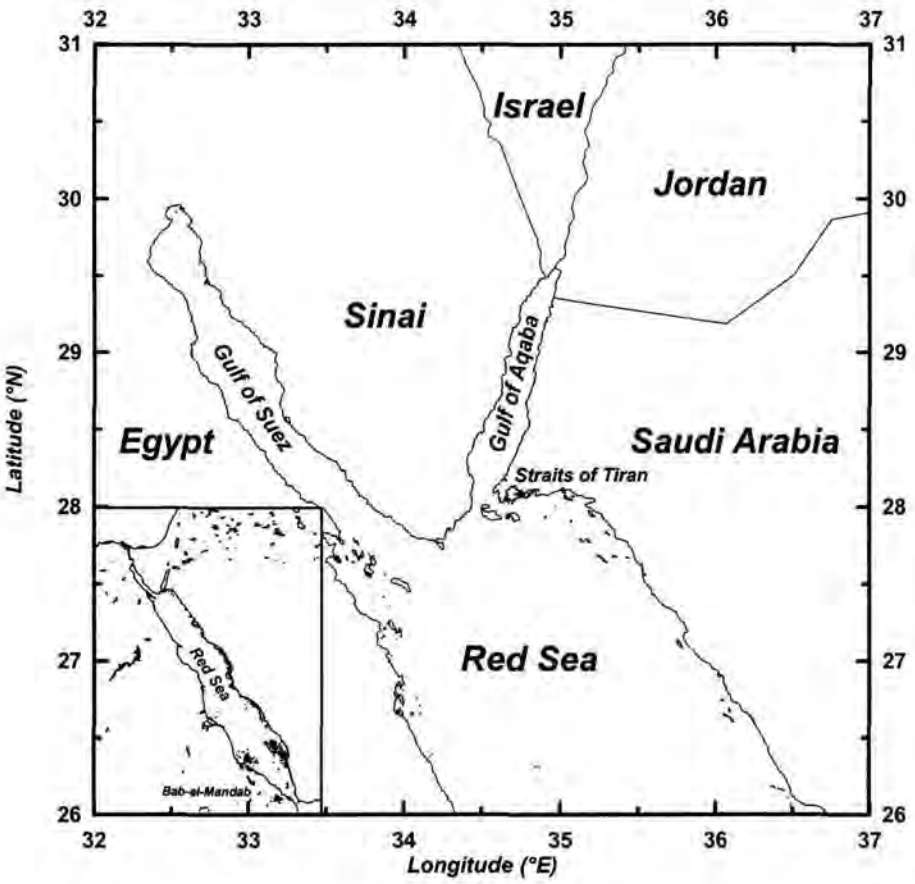

Figure 1.3. Location map of the Red Sea showing the Straits of Tiran, the Gulf of Aqaba and the Gulf of Suez.

1.4.2. Climate

The Gulf of Aqaba is situated between the Sinai desert and the western Arabian desert. The area is extremely arid and the evaporation is very high. Summer temperatures on land may reach up to 45°C, while it is as low as 4°C in winter.

Rainfall in the area is about 37 mm per year. There are however, exceptionally rainy years with as much rain as 70 mm (Reiss and Hottinger, 1984). Flash floods through major wadis in winter transport terrestrial material into the Gulf, resulting in large deltas and incision of submarine canyons. Produced by localized heavy rainfalls, most floods activate the wadis along restricted segment of the coast, thus causing damage to the coastal roads and to the fringing reefs.

Evaporation over the Gulf is about 400 cm/year (Reiss and Hottinger, 1984). The relative humidity in shore localities averages 30-55%. Over most of the Gulf wind blow along the main axes, predominantly from the north, switching abruptly to the southerlies in short gales of a few days duration and predictable seasons (Paldor and Anati, 1979).

1.4.3. Oceanography

Despite the fact that the Gulf of Aqaba is one marine unit, there are still certain differences in relation to its currents, temperature, salinity and coral reef communities which make the northern end different from the southern one and even the eastern side from the western side.

Tides in the northern Gulf of Aqaba are semi-diurnal. However, a distinct diurnal inequality in the high and low tides has been reported by Hulings (1989) who described them as "mixed" rather than semi-diurnal. Extremely low tides have been reported every 10 years. When this happens the reef crest may expose during the daytime, it might kill most of the exposed corals. This prevents the coral population from maintaining a steady state (Reiss and Hottinger, 1984). The currents in the northern Gulf flow in a clockwise direction (Hulings, 1979). A reversal in direction is coupled with changes in wind direction, especially with prolonged southerly winds (Hulings, 1989). However, it was found that the currents on the Jordanian coastline (at a depth of 20-60 m) ran parallel to the eastern side with speed values of 5-10 cm/sec (Leger et al., 1986).

The Gulf is unusually quiet body of water, with clear visibility and little wave action through out the year. The high transparency is partly related to the absence of rivers or major

streams flowing into the sea. Thus there is a poor supply of mineral salts such as nitrogen or phosphorus compounds to the water keeping the planktonic primary production very low. However, the extensive sunlight and the warm water lead to the tremendous development of corals. Wind-borne sediments account for some input of suspended matter, nutrients and metals (Hulings, 1989).

Seawater temperatures in the Gulf of Aqaba are higher in the north than in the south. The lowest water temperature occurs in early March (20.5°C), with the highest in August and September (27°C), and may reach 29°C in shallow coastal areas during the warm months (Hulings, 1979). There is a strong summer thermal stratification during the period April-October and mixed water in winter during the period January-March. Short transition conditions prevail between the stratification and mixed seasons (Klinker et al., 1976; Badran, 1996, Manasreh, 1998).

The lack of regular fresh water and the high evaporation rate within the Gulf cause the particularly saline conditions and contribute significantly to the oligotroghic nature of Gulf system. The salinity in the Gulf of Aqaba is relatively high and ranges between 40-40.8‰, vertical salinity differences are very small (Klinker et al., 1976; Manasreh, 1998).

Isohaline conditions exist in the upper 300 m during summer when waters of salinity 40.5‰ overlay waters of salinity 40.6-40.7‰. The upper isohaline water is restricted to the northern part of the Gulf. Whereas the deeper water extend all the length of the Gulf at a depth range 300-600 m. Below 600 m salinity is constant all over the year and along the Gulf at a value 40.8‰. In winter the halocline disappears and waters of salinity between 40.6-40.7‰ comprised a thick layer between the surface and 600 m (Klinker et al., 1976; Manasreh, 1998).

1.4.4. Coral reefs within the Gulf of Aqaba

The Gulf of Aqaba is characterized by a high diversity of coral reef communities, which represent the northern limit (29°32'N) for reef corals in the western Indo-Pacific region (Schuhmacher et al., 1995). They are mostly of the fringing type, because the Red Sea and the Gulf of Aqaba are devoid of a true continental shelf and the offshore profiles are very steep, therefore the reefs are narrow and they closely follow the shorelines (Gvirtzman and Buchbinder, 1978).

Furthermore, uplifted Pleistocene coral reef terraces are distributed along the coasts of Gulf (Al-Rifaiy and Cherif, 1988). These reefs developed since 306 kyr ago (Reiss and Hottinger, 1984) as a response to late Quaternary climatic fluctuations and eustatic sea level changes together with tectonic uplift rates of about 0.1 mm/year (Strasser et al., 1992; Gvirtzman, 1994). These fossil corals can provide unique informations about the complete history of reef development, sea level and paleoclimatic changes in the area.

1.5. Materials and methods

1.5.1. Coral material

The corals investigated in this thesis (*Porites spp.*) were recovered at the northern end of the Gulf of Aqaba (Figure 1.4). One colony (El-15) was collected in front of a narrow fringing reef off the Interuniversity Institute in Eilat (29°31′N and 34°56′E) at a depth of 15 in April 1996, while several colonies (Aq7, Aq19, Aq29 and Aq42) were collected from a depth transect in front of the Marine Science Station in Aqaba (29°27′N and 34°90′E). The transect was laid out on the reef between the reef flat and the deep fore reef down to 42 m, the coral colonies were collected at depths of 7, 19, 29 and 42 m in April 1999.

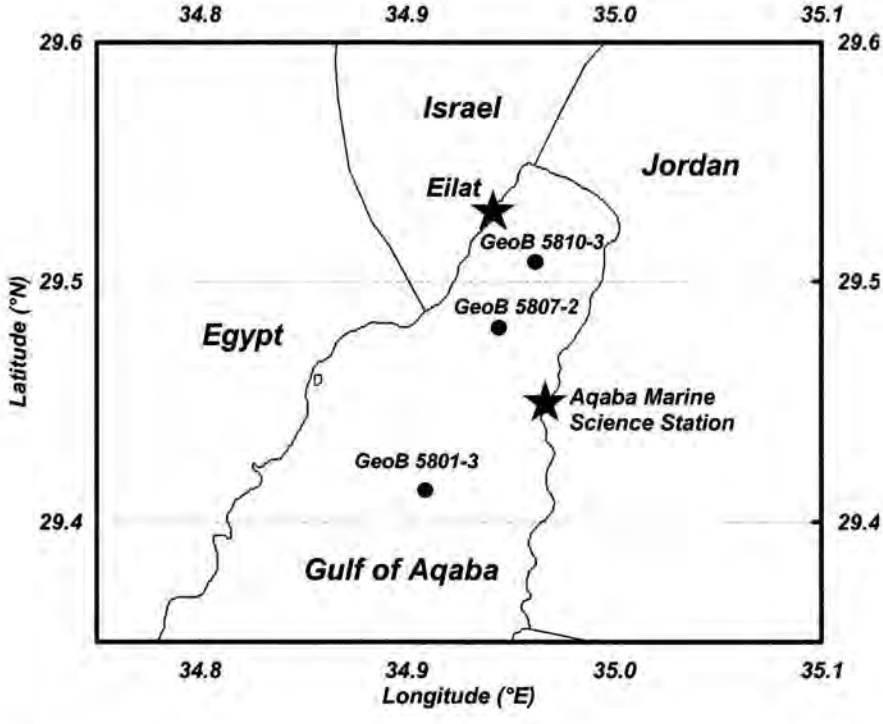

Figure 1.4. Map of the northern end Gulf of Aqaba showing the sampling locations of coral colonies from Aqaba and Eilat (stars) and sediment multicores (dots) examined in this study.

Coral colonies were harvested by SCUBA diving by removal of an upward growing columns (5-10 cm in diameter and 20 cm long) under water using hammer and chisel. After sampling, the corals were cleaned under high-pressure tap water to remove the residual organic matter and then dried under the sun for 24 hours.

1.5.1.1. Stable isotope sampling

All the columns of Eilat and Aqaba coral colonies were sectioned longitudinally into slabs of about 4-6 mm thickness parallel to the axis of maximum growth. The slabs were cleaned and X-rayed using industrial X-ray machine (Model Eresco 160 SLG), at 45 kV exposure conditions and Agfa Strukturix D4-film. Black and white prints of the X-radiographs revealed a clear skeleton density banding pattern of alternating bands of high and low density (Figure 1.1) and were used to choose suitable sampling profiles.

Two different approaches were used in stable isotope sampling depending on the desired temporal resolution. In order to attain high-resolution sampling, we followed the procedure of Pätzold (1986). Samples for isotopic analysis were obtained by cutting small rods out of the skeleton slabs following the growth of a single corallite from the surface vertically down to 4cm (Figure 1.1b). The rods were 2.5 mm in diameter, and 4-5 cm long containing minimum 4 years of growth. Using a precision lathe with a low speed grindstone the rods were milled down in steps that varied between colonies from 125μm to 500μm depending on the growth rate to produce a range of 26-52 samples/year.

For coarse sampling resolution, samples were collected by low-speed drilling using a dentist drill with a 0.6 mm diameter bit. Distance between samples was about 1 mm and the drilling depth was 3 mm (Figure 1.1a). Using this procedure a number of 7 to 12 samples (in average 9) per year were obtained along the maximum growth axis.

1.5.1.2. Stable isotopes analysis

For stable oxygen isotopic analysis, the powdered carbonate samples (100-200μg) were reacted with 100% orthophosphoric acid at 75°C to produce carbon dioxide. The isotope measurements were performed using an automated carbonate preparation device attached to a Finnigan MAT 251 mass spectrometer at the stable isotope laboratory of the Geoscience Departement of the University of Bremen, Germany.

Results are given in the conventional δ notation relative to the VPDB (Pee Dee belemnite) reference standard. The value of $\delta^{18}O$ and $\delta^{13}C$ are:

$$\delta^{18}O(‰) = \{[(^{18}O/^{16}O)_{sample} - (^{18}O/^{16}O)_{standard}] / (^{18}O/^{16}O)_{standard}\} \times 1000$$

$$\delta^{13}C(‰) = \{[(^{13}C/^{12}C)_{sample} - (^{13}C/^{12}C)_{standard}] / (^{13}C/^{12}C)_{standard}\} \times 1000$$

The reproducibility (±σ) is better than ±0.07‰ for $\delta^{18}O$ and ±0.05‰ for $\delta^{13}C$ based on replicate measurements of internal laboratory standard.

1.5.1.3. Skeletal growth parameters

The annual extension rates of the corals were determined from the seasonal cycle of $\delta^{18}O$ as the distance from maximum $\delta^{18}O$ value in a given year to the maximum value of the following year. The absolute bulk density was measured by gamma-densitometry on a Multi Sensor Core Logger (Geotek Ltd., UK) with a Cs^{137} source and 1 mm collimator at the Ocean Drilling Core Repository in Bremen. The method is based upon the attenuation of a gamma photon beam, depending on the thickness and density of the skeleton material (Chalker and Barnes, 1990). The coral slabs were placed on a computer-controlled conveyer belt underneath the collimator and moved in steps of 1 mm, calibrations involved 20 seconds to 5 minutes count, whereas 2 minute counts were used when tracking a cross skeletal slabs. For bulk density calculations from gamma-counts, there exist a log-linear relationship between the attenuation of counts and the mass thickness (skeletal density * slice thickness). A specific mass attenuation coefficient was calibrated by a shell-cube of giant clam *Tridacna*, which consist of aragonite. The annual mean bulk densities were calculated from the seasonal cycles of density variations, which were measured along adjacent profiles nearby the drilled profiles. The calcification rate was then calculated as a product of linear extension and skeletal density (Chalker et al., 1985; Lough and Barnes, 2000) as follows:

$$linear\ extension\ rate\ (cm\ year^{-1}) = \frac{calcification\ rate\ (gcm^{-2}\ year^{-1})}{bulk\ density\ (gcm^{-3})}$$

1.5.2. Sediment material

During Meteor cruise M44/3 in 1999; sediment cores were taken from the Gulf of Aqaba and the Red Sea (Pätzold et al., 2000). In this thesis, we have focused on three multicores sampled

at different water depths along a North-South transect from the northern end of the Gulf of Aqaba (Figure 1.4, Table 1.1).

Table 1.1. Positions and water depths of the analysed sediment cores from the northern end of the Gulf of Aqaba.

GeoB Number	*Latitude N*	*Longitude E*	*Water Depth (m)*	*Sediment recovery (cm)*
GeoB 5801-3	29°24.90′	34°54.70′	826	40
GeoB 5807-2	29°28.81′	34°56.78′	646	39
GeoB 5810-3	29°30.21′	34°57.73′	441	35

1.5.2.1. Foraminifera stable isotope analyses

Sub-samples for faunal analysis were taken at 0.5 cm intervals from each multicorer. The sediments were wet sieved with sieves of 63 and 150μm mesh size and dried in an oven at 55°C. From the 150μm fraction 12-18 specimens of the planktonic foraminifera *Globigerinoides sacculifer* (without final chamber) and *Globigerinoides ruber* (white) of 350 to 400 μm diameter (maximum extension) of species were used for stable isotope measurements. Analyses were carried out on a Finnigan MAT 251 mass spectrometer equipped with an automated carbonate preparation device at the stable isotope laboratory, Geoscience Department, Bremen University, Germany. Precision based on replicates of an internal limestone standard, was better than 0.07 ‰ and 0.05‰ for $\delta^{18}O$ and $\delta^{13}C$ respectively. Results are expressed in ‰ deviations from the VPDB standard.

1.5.2.2. ^{14}C AMS dating and calibration

Accelerator Mass Spectrometry (AMS) ^{14}C dating samples were taken from the top, intermediate and bottom parts of each multicore. About 700 to 1000 specimens of the *Globigerinoides sacculifer* and *Globigerinoides ruber* (250-500μm) were hand picked for this purpose. While carbonate hydrolysis and CO_2 reduction were performed in Bremen University, Germany, AMS measurements were carried out at the Leibniz-Labor for Radiometric Dating and Isotope Research at Christian-Albrechts-University, Kiel, Germany.

The ^{14}C AMS dating method is based on rate of decay of the radioactive carbon isotope ^{14}C. This isotope is produced naturally in the atmosphere by nuclear reaction between slow cosmic-ray neurons and the nucleus of stable ^{14}N:

$$ {}^{1}_{0}n + {}^{14}_{7}N \rightarrow {}^{14}_{6}C + {}^{1}_{1}H $$

where ${}^{1}_{0}$n is the neutron and ${}^{1}_{1}$H is the proton.

The ^{14}C atoms are then incorporated into the carbon dioxide molecules ($^{14}CO_2$) which mixed rapidly throughout the atmosphere and hydrosphere and absorbed, by every living thing, whether plant or animal. However, when the organism dies the ^{14}C stops being absorbed, and the ^{14}C activity declines as a result of radioactive decay. The radioactivity is given by:

$$ A = A_{\circ} e^{-\lambda t} $$

where A is ^{14}C measured activity ($dm^{-1}g^{-1}$), $A_{\circ}$ is the initial activity, t is the time in year and λ is the decay constant which equals ln2/Libby half-life (5568 ±30years).

All the ages obtained this study were calibrated and transformed into calendar years A.D. using the CALIB 4.3 calibration software. The values for ΔR of 100 years was used, this value corresponds to a reservoir age of about 420 years (Stuiver and Braziunas 1993; Stuiver et al., 1998a; 1998b).

1.5.3.3. Organic carbon, total nitrogen and carbonate analysis

Sediment samples (sampling step 1 cm) were freeze-dried and ground for the determination of total carbon (C_{tot}) and nitrogen (N_{tot}), and total organic carbon (C_{org}) contents. Values were obtained by combustion at 1050°C using a Heraeus CHN-O-rapid elemental analyser (Müller et al., 1994) at the Geoscience Department at Bremen University, Germany. For the determination of organic carbon, 25 mg aliquots of the dried sediments were weighted in a silver foil crucibles, wetted with a few drops of ethanol to suppress foaming during acidification, decalcified by drop wise addition of 6 N HCl, and dried on a hot plate at about 80°C. Total carbon and nitrogen were determined on untreated sample aliquots (25 mg) using tin crucibles for weighting. The carbonate content of the samples was calculated from the difference between total and organic carbon and expressed as calcite [$CaCO_3 = 8.33 * (C_{tot} - C_{org})$]. All analyses were performed in duplicate and expressed in weight percent dry, salt-free sediment assuming a pore-water salinity of 40‰. The relative precision of the measurements, based on duplicates and control analysis of lab-internal reference sediment sample (WS1), was better than 3%.

1.5.3.4. Stable isotope analysis of organic matter

The $\delta^{13}C_{org}$ of the sediment was measured with a Finnigan Delta E mass spectrometer and commercial Heraeus CHN-Rapid analyser interfaced by an automated trapping box at the Geoscience Department at Bremen University, Germany. The samples were prepared as described for total organic carbon measurements. $\delta^{13}C$ values are reported against the VPDB standard. Reproducibility for $\delta^{13}C_{org}$ measurements based on internal standards was better than 0.15‰.

1.6. Environmental data

1.6.1. Seawater temperature and salinity records

StowAway TidbiT temperature loggers (Figure 1.5) were deployed along the depth transect in front of the Marine Science Station at Aqaba in April 1999 next to the coral colonies at depths of 7, 19, 29 and 42 m. The loggers provided a continuous record of *in situ* temperature readings (1 hour interval) till June 2000. The accuracy of measurements for the temperature loggers was checked each 6 months by calibration against mercury thermometer, and it ranged between ± 0.10 and 0.15 °C.

Figure 1.5. StowAway TidbiT temperature logger that was used in the study to provide high-resolution (hourly interval) continuous temperature records from different water depths and over long time period.

Furthermore, Monthly measurements of sea surface temperature from Eilat between 1988-2000 were obtained (Amatzia Genin, personal communication). The measurements were based on daily observations in the upper 20 cm of the water column with a pre-calibrated mercury thermometer (precision 0.1°C) fixed in a bucket. Whereas, monthly temperature and salinity records from Aqaba were obained between 1997-2000 (Riyad Manasreh, personal communication).

The measurements were based on biweekly observations and were performed in front of the Marine Science Station at Aqaba, in a fixed coastal station (from surface down to 50m deep) about 300m a way from the study transect, using a conductivity-temperature-depth

sensor (OS200 CTD) instrument. The precision of the CTD is better than ±0.001°C and ±0.003‰ for temperature and salinity respectively.

1.6.2. Isotopic composition records of seawater

Water samples for stable isotope analysis were collected by SCUBA divers periodically at a monthly resolution over 14-month period (April 1999 to June 2000). Along the depth transect from surface waters and from each depth (7, 19, 29 and 42m) 500 ml polyethylene bottles were filled with seawater next to coral colonies. Immediately after sampling, duplicate samples of 100 ml of seawater were transferred into brown borosilicate glass bottles. For oxygen isotope analysis, water samples of the 100 ml were taken and stored without further treatment, while the other 100 ml samples were carefully poisoned with 1 ml of a saturated $HgCl_2$ solution for carbon isotope analysis. Both bottles were sealed with melted paraffin and stored at 4°C till measurements were carried out.

The stable isotope measurements followed the classical procedure of equilibration of water with CO_2 at 25°C for the water ^{18}O analysis (Epstein and Mayeda, 1953); extraction of the total dissolved inorganic carbon as CO_2 from water by acidification with phosphoric acid for the - $\delta^{13}C_{\Sigma CO2}$ analysis (Kroopnick, 1974).

The isotopic data were obtained on a Finnigan Delta mass spectrometer at the Geoscience Department, Bremen University, Germany with a precision of 0.1‰ and 0.16‰ for $\delta^{18}O$ and $\delta^{13}C$ respectively. The data are given as the per mil deviation of the ^{18}O:^{16}O or ^{13}C:^{12}C ratio R of the sample respectively relative to the VSMOW oxygen isotope standard (Craig, 1961; Hut, 1987) and to VPDB carbon isotope standard (Craig, 1957). The $\delta^{18}O$ values in VSMOW were converted to the VPDB scale by adding a constant of –0.27‰ (Hut, 1987).

$$\delta = \frac{R_{\text{Sample}}}{R_{\text{Standard}}} \times 1000$$

1.7. Focus of this thesis

Despite the general applicability of corals as paleoclimate proxies is uncontested, and corals can provide histories of large scale climate variability which are in some cases equivalent in quality and resolution to those derived from instrumental data, it is subjected to limitations, which may affect the reliability of the proxy particularly on the subannual time scale. However, calibration studies may serve to improve the accuracy of records obtained from these proxies.

Some of these limitations suggest that environmental signals obtained from corals are subjected to smoothing and distortion results from calcification throughout the thickness of coral tissue layer (Barnes et al., 1995; Taylor et al., 1995). Furthermore, it is often assumed that coral grow at a uniform rates which is probably not the case, the changes or interruption in coral growth rates on the annual time scales may change the absolute isotopic values (e.g., Land et al., 1975; Pätzold, 1986; McConnaughey, 1989; Leder et al., 1996). Other studies found that some physiological effects might also change the environmental signals produced by corals (McConnaughey, 1989; Allison et al., 1996). Reducing the sampling resolution was also proposed to cause attenuation of the climatic signals obtained from corals (Leder et al., 1996).

In the Red Sea, the coral based paleoclimate studies are scarce (Klein et al., 1992; 1993; 1997; Heiss, 1996; Heiss et al., 1999; Felis et al., 1998; 2000; Moustafa et al., 2000). Most of these studies have made there calibrations depending on one coral from certain depth with bimonthly/monthly resolution, and based on satellite (IGOSS) or gridded (COADS) sea surface temperature records without measurements of seawater $\delta^{18}O$ variations (Klein et al., 1992; Heiss et al., 1999).

The focus of this thesis therefore is to carry out a coral $\delta^{18}O$ calibration study from the northern Gulf of Aqaba via *in situ* monitoring of seawater temperature (SST), salinity (SSS), and a regular water sampling for $\delta^{18}O$. The produced high-resolution time series data on the chemical and physical properties of seawater (SST, SSS, $\delta^{13}C$, $\delta^{18}O$) were utilized to assess the ability of *Porites* corals to accurately record environmental variations in order to examine the robustness of coral records and to constrain the environmental sources of the isotopic variations. Additionally, the thesis aims to evaluate the effect of some biological factors such as extension rate, density, calcification rate, tissue layer thickness and coral species that may change the environmental signals produced by corals and to establish acceptable $\delta^{18}O$/temperature relation for the region.

Moreover, the thesis focused on high-resolution paleoenvironmental data that may obtain from sediment records in such areas with high sedimentation rates that can document changes at decadal time scale. Therefore, the carbon isotope composition of planktonic foraminifera from sediment cores was used to track changes of seawater DIC during the last 1000 years and to detect the effect of anthropogenic CO_2 increase in the atmosphere and in the northern Gulf of Aqaba waters.

1.8. Thesis structure

The thesis consists of three manuscripts (Chapter 2-4) submitted to or already published in reviewed international scientific journals. The following gives a short overview of these manuscripts.

Chapter 2

Stable oxygen isotope records of corals from the northern Gulf of Aqaba: environmental and biological effects

Puplished as:

Al-Rousan, S., S., Al-Moghrabi, J., Pätzold and G., Wefer, Stable oxygen isotope records of corals from the northern Gulf of Aqaba: environmental and biological effects. Marine Ecology Progress Series in press 2002.

This manuscript evaluates the effect of environmental and some biological factors on the skeletal $\delta^{18}O$ composition of two *Porites* coral colonies collected from the northern end of the Gulf of Aqaba. The results suggest that a large majority of the seasonal variations in coral oxygen isotope from the area can be explained by SST variations. However, coral $\delta^{18}O$ was found to be growth dependent and a simple exponential model can explain the relation between the two variables. Furthermore, significant offsets in $\delta^{18}O$ coral records from the two colonies are related to coral species differences. The manuscript discusses also the relation between some growth parameters with the skeletal $\delta^{18}O$ values.

Chapter 3

Stable oxygen isotopes in *Porites* corals monitor weekly temperature variations in the northern Gulf of Aqaba, Red Sea

To be submitted to Coral Reefs as:

Al-Rousan, S., S., Al-Moghrabi, J., Pätzold and G., Wefer, Stable oxygen isotopes in *Porites* corals monitor weekly temperature variations in the northern Gulf of Aqaba, Red Sea.

The article deals with high-resolution coral $\delta^{18}O$ records (weekly/biweekly) from the northern end of the Gulf of Aqaba, calibrated against high-resolution *in situ* temperature, salinity and isotopic composition of seawater measurements over 14 months from different water depths. Results show that high-resolution coral $\delta^{18}O$ records from all depths were able to capture fine details of the weekly temperature records and were able to resolve more that 95% of the weekly temperature variations. However attenuation and amplification of the corals seasonal amplitudes were recorded in deep slow growing corals due to changes or interruption in coral growth rates on the annual time scales. Relations between seawater $\delta^{18}O$ and salinity, and coral $\delta^{18}O$, seawater temperature and $\delta^{18}O$ were also investigated.

Chapter 4

Invasion of anthropogenic CO_2 recorded in planktonic foraminifera from the northern Gulf of Aqaba

To be submitted to Earth and Planetary Science Letters as:

Al-Rousan, S., J., Pätzold and G., Wefer, Invasion of anthropogenic CO_2 recorded in planktonic foraminifera from the northern Gulf of Aqaba

The third manuscript deals with high-resolution (~10years) records of the stable carbon isotope composition of the planktonic foraminifera *G. sacculifer* from the northern Gulf of Aqaba during the last 1000 years. Results show a uniform and consistent planktonic $\delta^{13}C$ pattern before 1750s, and a gradual decrease of approximately 0.63‰ in the last two centuries. This decrease seems to track the decrease of $\delta^{13}C_{DIC}$ in the surface waters that is mainly caused by the increase of anthropogenic input of ^{13}C depleted CO_2 into the atmosphere. Variations in the $\delta^{13}C$ of organic matter also show a trend toward lighter values closely follow those of the foraminifera and support the interpretation.

CHAPTER TWO

2. Stable oxygen isotope records of corals from the northern Gulf of Aqaba: environmental and biological effects

("Marine Ecology Progress Series" In press 2002)

Saber Al-Rousan [1, 2,*], Jürgen Pätzold [1], Salim Al-Moghrabi [2] and Gerold Wefer [1]

[1] Fachbereich Geowissenschaften, Universität Bremen, D-28359 Bremen, Germany

[2] Marine Science Station, P.O. Box 195, Aqaba, Jordan

*email: alrousan@uni-bremen.de

2.1. Abstract

Monthly $\delta^{18}O$ records of two coral colonies (*Porites* cf. *lutea and Porites* cf. *nodifera*) from different localities (Aqaba and Eilat) from the northern Gulf of Aqaba, Red Sea, were calibrated with recorded sea surface temperatures between 1988-2000. The results show high correlation coefficients between SST and $\delta^{18}O$. Seasonal variations of coral $\delta^{18}O$ in both locations could explain 91% of the recorded SST. Different $\delta^{18}O$/SST relations from both colonies and from the same colonies were obtained, indicating that $\delta^{18}O$ from coral skeletons were subjected to extension rate effect. Significant $\delta^{18}O$ depletions are associated with high extension rates and heavier values with low extension rates.

The relation between coral skeletal $\delta^{18}O$ and extension rate is not linear and can be described by a simple exponential model. An inverse relationship extends over extension rates from 1 to 5 mm/yr, while for more rapidly growing corals and portions of colonies the relation is constant and the extension rate did not appear to have significant effect. We recommend that $\delta^{18}O$ values should be obtained from fast growing corals or portions where the isotopic disequilibrium is fairly constant (extension rate >5 mm/yr).

The results show that difference in coral species may produce a significant $\delta^{18}O$ profile offset between two colonies which is independent from environmental and extension rate effects. We conclude that skeletal extension rate and coral species have an important influence on coral $\delta^{18}O$ and must be considered when using $\delta^{18}O$ records for paleoclimatic reconstructions.

2.2. Introduction

Massive growing corals can be used as environmental recorder because their annual growth bands allow the reconstruction of accurate chronologies (Knutson et al., 1972). Massive hermatypic coral skeletons are excellent monitors of tropical water environments. Corals of this type live in the surface-ocean mixed layer, grow continuously at rates of several millimetres to centimetres per year, and during growth they incorporate isotopic species into their skeleton.

The stable oxygen isotopic composition ($\delta^{18}O$) of hermatypic corals has been utilized in numerous reconstructions of past sea surface temperatures and salinities (e.g. Charles et al., 1997; Gagan et al., 2000). Coral $\delta^{18}O$ reflects a combination of local SST and the $\delta^{18}O$ value of

ambient seawater (Epstein et al., 1953; Wefer and Berger, 1991). However, changes in coral growth rates may change the absolute isotopic values. The variations in extension and calcification rates have an impact on the fractionation of stable isotopes and have been a subject of discussion for a long time (Land et al., 1975; Goreau, 1977; Weil et al., 1981; Pätzold, 1986; McConnaughey, 1989; de Villiers et al., 1995; Leder et al., 1996; Allison et al., 1996; Cohen and Hart, 1997). Significant skeletal $\delta^{18}O$ depletion in faster growing areas of coral skeleton rather than slower growing areas has been reported for the first time by Land et al. (1975). Allison et al. (1996) observed in *Porites lutea* from Phuket, South Thailand, that the growth rate/$\delta^{18}O$ relationship is linear at all extension rates, while McConnaughey (1989) found this relation in *Pavona clavus* from Galapagos only in parts of corals extending at less than 5 mm/year. For more rapidly growing parts of the coral, extension rate did not appear to have a significant effect in $\delta^{18}O$.

Few studies have examined skeletal $\delta^{18}O$ variations within and among species. From studies on corals from Kaneohe Bay, Hawaii, Grottoli (1999) found that $\delta^{18}O$ values are constant with variable depth for a given species, and that this parameter exhibits interspecific variability. Species-specific offsets in $\delta^{18}O$ have been also reported by Weil et al. (1981) and Wellington et al. (1996).

In this study we examined skeletal $\delta^{18}O$ composition of two *Porites* colonies collected from the northern end of the Gulf of Aqaba at a depth of 19 m from Aqaba (*Porites* cf. *lutea*) and another colony from Eilat at 15 m (*Porites* cf. *nodifera*). To evaluate the effect of extension rate that is independent of the *in situ* temperature, variations of $\delta^{18}O$ of seawater and specific-species effects, samples for $\delta^{18}O$ analysis were taken from each specimen along synchronous growth profiles with different extension rates. Previously published and unpublished coral $\delta^{18}O$ data from the area were also included in this study for comparison. However, results from this study can be used to evaluate and correct coral $\delta^{18}O$ values obtained from modern and fossil corals for extension rate effects.

2.3. Materials and methods

The study is located at the northern end of the Gulf of Aqaba (Figure 2.1) which is the northward extension of the desert-enclosed Red Sea. The maximum depth of the Gulf is 1830 m with 180 km long and 5-26 km width. Oligotrophic conditions prevail in the Gulf waters and

evaporation (350 cm/year) greatly exceeds precipitation (3 cm/year) (Reiss and Hottinger, 1984).

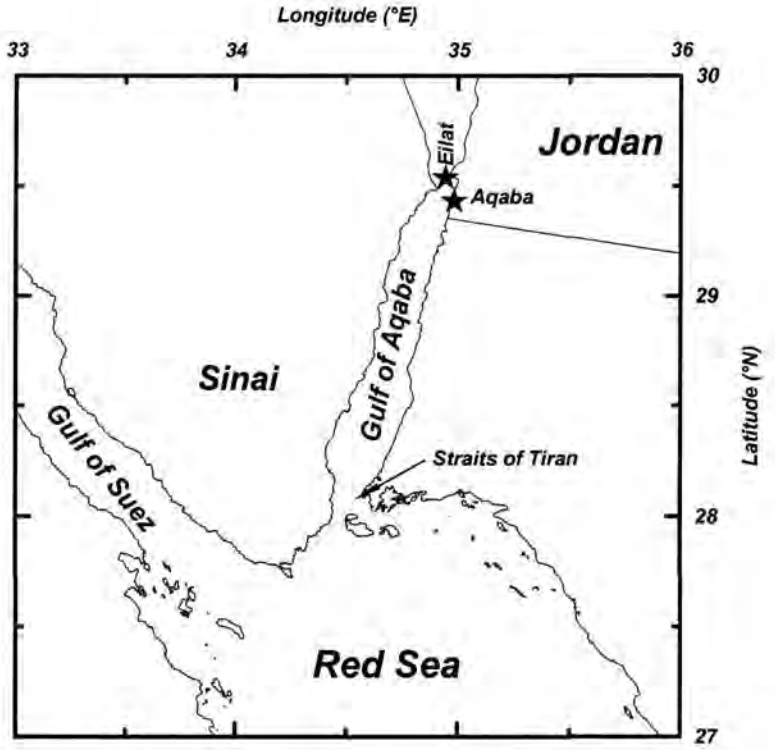

Figure 2.1. Location map of the Gulf of Aqaba showing the collection sites (stars) of *Porites* spp. coral colonies from Aqaba and Eilat, northern Gulf of Aqaba.

A column of a *Porites* cf. *nodifera* colony was collected in front of the Interuniversity Institute in Eilat (29°31′N and 34°56′E) at a depth of 15 m in April 1996 (El-15), while another column of *Porites* cf. *lutea* colony (Aq-19) was collected in front of the Marine Science Station in Aqaba (29°27′N and 34°90′E) at a depth of 19 m in April 1999. Both coral columns were sectioned along their longitudinal axes to obtain slabs of about 4 mm thickness. X-radiographs were prepared to reveal annual density bands for determining sampling profiles (Figure 2.2). Aragonite sub-samples were collected by low-speed drilling using a dentist drill with a 0.6 mm diameter bit. Distance between samples was about 1 mm and the drilling depth was 3 mm. A number of 7 to 12 samples (in average 9) per year from both corals were obtained along the maximum growth axis (main profile). In addition continuously sampling of stable isotopic profiles was drilled along lateral corallites from the sides of both colonies which showed low growth rate (Figure 2.2).

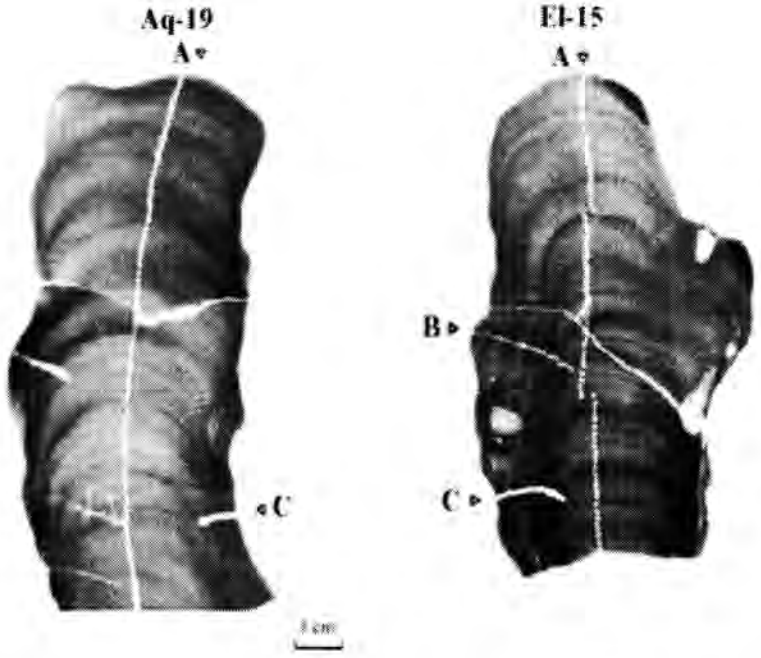

Figure 2.2. X-radiograph positive prints of the two coral slabs (Aq-19 and El-15) showing the skeletal density bands and the sampling profiles for stable isotope analysis (profiles A, B, and C) as indicated by the arrow heads.

The isotopic composition of the samples was measured with a Finnigan MAT 251 mass spectrometer at Bremen University. All values are reported in per mil relative to VPDB. Average measurement precision for $\delta^{18}O$ was ±0.07 ‰.

The chronologies of both corals were constructed by designating the maximum $\delta^{18}O$ value within each year as mid-March (the coldest month in the year according to recent SST records from Eilat and Aqaba). Linear interpolation of twelve equidistant values for the main profiles (six for the side profiles) per year between these maxima was applied, using AnalySeries 1.1 software package (Paillard et al., 1996). This procedure provided a monthly and bimonthly sampling resolution.

Absolute bulk density was measured by gamma-densitometry on a Multi Sensor Core Logger (Geotek Ltd., UK) with a Cs^{137} source and 1 mm collimator at the Ocean Drilling Core Repository in Bremen. The method is based upon the attenuation of a gamma photon beam, depending on the thickness and density of the skeleton material (Chalker and Barnes, 1990). Annual mean bulk densities were calculated from the seasonal cycles of density variations which were measured along adjacent profiles nearby the drilled profiles.

Monthly measurements of sea surface temperature from Eilat between 1988-2000 were used for comparison (Amatzia Genin, personal communication). The measurements were based on daily observations in the upper 20 cm of the water column (200 m distance to the site where the coral was collected) with a pre-calibrated mercury thermometer (precision 0.1°C) fixed in a bucket. On the other hand, the monthly temperature record from Aqaba was obtained between 1997-2000 (Riyad Manasreh, personal communication). The measurements were based on biweekly measurements in the upper meter of the water column using an OS200 CTD instrument (precision 0.001°C). The measurements were performed in front of the Marine Science Station, 300 m away from the coral site.

2.4. Results

2.4.1. Sea water temperature records

No major significant differences were observed between recorded SST in Aqaba and Eilat. In both locations sea surface temperatures show the same regular seasonal cycle and having the same seasonal amplitude (5.5°C). It averages 23.6°C with maximum temperatures of 26.4°C (on average) in August/September, and minimum temperatures of 20.9°C (on average) in February/March (Figure 2.3).

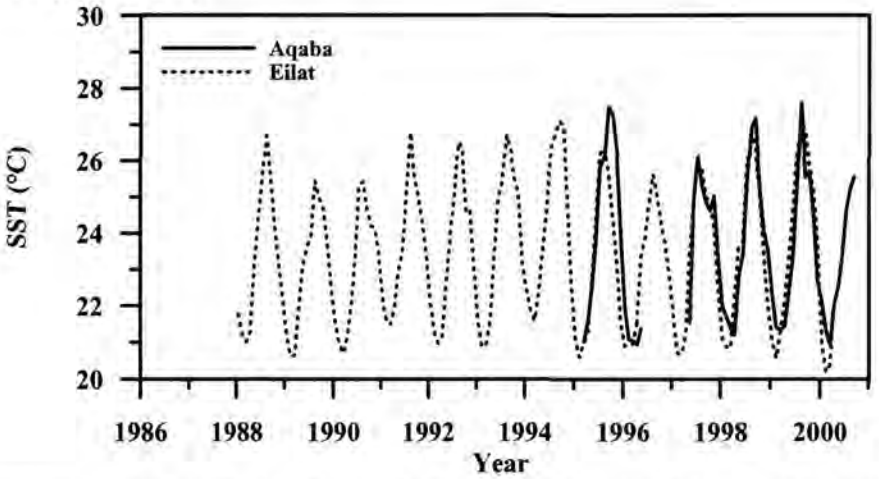

Figure 2.3. Monthly-recorded sea surface temperatures in Aqaba between 1997-2000 (Manasreh, unpublished data) and in Eilat between 1988-2000 (Genin, unpublished data).

2.4.2. Salinity and $\delta^{18}O$ of sea water

Seawater $\delta^{18}O$ is related to changes in salinity as a response to changes in evaporation, precipitation and mixing of waters from different sources. This relation between $\delta^{18}O_w$ and

salinity is different from ocean to ocean. In the Red Sea a change of 1‰ salinity causes a change of 0.29‰ in $\delta^{18}O_w$ according to Craig (1966) and Andrié and Merlivat (1989). At the northern end of the Gulf of Aqaba the salinity of the surface waters is close to 40.5‰ and varies by less than 0.5‰ throughout the year (Wolf-Vecht et al., 1992).

Manasreh (1998) reported average minimum salinities of 40.34‰ occur during winter (February) and maximum salinities of 40.56‰ during summer (June). These minor variations in the surface seawater salinity throughout the year are considered to have little effect on the seasonal variation of the seawater $\delta^{18}O$ (Klein et al., 1992) (0.225‰ salinity =0.065‰ $\delta^{18}O$, Craig, 1966). Therefore, the seasonal $\delta^{18}O$ variation in the coral skeleton of the northern Gulf of Aqaba should be mainly controlled by SST (Heiss et al., 1999).

2.4.3. Calibration of $\delta^{18}O$ in coral skeletons

The x-radiograph positive prints of the coral slabs reveal a clear and regular skeletal density-banding pattern. The alternating bands of high and low densities are annual as confirmed by the strong seasonal cycle in $\delta^{18}O$.

The comparison between local SST records and coral $\delta^{18}O$ time series is a necessary first step in the calibration of coral $\delta^{18}O$ records. The oxygen isotope profiles of both corals show well-organized cyclic variations along the axis of maximum extension rate (fast growing tops) (profiles El-15A and Aq-19A) (Figure 2.4).

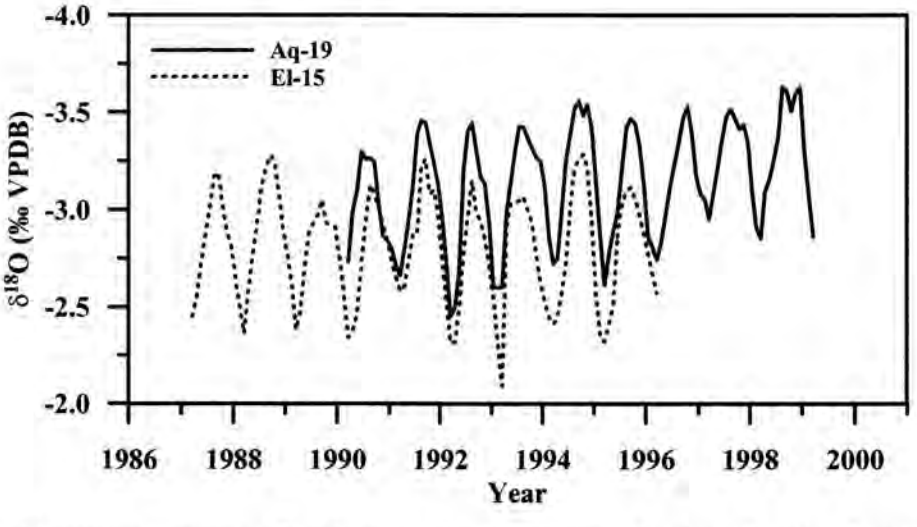

Figure 2.4. Stable oxygen isotope profiles from samples drilled vertically along the axis of maximum extension rate of *Porites* cf. *lutea* coral from Aqaba and *Porites* cf. *nodifera* coral from Eilat between 1987 and 1999.

$\delta^{18}O$ in the Aqaba coral ranged between –2.45 to –3.55‰ with an average of –3.10‰ and between –2.10 to –3.28‰ with an average of –2.79‰ in the Eilat coral. Each $\delta^{18}O$ profile shows strong seasonal variations with similar amplitudes. These are on average 0.80‰ in Aqaba and 0.83‰ in Eilat. Both profiles correspond remarkably well to the monthly SST measurements in Eilat and Aqaba (Figure 2.5). The correlation coefficients are rather high and range between –0.84 in Eilat coral (in the time interval 1988-1995) and –0.81 from Aqaba coral (in the time interval 1995-1999). Unfortunately no instrumental temperature data were available from Aqaba during the period 1988-1995.

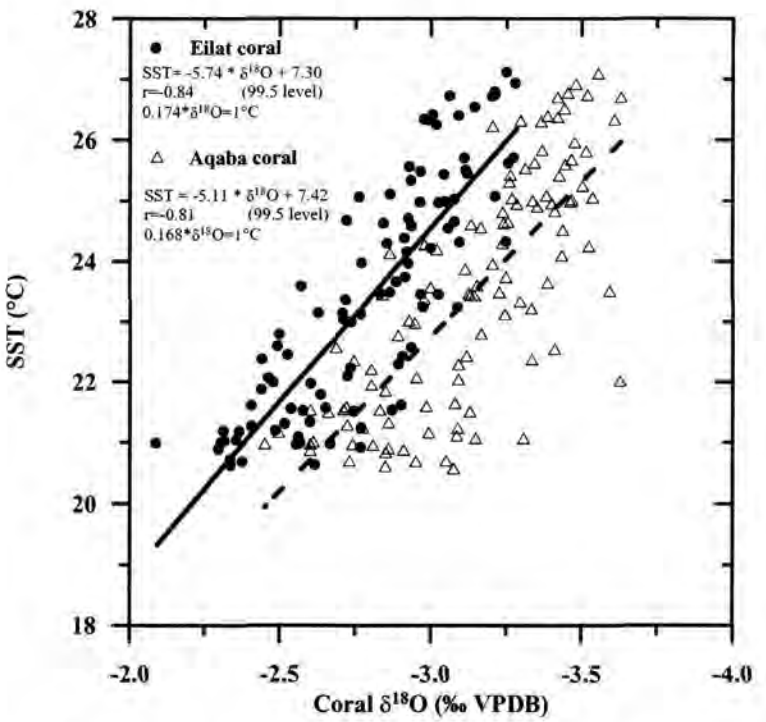

Figure 2.5. Comparison of monthly coral $\delta^{18}O$ variations (from profiles drilled vertically along the maximum extension rate) with monthly recorded sea surface temperature at a) Aqaba and b) Eilat.

Monthly records of $\delta^{18}O$ in both locations from the main growth profile (El-15A and Aq-19A) were calibrated with recorded SST, and the following equations are the results of the calculations:

$$SST\ (°C) = -5.93\ (\delta^{18}O_{coral}) + 4.63 \qquad r = -0.81 \qquad (99.5\%\ level)\ Aqaba\ coral$$

$$SST\ (°C) = -5.75\ (\delta^{18}O_{coral}) + 7.30 \qquad r = -0.84 \qquad (99.5\%\ level)\ Eilat\ coral$$

The $\delta^{18}O$/SST relationship from these equations varies between 0.168‰/°C from Aqaba and 0.174‰ /°C from Eilat coral. The correlation from the annual averages of the $\delta^{18}O$ record and

the annual average SST of the two corals were low (–0.25 to -0.31) despite the annual $\delta^{18}O$ record follows that of the annual SST record.

2.4.4. Extension rate and skeletal $\delta^{18}O$

Comparing the $\delta^{18}O$ records from Aqaba and Eilat (from the main profiles, El-15A and Aq-19A) in the period 1990-1995, the results show that Aqaba coral is several parts ‰ more depleted in $\delta^{18}O$ than Eilat coral. The offset between the two colonies ranged between 0.27-0.36‰ with an average of 0.29‰, which appears to be constant over the length of all covered years (Figure 2.4).

Annual extension rates were determined from the seasonal cycle of $\delta^{18}O$ as the distance from maximum $\delta^{18}O$ value (which represents the minimum recorded temperature) in a given year to the maximum value of the following year. The Eilat coral showed lower mean annual extension rates which ranged between 7 to 13 mm/year (11.2 mm/year in average), while it ranged between 12 to 21 mm/year (15.2 mm/year in average) in the Aqaba coral.

We examined the relationship between annual extension rates and mean annual $\delta^{18}O$ in Aqaba and Eilat. The $\delta^{18}O$ values obtained along the slower extension rate profile (El-15A) were more enriched in $\delta^{18}O$ than the faster extension rate profile (Aq-19A).

2.4.5. Coral $\delta^{18}O$ from synchronous growth profiles

To evaluate the extension rate effect that is independent of the *in situ* temperature and variations on $\delta^{18}O$ of seawater, $\delta^{18}O$ samples were taken from each specimen along synchronous growth profiles with different extension rates.

The bimonthly $\delta^{18}O$ profiles from the slower growing sides of the Eilat coral (El-15B and El-15C) show strong seasonal variations with 0.82 and 0.89‰ seasonal amplitude, which is similar to that obtained from the main profile from the same colony (El-15A).

The $\delta^{18}O$ values from profile El-15B ranged between –2.04 and –3.30‰ with an average of –2.68‰ which is heavier than that obtained from the main profile by 0.11‰ (Figure 2.6a). The extension rate in this profile ranged between 2-5 mm/year with an average of 3.9 mm/year. Also $\delta^{18}O$ values from El-15C profile ranged between –1.75 to –2.87‰ with average –2.23‰

which is 0.15‰ heavier than that from El-15B (Figure 2.6a). The extension rate in this profile ranged between 1.5 and 3 mm/year and averaged 2.3 mm/year.

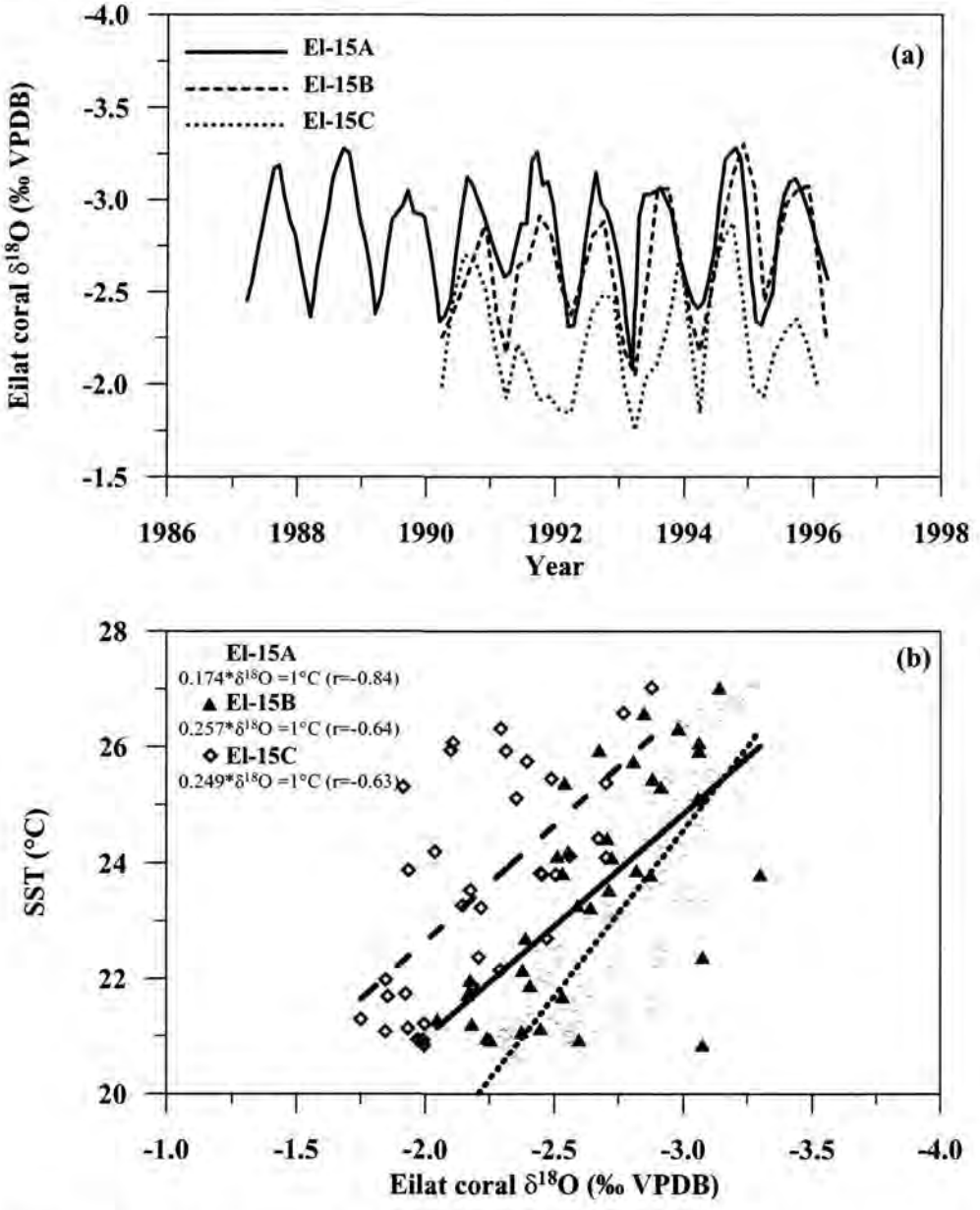

Figure 2.6. a) Seasonal variation in $\delta^{18}O$ (VPDB) composition of Eilat coral along different profiles. b) Linear relation between $\delta^{18}O$ and recorded sea surface temperature along different coral extension rate profiles (El-15A (11.2 mm/year), El-15B (3.9 mm/year) and El-15C (2.3 mm/year)).

A bimonthly $\delta^{18}O$ profile from the Aqaba coral (Aq-19C) with extension rates between 1 and 2.5 mm/year (1.9 mm/year in average) was also obtained. $\delta^{18}O$ values showed a seasonal amplitude of 0.73‰. Values ranged between –1.85 and –2.98‰ and averaged -2.29‰, which is similar to that obtained from the slowest growth profile from Eilat coral (El-15C), but is

higher by 0.81‰ than the average value from the main profile from the same colony (Aq-19A) (Figure 2.7a).

Calibration of $\delta^{18}O$ from these profiles with recorded SST in bimonthly resolution, produced different $\delta^{18}O$/SST equations (Figure 2.6b, 2.7b) which vary between 0.21‰/°C, 0.25‰/°C and 0.24‰/°C with correlation coefficients of 0.69, 0.64 and 0.63 from Aq-19C, El-15B, El-15C, respectively.

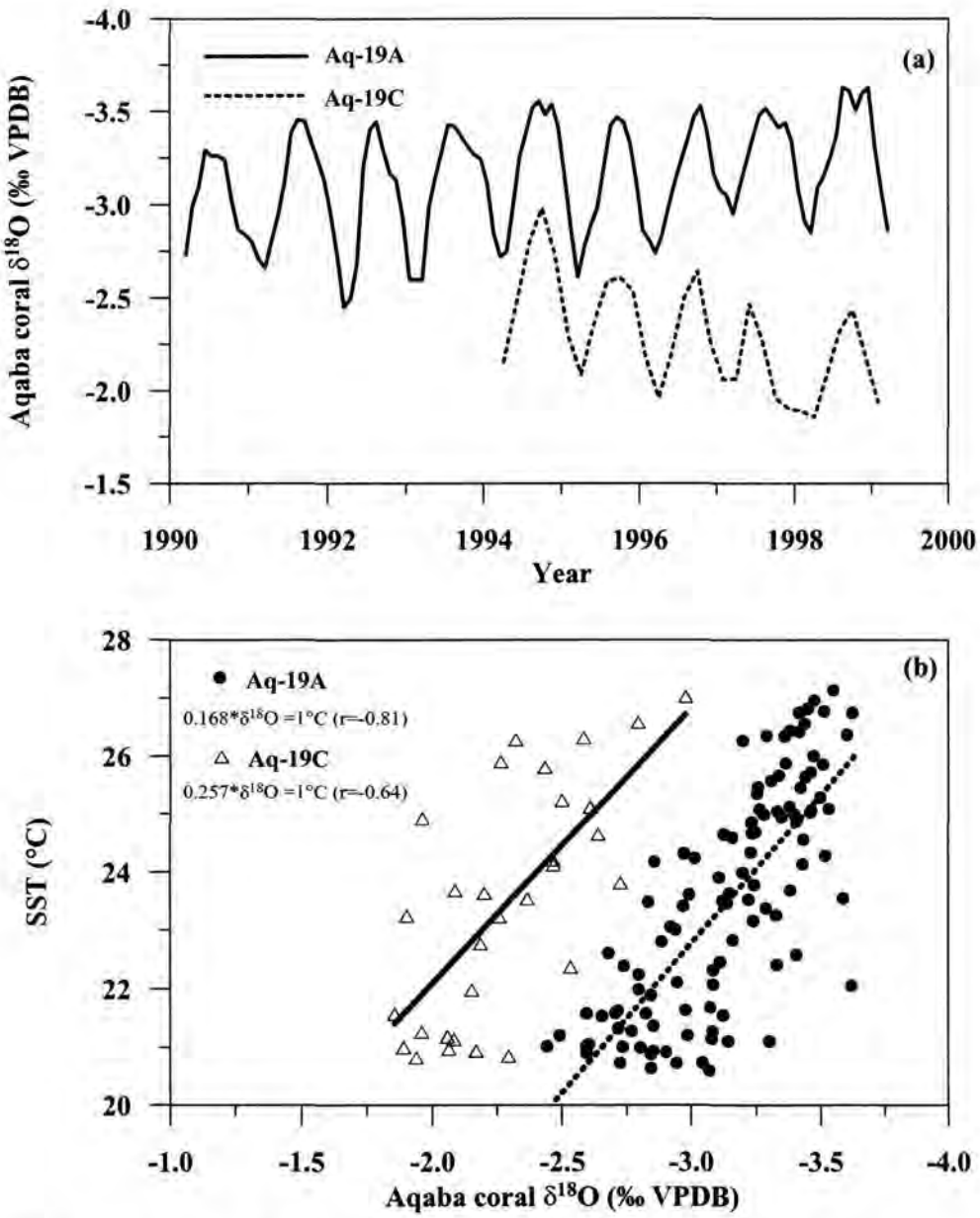

Figure 2.7. a) Seasonal variation in $\delta^{18}O$ (VPDB) composition of Aqaba coral along two different profiles. b) Linear relation between $\delta^{18}O$ and recorded sea surface temperatures along two different coral extension rate profiles (Aq-19A (15.2 mm/year), Aq-19C (1.9 mm/year)).

2.4.6 Relation between growth variables

Calcification rate was calculated as a product of linear extension and skeletal density (Chalker et al., 1985; Lough and Barnes, 2000). Calcification values along all profiles ranged between 2.2-0.157 g/cm^{-2}year with average 0.92 g/cm^{-2}year, and decreases from the top to the sides of the colonies due to decrease in extension rate.

The relations between density, extension and calcification rate from this study (Figure 2.8) are similar to the widely known growth relations from other studies (Wellington and Glynn, 1983; Dodge and Brass, 1984; Scoffin et al., 1992; Lough and Barnes, 2000). Average annual extension was inversely correlated with average annual density (r=0.88) and significantly correlated with average annual calcification (r=0.98). Average skeletal density was inversely correlated with average annual calcification (r=0.84) and skeletal oxygen isotope (r=0.80). Thus, we conclude that variations in average annual calcification were mostly caused by variations in extension rate as found by Barnes and Lough (1993) and Lough and Barnes (2000).

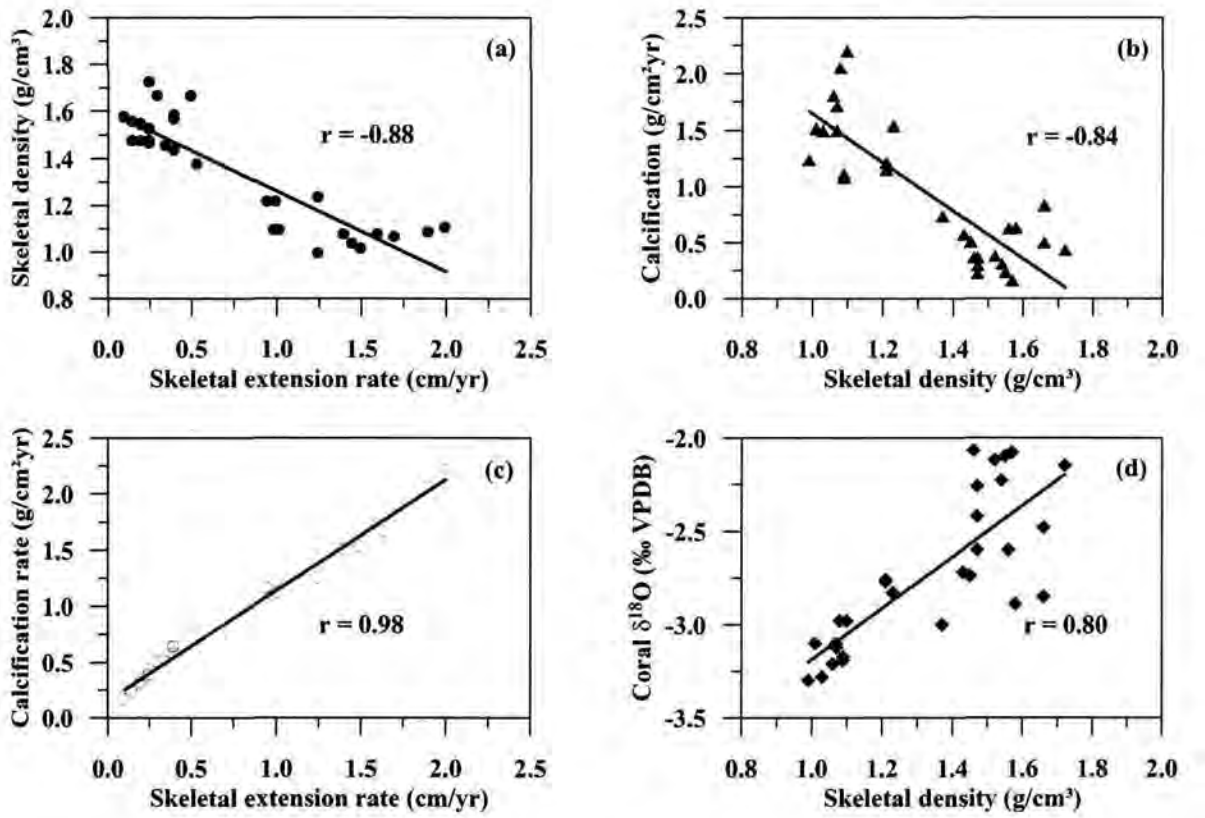

Figure 2.8. Scatter diagram of average annual growth data for Aqaba and Eilat corals. a) density vs. extension, b) calcification vs. extension, c) calcification vs. density, and d) density vs. skeletal stable oxygen isotopes. Regression lines and correlation coefficients are shown.

2.5 Discussion

2.5.1. Calibration of coral $\delta^{18}O$

Our $\delta^{18}O$/SST slopes from Aqaba and Eilat coral main profiles (0.168 and 0.174‰/°C) are less than the widely recognized values of 0.22‰ for calcite (Epstein et al., 1953) and 0.23‰/°C for aragonite (Grossman and Ku, 1986) but they are quite similar to values determined by Gagan et al. (1994) for *Porites* at a weekly resolution from the Great Barrier Reef (0.18‰/°C) and by Quinn et al. (1998) for a New Caledonia *Porites* on a monthly scale (0.172‰ /°C).

Felis et al. (1998) and Moustafa (2000) determined a value of 0.165‰/°C as the most reasonable one for calibration for *Porites* from Ras Umm Sid, Red Sea (using IGOSS temperature data set). Heiss et al. (1999) also found a value of 0.166 and 0.187‰/°C from monthly resolution in horizontal and vertical profiles from a *Porites* colony from Aqaba.

For the annual time scale the correlation coefficient decreases to -0.25 and -0.31. Quinn et al. (1998) found the same situation in New Caledonia corals in which the correlation coefficient decreased from -0.87 in the seasonal time scale to –0.53 in the annual time scale. They explained this decrease due to salinity changes in which the seasonal variations in salinity are small compared to that for temperature, while the interannual changes in salinity are proportionally larger than seasonal changes.

This may be also the situation in the northern Gulf of Aqaba. A regular measurement of seawater salinity for three years (1997-2000) showed no systematic annual pattern (Riyad Manasreh 2000, personal communication) and the average annual values differ from year to year. The interannual variations during this period are as much as 0.4‰ compared to 0.225‰ on the seasonal scale. The potential impact of 0.4‰ interannual salinity variations on $\delta^{18}O$ of Red Sea water and hence on coral $\delta^{18}O$ is 0.12‰ (after Craig, 1966). This effect could explain part of the difference of the seasonal and mean annual slopes of $\delta^{18}O$/SST.

The measured SST in Eilat and Aqaba reveal an average annual cycle of about 5.5°C. Using the gradient of 0.165‰/°C for coral $\delta^{18}O$-temperature dependence from the northern Red Sea (Felis et al., 1998; Moustafa, 2000), the average seasonal coral $\delta^{18}O$ amplitude of 0.83‰ would reflect a temperature change of about 5.0°C, which is about 91% of the average seasonal SST amplitude. The expected variation of 0.065‰ $\delta^{18}O$ of seawater (related to 0.225‰ change in salinity) has a magnitude of 7.8% of the average seasonal coral $\delta^{18}O$ variation. This indicates that a large majority of the variations in coral oxygen isotope data can be explained

by the sea surface temperature variations, and only a small fraction can be attributed to $\delta^{18}O$ variations of surface water.

It is obvious from our results that different $\delta^{18}O$/SST relations can be obtained from different colonies and within the same colony. These variations are most likely mediated by coral biology, which would be outlined in the next section.

2.5.2. Extension rate effect on skeletal $\delta^{18}O$ composition

Both main $\delta^{18}O$ profiles from the two colonies (El-15A and Aq-19A) show similar amplitudes (0.80 and 0.83‰) which implies that both corals respond similarly to environmental signals. The offset between the $\delta^{18}O$ profiles which is about 0.29‰ on average (more depleted $\delta^{18}O$ values in the Aqaba coral) does not reflect changes in temperature and/or salinity between the two sites (similar physical environment) and should be a biological mediated signal.

Despite the profiles from the coral sides (El-15B, C and Aq-19C) were sampled at lower resolution, we received more or less the same seasonal amplitude as that obtained from the main profiles at a monthly resolution sampling. Analysis of $\delta^{18}O$ along the main and synchronous growth profiles produced different trends in $\delta^{18}O$ values (Figure 2.5, 2.6b, 2.7b).

These results indicate that the $\delta^{18}O$ values are subjected to extension and calcification rate effects, i.e. the faster growing profile (Aq-19A) is 0.29‰ more depleted in $\delta^{18}O$ than the slower growing one (El-15A). Continuation of the heavier $\delta^{18}O$ trend with slow extension rate was also observed from synchronous growth profiles from both colonies (Aq-19C, El-15B, El-15C).

The relation between coral $\delta^{18}O$ and skeletal growth rate from this study is not linear and can be explained by simple exponential model (Figure 2.9)

$$Coral\ \delta^{18}O = -3.067 + exp\ [1.069 + (-0.744) * E.r] \qquad Aqaba\ coral \quad r = 0.96$$

$$Coral\ \delta^{18}O = -2.795 + exp\ [1.016 + (-0.757) * E.r] \qquad Eilat\ coral \quad r = 0.97$$

Where E.r is the coral extension rate in mm/year, and $\delta^{18}O$ in ‰VPDB.

Coral $\delta^{18}O$ data from Aqaba and Eilat and from the same genus *Porites* with different extension rates S4 (6.8 mm/yr), MB30 (3.3 mm/yr), IS50 (2.0 mm/yr) and S6 (14.8 mm/yr) (Klein et al., 1993; Pätzold and Klein unpublished data), Aq-193 (20 mm/yr), Aq-292 (5.3

mm/yr) and Aq-424 (3.5 mm/yr) (Al-Rousan, unpublished data) were also plotted in the same diagram (Figure 2.9). The data were fitted in the curve and supported the reliability of the exponential model.

The inverse relationship between $\delta^{18}O$ and extension rate from this model extends over growth rate 1-5 mm/yr as in, Aq-19C, Aq-292, Aq-424, El-15B, El-15C, MB30, and IS50. For more rapidly growing corals and portions of corals like in profiles Aq-19A, Aq-193, El-15A, S4 and S6 (Figure 2.9) the relation is constant and the extension rate did not appear to have significant effect on coral $\delta^{18}O$.

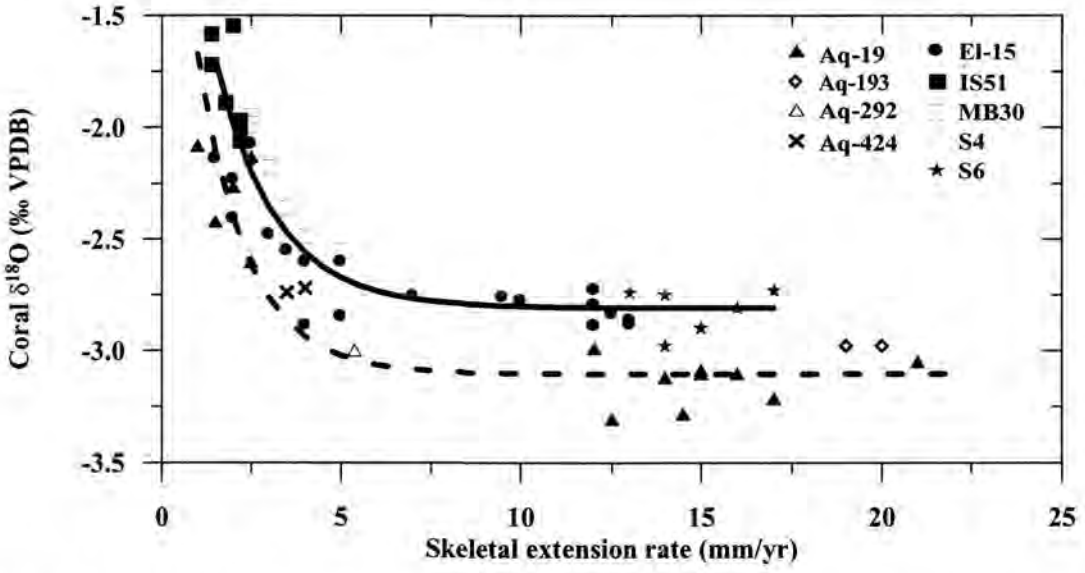

Figure 2.9. Exponential relationship between skeletal $\delta^{18}O$ and skeletal extension rate of *Porites* spp. colonies sampled along vertical (main axis) and horizontal (coral sides) profiles for corals collected from the northern Gulf of Aqaba, Red Sea. Data of IS51, MB30 and S4 are from Klein et al. (1993), S6 from Pätzold and Klein (unpublished data), and Aq-193, Aq-292 and Aq-424 from Al-Rousan (unpublished data).

These results are similar to the findings of McConnaughey (1989), who found an inverse relationship from Galapagos *Pavona clavus* corals that grew at rates less than 5 mm/year, and extension rate did not appear to have any significant effect at rates more than 5 mm/yr. Quinn et al. (1998) also found this negative correlation in New Caledonia corals and Allison et al. (1996) in corals from Phuket, South Thailand, but at all extension rates. Higher $\delta^{18}O$ and Sr/Ca values in slower growing transects were reported by de Villiers et al. (1995) on *Pavona clavus* from Galapagos Island. In contrast, Leder et al. (1996) found that $\delta^{18}O$ of rapidly growing portions (8 mm/year) of a colony was 0.1-0.2‰ heavier than the slowest growing portions (1.1

mm/year) and explained this as a result of reduced sampling resolution in slower growing portions of the coral and not a result of variable kinetic effects.

We conclude that growth rate has an important control on the isotopic composition of coral skeletons. Our results support the conclusion drawn by McConnaughey (1989), that the depletion of $\delta^{18}O$ is characteristic for kinetic fractionation associated with rapid calcification, and the isotope disequilibria tends to be fairly consistent in rapidly growing parts of photosynthetic corals. For that reason we suggest that $\delta^{18}O$ should be obtained from fast growing portions where the extent of isotopic disequilibria is largest, because isotopic disequilibria is too variable in slow growing parts.

2.5.3. Calcification rate and species-specific effects

As shown in Figure 2.9, a $\delta^{18}O$ offset between Aqaba and Eilat colonies still exists. We calculated the calcification rate along the drilled profiles. Due to the high correlation between extension and calcification rate (Figure 2.8c) the relation between calcification and $\delta^{18}O$ failed to explain the offset between the main $\delta^{18}O$ profiles from the two colonies. A similar exponential equation was reproduced (Figure 2.10). We found that high extension profiles revealing low skeletal densities (Aq-19A) were depleted in $\delta^{18}O$ compared to low extension profiles showing high densities (El-15A) which may have the similar calcification rate.

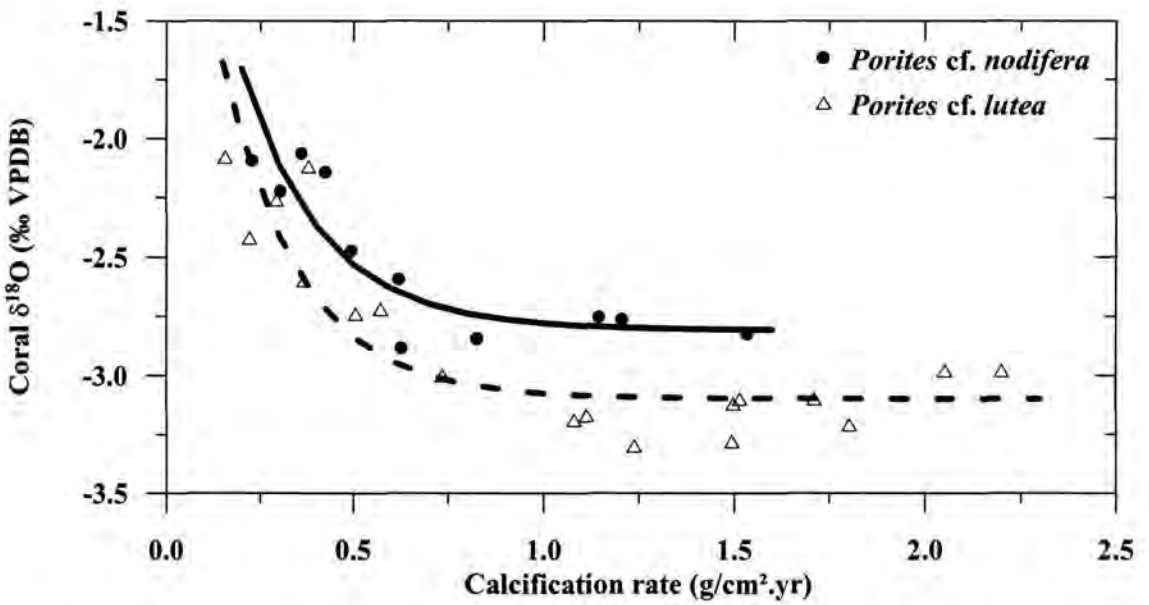

Figure 2.10. Exponential relationship between skeletal $\delta^{18}O$ and skeletal calcification rate for two different *Porites* spp. corals (*Porites* cf. *nodifera* and *Porites* cf. *lutea*) collected from the northern Gulf of Aqaba, Red Sea.

The offset between $\delta^{18}O$ profiles cannot always be explained as a function of extension and /or calcification rate. For this reason both corals were taxonomically identified. We found that Aq-19, Aq-193, Aq-292 and Aq-424 are *Porites* cf. *lutea* which are depleted in $\delta^{18}O$ by about 0.29‰, compared to El-15 which belongs to *Porites* cf. *nodifera* species. Wellington et al. (1996) found that certain species are enriched or depleted in $\delta^{18}O$ relative to other species from the same genus living under the same environmental conditions, where as Grottoli (1999) in Hawaii corals found that $\delta^{18}O$ varies among species, species-specific offsets in $\delta^{18}O$ have been also reported by Weil et al. (1981). The $\delta^{18}O$ offset between coral species may reflect some genetic differences which alter the extent of isotopic disequilibria (Allison et al., 1996).

The results from this study show that the linear extension rate and species variation should be considered when interpreting coral $\delta^{18}O$ data for paleoclimatic studies. Further studies are also needed to study the variation of $\delta^{18}O$ of other *Porites* species.

2.6. Conclusions

The high correlation between coral $\delta^{18}O$ and recorded SST (-0.84) in both Aqaba and Eilat in the northern Red Sea suggests that a large majority of the seasonal variations in coral oxygen isotopes can be explained by the sea surface temperature variations, and only a small fraction can be attributed to $\delta^{18}O$ variations of surface water. These results support the concept of using northern Red Sea corals as recorders of sea surface temperature variability. Interannual salinity variations in the Gulf of Aqaba (as recorded in recent studies) seem to be responsible for decreasing the correlation between coral $\delta^{18}O$ and SST at the annual time scale.

Different $\delta^{18}O$/SST relations from two different colonies and also from the same colonies were obtained, indicating that $\delta^{18}O$ of coral skeletons is subjected to an extension rate effect. Significant $\delta^{18}O$ depletion is observed at high extension rates, and heavier values at low extension rates. The relation between $\delta^{18}O$ and extension rate is not linear and can be explained by a simple exponential model, in which the inverse function extends over extension rates 1-5 mm/yr. For more rapidly growing corals and portions of coral colonies, the relation is constant and the extension rate did not appear to have any significant effect on coral $\delta^{18}O$. The offset in $\delta^{18}O$ profiles cannot be always explained as a function of extension and/or calcification rate and may result from coral species differences.

We suggest that $\delta^{18}O$ values from *Porites* corals should be obtained from fast growing corals or portions of the colonies (>5 mm/yr), where the isotopic disequilibrium is fairly constant. Skeletal extension rate and coral species should be considered when interpreting and comparing coral paleoclimatic data from various coral species with different extension rates.

2.7. Acknowledgments

We wish to thank Y. Loya for coral sample collection at Eilat. Special thanks are also due to R. Manasreh and A. Genin for providing temperature records from Aqaba and Eilat. All isotopic measurements were carried out at Bremen University. We are grateful to M. Segl for stable isotope analysis and U. Röhl for introduction to the Multi Sensor Core Logger. This work is part of the Red Sea Program (RSP II), funded by the German Federal Ministry of Education, Science, Research, and Technology (BMBF).

CHAPTER THREE

3. Stable oxygen isotopes in *Porites* corals monitor weekly temperature variations in the northern Gulf of Aqaba, Red Sea

(to be submitted to "Coral Reefs")

Saber Al-Rousan [1,2,*], Jürgen Pätzold [1], Salim Al-Moghrabi [2] and Gerold Wefer [1]

[1] Fachbereich Geowissenschaften, Universität Bremen, D-28359 Bremen, Germany

[2] Marine Science Station, P.O. Box 195, Aqaba, Jordan

* email: alrousan@uni-bremen.de

3.1. Abstract

To assess the ability of *Porites* corals to accurately record environmental variations, high-resolution (weekly/biweekly) coral $\delta^{18}O$ records were obtained from four coral colonies from the northern Gulf of Aqaba, which grew at depths of 7, 19, 29 and 42m along one transect. Next to each colony, hourly temperatures, biweekly salinities and monthly $\delta^{18}O$ of seawater were continuously recorded over a period of 14 months (April 1999-June 2000).

Contrary to water temperature, which shows a regular and strong seasonal variation and change with depth, seawater $\delta^{18}O$ exhibits a weak seasonality and change with depth. Positive correlations between seawater $\delta^{18}O$ and salinity were observed indicating that seawater $\delta^{18}O$ is governed by changes in salinity. The two parameters were related to each other by the equation $\delta^{18}O_{Seawater\ (VSMOW)} = 0.281 * SSS\ (‰) - 9.14$.

The high-resolution coral $\delta^{18}O$ records from this study show regular pattern of seasonality and are able to capture fine details of the weekly average temperature records. They resolve more than 95% of the weekly temperature variations. On the other hand attenuation and amplification of coral seasonal amplitudes were recorded in deep slow growing corals, which were not related to environmental effects (temperature and/or seawater $\delta^{18}O$), or sampling resolution, but result from subannual variations in extension rate. Furthermore no smoothing or distortion of the isotopic signals was observed due to calcification within the tissue layer as suggested by earlier studies. The calculations from coral $\delta^{18}O$ calibrations against the *in situ* measurements show that temperature (T) is related to coral $\delta^{18}O$ (δ_c) and seawater $\delta^{18}O$ (δ_w) by the equation $T = -5.38 * (\delta_c - \delta_w) - 1.08$.

Our results demonstrate that coral $\delta^{18}O$ from the northern Gulf of Aqaba is a reliable recorder of temperature variations and there is a minor contribution of seawater $\delta^{18}O$ to this proxy, which could be ignored.

3.2. Introduction

Due to the relatively short temporal coverage of instrumental climate records, high-resolution proxy archives are increasingly used to study the climatic changes over decades or even centuries. Records preserved in corals, especially *Porites spp.*, reliably yield continuous and quantitative reconstructions of environmental and climatic parameters, with monthly to weekly

resolution back to several hundred years ago. This is due in part to their annual growth bands that allow for the construction of accurately dated chronologies (Knutson et al., 1972).

Isotopic measurements from coral skeletons have been widely used as a proxy of environmental conditions. The stable oxygen composition of coral skeletons have been utilized in numerous reconstructions of past sea surface temperatures and salinities (e.g. Pätzold, 1984; Linsely et al., 1994; Charles et al., 1997; Gagan et al., 2000; Kuhnert et al., 2000; Felis et al., 2000). Coral $\delta^{18}O$ reflects the temperature and the oxygen isotopic composition of the ambient seawater in which the coral grew (Fairbanks and Dodge, 1979; Swart et al., 1983; Aharon et al., 1991; Wefer and Berger, 1991).

In order to use corals to reconstruct paleotemperatures, it is necessary to clarify the relation between coral $\delta^{18}O$ and the recorded SSTs in respective sites. The slope of the linear $\delta^{18}O$/SST relationship is similar in most calibration studies (McConnaughey, 1989; Gagan et al., 1994; Leder et al., 1996) and ranges from 0.18 to 0.20‰/°C. However the regression lines may offset. Most of these studies used gridded SST instead of the local measurements, which may affect the results of the reliability of the proxy on short time scale, due to short-term local climate signals incorporated in the coral $\delta^{18}O$. Furthermore, seawater $\delta^{18}O$ from these studies was not considered (Quinn et al., 1998) or assimilated to an annual value (McConnaughey, 1989) or derived from salinity (Carriquiry, 1994). Studies including continuous records of reef-site salinity and $\delta^{18}O$ of seawater at similar time scale are very rare (Wellington et al., 1996, Leder et al., 1996).

Although the general applicability of coral $\delta^{18}O$ as climate proxy is uncontested, it is subject to limitations, particularly on the subannual time scale. Modeling studies for coral skeletogenisis suggested that environmental signals obtained from corals are subjected to smoothing and distortion results from calcification throughout the thickness of coral tissue layer (Barnes et al., 1995; Taylor et al., 1995). However changes or interruption in coral extension rates may change the absolute isotopic $\delta^{18}O$ values, in which more negative values associated with high-extended corals (Land et al., 1975; Pätzold, 1986; Cohen and Hart, 1997). Other studies found that some physiological effects might also change the environmental signals produced by corals (McConnaughey, 1989; Allison et al., 1996). Reducing the sampling resolution was also proposed to cause attenuation of the climatic signals obtained from corals (Leder et al., 1996).

In the Red Sea, the coral based paleoclimate studies are scarce (Klein et al., 1992; 1993; 1997; Heiss, 1996; Heiss et al., 1999; Felis et al., 1998; 2000; Moustafa et al., 2000). Most of these studies have made there calibrations depending on corals from one depth with bimonthly/monthly resolution, and based on satellite (IGOSS) or gridded (COADS) sea surface temperature records without measurements of seawater $\delta^{18}O$ variations (Klein et al., 1992; Heiss et al., 1999).

Here we present a 14-month calibration study carried out on *Porites spp.* colonies collected in front of the Marine Science Station in Aqaba from a depth transect extended over 7,19, 29 and 42 m depth. In order to examine the robustness of coral records, to check the ability of corals to preserve small changes in the annual temperature cycle and to constrain the environmental sources of the isotopic variations. We have measured *in situ* seawater temperature, salinity and isotopic composition of seawater over the period between April 1999 to June 2000 from all four depths. These time series are compared against weekly/biweekly isotopic records obtained from coral skeletons that where collected along the depth transect.

3.3. Oceanography and climate

The Gulf of Aqaba is the northeastern extension of the desert-enclosed Red Sea (Figure 3.1a), which represents a unique northern hemisphere site where corals grow at up to 29.5°N. The Gulf is a semi-isolated basin separated from the Red Sea proper by the Straits of Tiran which are about 240 m deep. The maximum depth of the Gulf is 1830 m with180 km length and 5-26km width.

It is located within the very warm portion of the Sahara bio-climatic zone. The climate is arid with high evaporation (~ 400cm/yr) and negligible precipitation (~ 2.2cm/yr) and runoff. The area is affected by the airflows from the Indian monsoonal trough and the Mediterranean low-pressure system (Hulings, 1989). The latter creates cooler and unsettled conditions during the period November through March. The mean sea surface temperatures are 23.5°C, and mean salinity values in the upper waters are 40.4-40.6‰ (Manasreh 2001, personal communications).

The physico-chemical environment of the Gulf waters shows strong seasonal fluctuations than do other subtropical seas. During summer (April-October), the water column is stratified and the surface layers are depleted in nutrients (Reiss and Hottinger, 1984). However, in winter (November-March) the thermocline disappears and deep convective mixing persists for several

months reaching 600m depth or more (Genin et al., 1995). During this period, the surface waters are enriched with nutrients brought up from deeper layers.

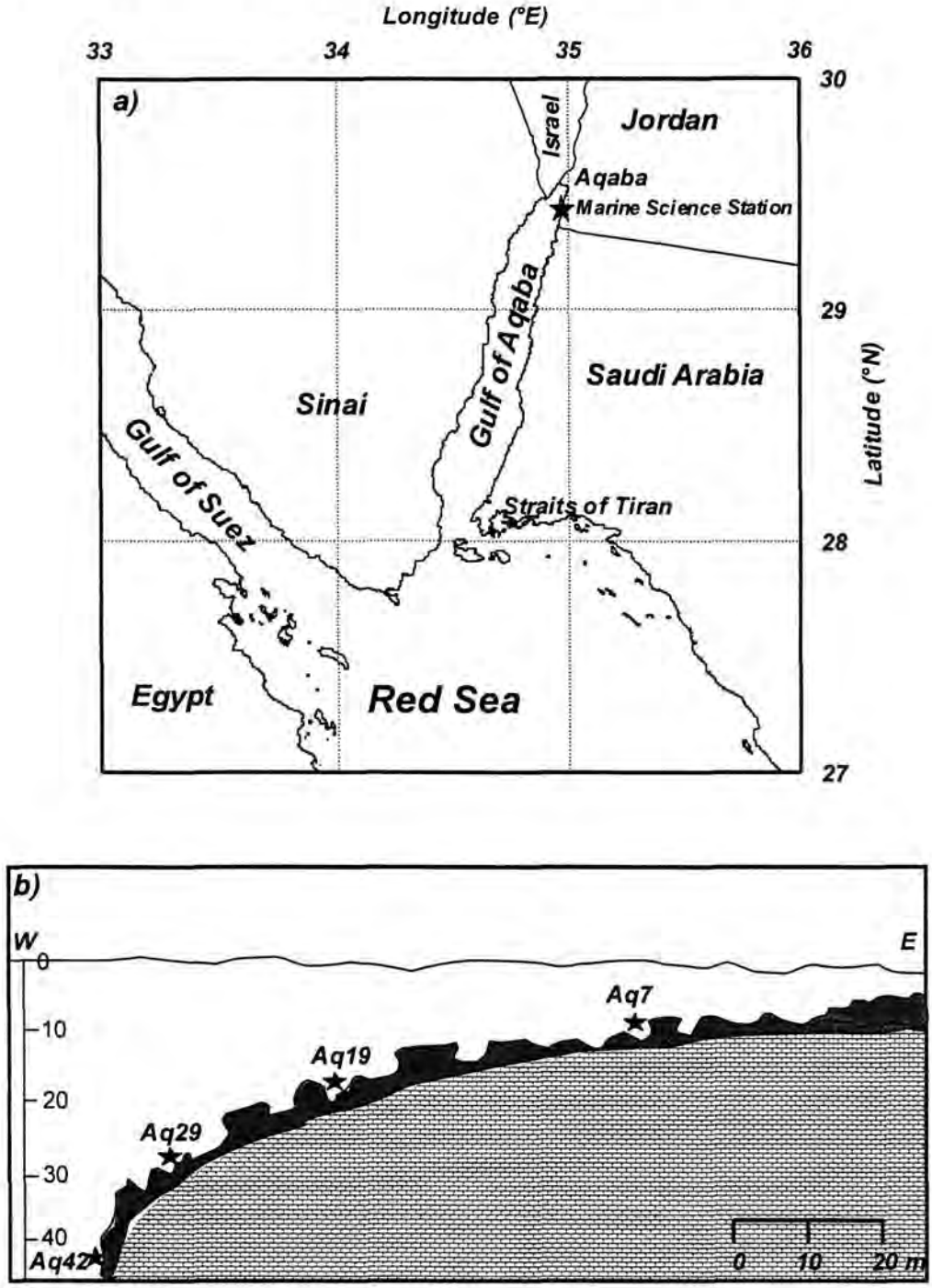

Figure 3.1. a) Map of the northern Gulf of Aqaba. The star indicates the sampling location near the Marine Science Station in Aqaba. b) Cross section along the reef transect in front of the Marine Science Station in Aqaba, the stars show the sites where corals and environmental data were collected.

Extremely oligotrophic conditions are prevailing in the Gulf due to the arid climate and because it receives its waters from the nutrient-depleted Red Sea surface water through the Straits of Tiran (Reiss and Hottinger, 1984). The deep light penetration and high transparency due to low amount of resuspended materials and fresh water flux (Levanon et al., 1979) results in extending the depth limit of hermatypic corals down to 130m as reported by Reiss and Hottinger (1984).

3.4. Materials and methods

3.4.1. Study area

A steeply EW oriented reef slope transect was chosen at the northern tip of the Gulf of Aqaba (29° 27`N and 34° 90`E) in front of the Marine Science Station in Aqaba (Figure 3.1a). The transect was laid out on the reef between the reef flat and the deep fore reef down to 42 m. Scleractinian corals were distributed along this transect at all depths (Figure 3.1b).

3.4.2. Environmental data

Temperature loggers StowAway TidbiT were deployed at each depth along the transect in April 1999 next to the coral colonies. The loggers provided a continuous record of *in situ* temperature readings (1 hour interval) during their deployment period (till June 2000). The accuracy of measurements for the temperature loggers was also checked each 6 months by calibration against mercury thermometer, and ranged between ± 0.10 and 0.15 °C.

During the study period, biweekly continuous measurements of seawater salinity were obtained (Manasreh, unpublished data); the record was measured in a fixed coastal station about 300m a way from the study transect from surface down to 50m deep using a conductivity-temperature-depth sensor (OS200 CTD).

3.4.3. Isotopic composition of seawater

Water samples for stable isotope analysis were collected by SCUBA divers at monthly intervals (April 1999 to June 2000). 500 ml polyethylene bottles were filled with seawater next to each monitored colony. Immediately after sampling, 100 ml of the seawater were transferred into brown borosilicate glass bottles without further treatment. The bottles were sealed with

melted paraffin to avoid air contamination and were kept in a refrigerator at 4°C until measurements were carried out at Bremen University.

The measurements followed the classical procedure of equilibration of water with carbon dioxide of known $\delta^{18}O$ at 25°C (Epstein and Mayeda, 1953). The isotopic data were obtained on a Finnigan Delta mass spectrometer with a precision of 0.1‰. The data are given as the per mil deviation of the ^{18}O: ^{16}O ratio R of the sample relative to the VSMOW oxygen isotope standard (Craig, 1961; Hut, 1987)

$$\delta = ((R\ sample/R\ standard) - 1) * 10^3$$

3.4.4. Coral samples

On June 21 2000, four columns of *Porites spp.* colonies Aq7, Aq19, Aq29 and Aq42 were collected along the monitored depth transect from 7, 19, 29, and 42m deep respectively. Colonies were harvested by SCUBA diving by removal of a heady shape columns (5-10 cm in diameter) under water using hammer and chisel. After sampling, the corals were cleaned under high-pressure tap water to remove the residual organic matter and then dried under the sun.

The corals were sectioned longitudinally into slabs of 4mm thickness parallel to the axis of maximum growth. The slabs were cleaned and X-rayed using industrial X-ray machine (Model Eresco 160 SLG) and Agfa Strukturix D4-film. Black and white prints of the x-radiographs were used to choose suitable profiles of annual growth patterns.

In order to attain high-resolution we followed the procedure of Pätzold (1986). Samples for isotopic analysis were obtained by cutting small rods out of the skeleton slabs following the growth of a single corallite from the surface vertically down to 4cm. The rods were 2.5mm in diameter, and 4-5cm long containing minimum 4 years of growth, the sticks were rigid enough and there was no need to soak them in resin.

Using a precision lathe with a low speed grindstone the rods were milled down in steps that varied between colonies from 125μm to 500μm depending on the growth rate to produce a range of 26-52 samples/year (Table 3.1).

Table 3.1. Annual skeletal extension rate, and number of samples drilled per year for coral colonies in this study.

Coral sample	Extension rate (mm/yr)	Number of Samples/yr
Aq7	10	36
Aq19a	20	52
Aq19b	20	40
Aq29	5.4	42
Aq42	3.5	26

For stable oxygen isotopic analysis, the powdered carbonate samples (100-200μg) were reacted with 100% orthophosphoric acid at 75°C to produce carbon dioxide. The isotope measurements were performed using an automated carbonate preparation device attached to a Finnigan MAT 251 mass spectrometer. Results are given in the δ notation relative to the VPDB isotopic standard. The reproducibility (±σs) for $\delta^{18}O$ is better than ±0.07‰ based on replicate measurements of internal laboratory standard.

To construct an age model for the coral isotope chronologies, AnalySeries 1.1 software package (Paillard et al. 1996) was used to convert the distance units into time scale units using features in the coral $\delta^{18}O$ records which could clearly be matched with the same events in the weekly/biweekly instrumental temperature records (wiggle matching) and locking these at their corresponding dates (Alibert and McCulloch, 1997). The lowest $\delta^{18}O$ values of each annual cycle were tied to the highest temperature (August) values and the highest tied to the lowest temperature values (March). About six additional tie points per year were added by this way in addition to the date of coral collection. Time between these points was interpolated.

3.5. Results

3.5.1. Seawater temperature

Daily, weekly, biweekly and monthly average temperatures were calculated from the hourly-recorded measurements from the four depths (Table 3.2). All records show similar, well-organized and strong seasonal pattern which characterized by short spikes of ~1 °C on the daily temperature record (Figure 3.2). Mean annual temperature range based on daily average for the

year (1999-2000) was 7.13°C with a maximum temperature of 27.91°C, which falls in August and minimum of 20.78 °C in March.

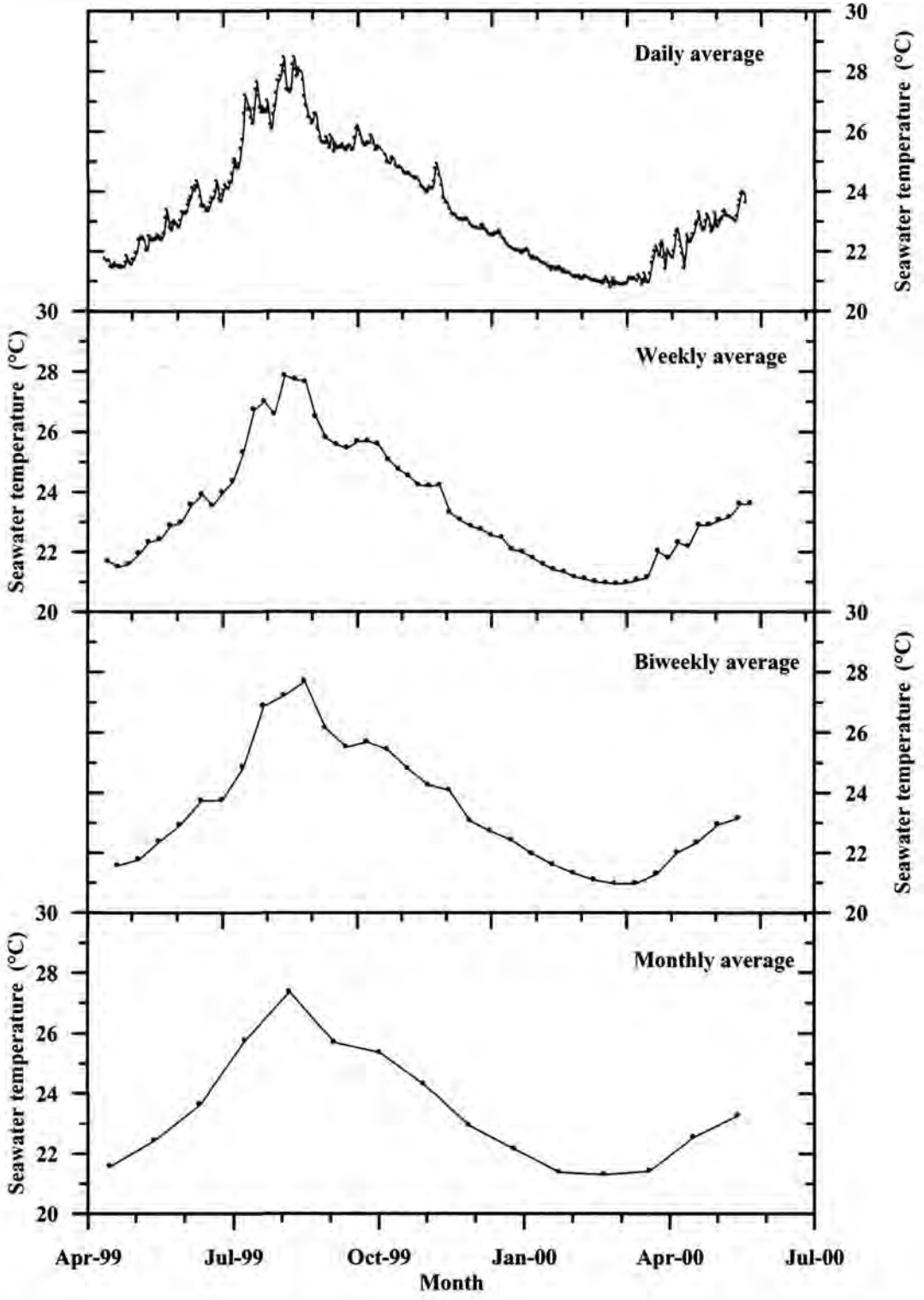

Figure 3.2. Time series of instrumental sea water temperature at 7m depth from the study sites, the averages are based on hourly temperature measurements using temperature loggers between April 1999-June 2000.

Table 3.2. Mean annual range of seawater temperatures calculated from hourly measurements along the depth transect between August 1999 and March 2000

Water Depth (m)	Daily (°C)	Weekly (°C)	Biweekly (°C)	Monthly (°C)
7	7.69	7.00	6.73	6.05
19	7.44	6.64	6.58	5.88
29	6.93	6.29	6.25	5.59
42	6.44	5.84	5.67	5.10
Average	7.13	6.44	6.31	5.66

3.5.2. Seawater salinity

Contrary to water temperature, salinity during the study period exhibits a weak seasonality and change with depth (Figure 3.3). Average salinity is close to 40.4‰ and shows variations less than 0.3‰ through the year. The average minimum salinities of 40.28‰ were recorded during winter (March 1999) and maximum salinities of 40.56‰ during summer (June 2000). Due to water stratification in summer, lower salinities were observed in deep waters (42m) between June and September (Figure 3.3).

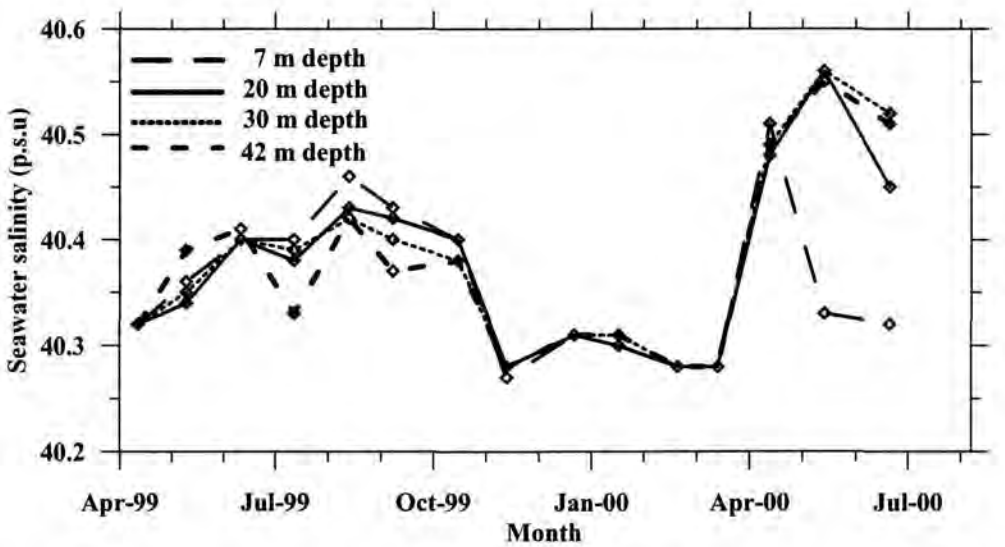

Figure 3.3. Seasonal variations of seawater salinity (p.s.u.) at four depths recorded in coastal waters from the northern Gulf of Aqaba between the period April 1999-June 2000.

3.5.3. Isotopic composition of seawater

Based on the monthly sampling over 14 month, the average $\delta^{18}O$ value of seawater at our sampling sites is about 1.86‰ relative to VSMOW (Vienna Standard Mean Ocean Water) reference standard, and the values range between 1.75-2.0‰ (Figure 3.4).

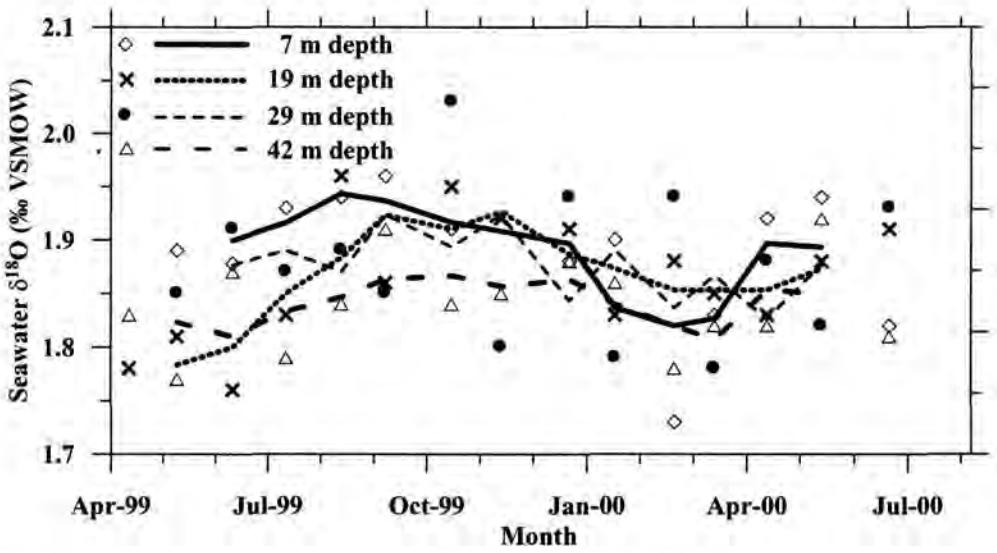

Figure 3.4. Seasonal variations in seawater $\delta^{18}O$‰ (relative to VSMOW) at the coral sites based on monthly sampling between April 1999-June 2000. The lines represent three points running averages.

A weak and instable seasonal pattern is observed, with minor variations between depths (Figure 3.4). Three points running averages were applied for the data to make the pattern clearer. The highest values were observed between July and September in shallower depths, while low values in deeper depths and during winter (Figure 3.4).

3.5.4. Skeletal $\delta^{18}O$ composition

All $\delta^{18}O$ profiles from the four coral skeletons recorded the same regular seasonal pattern and timing of small variations although they were sampled at different resolutions (Figure 3.5). These patterns are similar and matches closely the recorded temperature cycle. Short period (less than 2 weeks) and magnitude (0.2‰) temperature excursions or spikes were also recorded in all corals (Figure 3.5).

The average coral $\delta^{18}O$ composition ranges between –1.99 and –3.75‰ and averages are –3.16‰, -2.92‰, -3.00‰, and –2.72‰ for corals Aq7, Aq19, Aq29 and Aq42, respectively.

Seasonal amplitudes were determined from the seasonal cycle of $\delta^{18}O$ as the difference between minimum $\delta^{18}O$ value (in August 1999) and the maximum value (March 2000). The mean of all corals is 1.1‰, with averages for the individual colonies of 1.1‰, 1.2‰, 0.85‰ and 1.26‰ for corals Aq7, Aq19, Aq29 and Aq42, respectively.

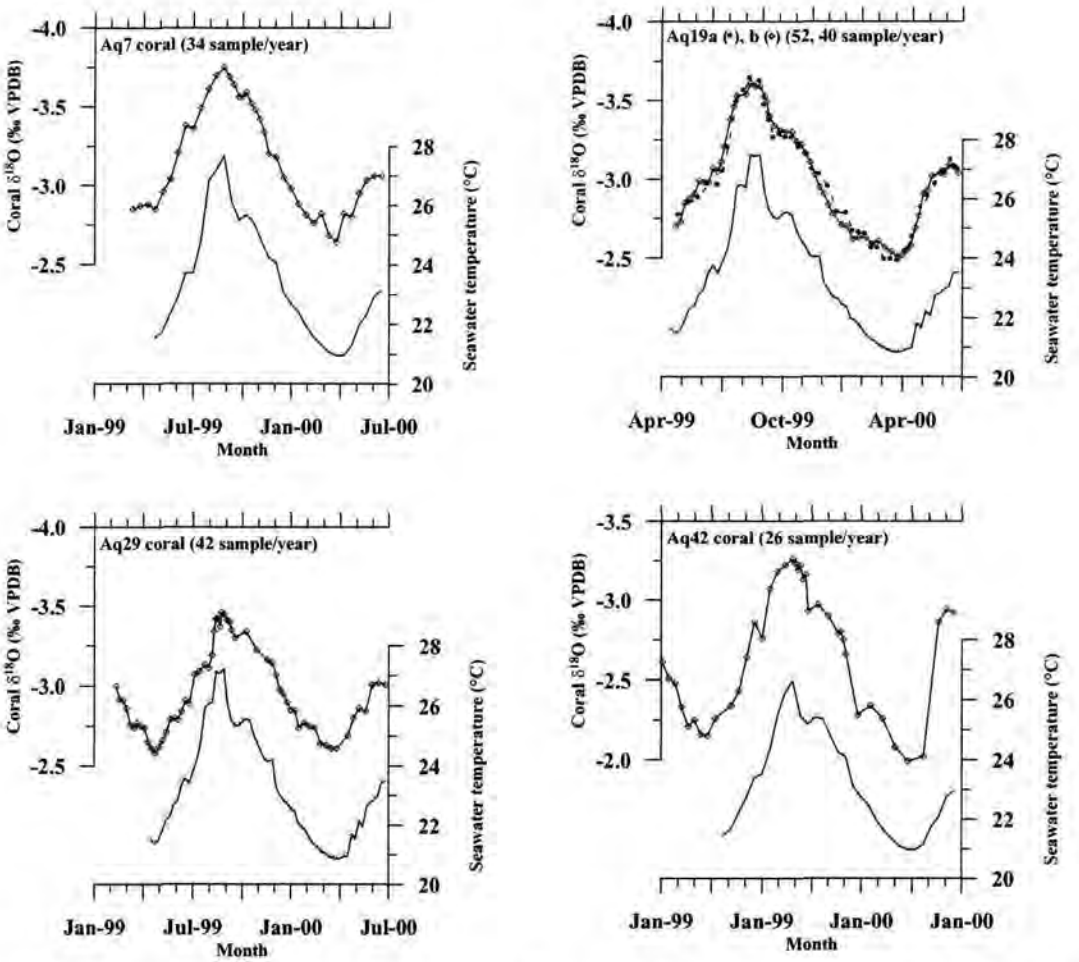

Figure 3.5. Time series of $\delta^{18}O$ profiles sampled at different resolutions form corals (Aq7, Aq19a, b, Aq29 and Aq42), and weekly/biweekly average temperature records taken along the depth transect from depths 7, 19, 29 and 42m.

Average annual extension rates were also measured as the distances from maximum $\delta^{18}O$ in 1999 to the maximum value in 2000. Corals from deep waters (Aq29, Aq42) showed lower mean annual extension rates, which ranged between 3.5 to 5.4 mm/year (Table 3.1), while extension rate ranged between 10 to 20 mm/year in shallow corals (Aq7, Aq19).

From the mean temperature 23.42°C and $\delta^{18}O$ seawater (1.59‰ VPDB which was converted from VSMOW using the correction of –0.27‰, Hut, 1987) at the four sites, the

theoretical $\delta^{18}O$ of the coral aragonite can be estimated (using the equation of Grossman and Ku, 1986). The values averaged 0.96‰, which indicate that our corals are depleted by about 3.91‰ from isotopic equilibrium.

3.6. Discussion

3.6.1. Seawater temperature

A thermal stratification of the water mass in the fore-reef in summer (between June and November) was observed from the temperature records. The shallow waters (7m) are about 1.2°C warmer than waters at deeper depths (42m) based on weekly data, in November the stratified layer began to disappear and mixing of the water column is prevailing till May (Figure 3.6).

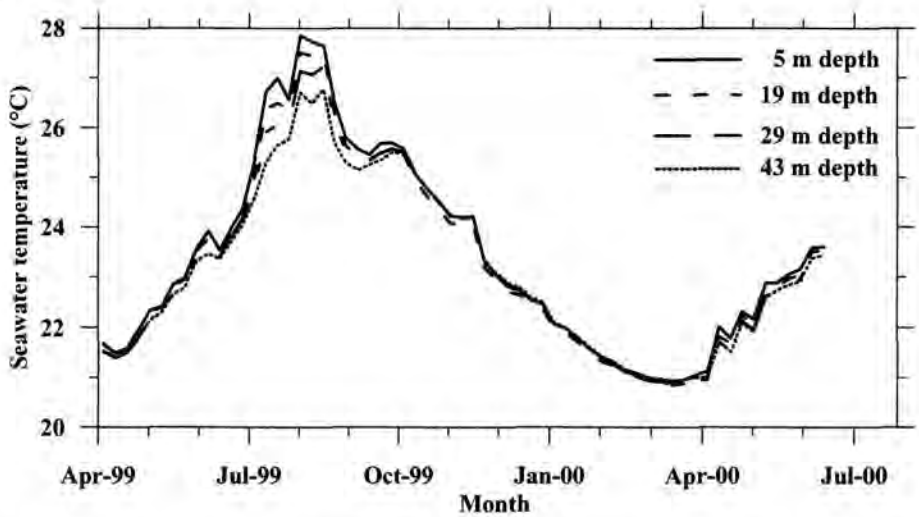

Figure 3.6. Weekly seawater temperature averages based on hourly measurements recorded along the depth transect from 7, 19, 29 and 42m deep, using temperature loggers over the period April 1999-June 2000.

3.6.2. Salinity and $\delta^{18}O$ of seawater

Salinity and $\delta^{18}O$ varied due to enrichment due to evaporation, depletion due to precipitation and runoff and mixing due to advection and diffusion (Delaygue et al., 2001). In the northern Gulf of Aqaba fresh water input due to precipitation and runoff is negligible; therefore the variation in salinity and $\delta^{18}O$ of seawater is the result of high evaporation (4m/yr, Reiss and Hottinger, 1984) and advection and diffusion of the water.

According to our monthly $\delta^{18}O$ of seawater and near biweekly salinity measurements, we found a positive correlation between salinity and $\delta^{18}O$ of seawater (Figure 3.7a). The relation can be expressed as follows:

$$\delta^{18}O_w = 0.281 * S\ (‰) - 9.14 \qquad (r=+0.60)$$

Where S is salinity (given in p.s.u) $\delta^{18}O_w$ is expressed relative to VSMOW.

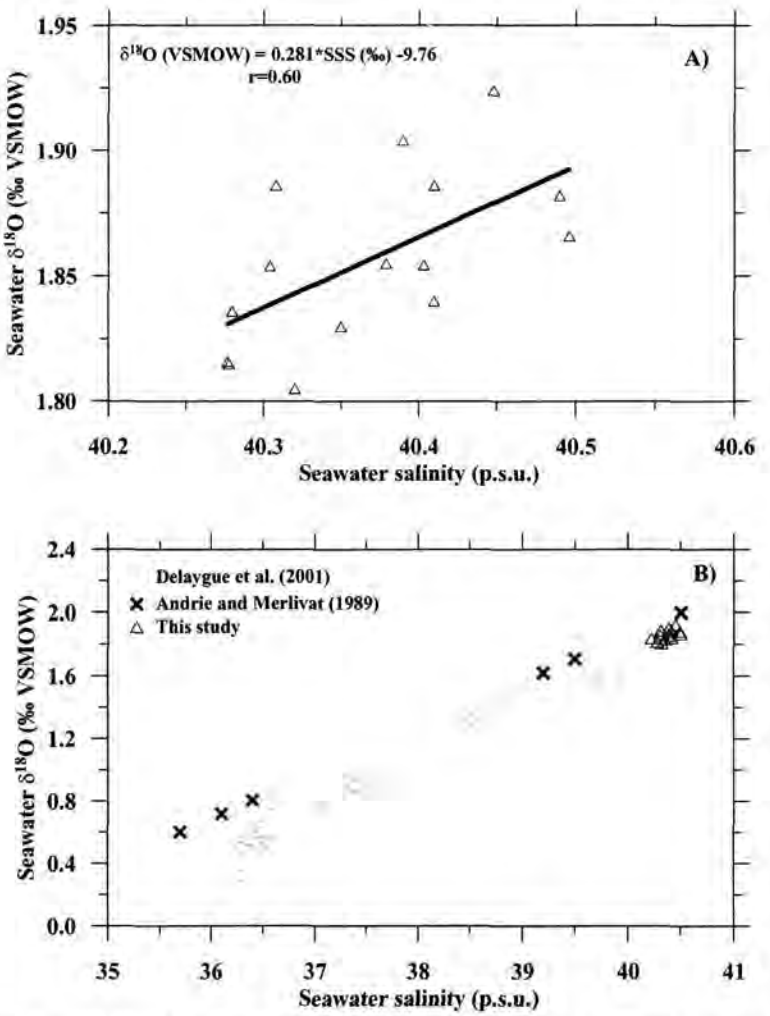

Figure 3.7. A) Linear regression of seawater $\delta^{18}O$‰ (relative to VSMOW) versus seawater salinity (p.s.u.) from the northern Gulf of Aqaba. B) Surface water $\delta^{18}O$‰/salinity regressions from the Red Sea, data from Delague et al. (2001) and Andrié and Merlivat (1989). Data from this study were also included for comparison.

The relation shows that the $\delta^{18}O$ of seawater is governed by salinity changes, and it compares with those previously reported by Craig (1966), Andrié and Merlivat (1989), Ganssen and Kroom (1991), and Delaygue et al. (2001) from the Red Sea. Some of the data are plotted in Figure 3.7b.

The relatively weak correlation (+0.60) in our results compared to those reported in the earlier studies, are explained by the narrow range of measured $\delta^{18}O$ and salinity. The salinity range in the northern Gulf of Aqaba is 40.28-40.56‰, while it ranges between 35.6 and 40.8‰ in the Red Sea proper.

Since our results of seawater $\delta^{18}O$ were scattered (Figure 3.4) and measurements were collected in a monthly resolution, weekly/biweekly values of the seawater $\delta^{18}O$ were derived based on the above equation and the biweekly salinity measurements in order to correspond to the coral $\delta^{18}O$ sampling resolution. For the calculations of the synthetic coral $\delta^{18}O$ in corals Aq19 and Aq29, the derived values of seawater $\delta^{18}O$ were interpolated to weekly resolution assuming that no significant changes in $\delta^{18}O$ of seawater will take place over one week time interval.

3.6.3. Synthetic coral $\delta^{18}O$

We have examined most of the paleotemperature equations in the literature to construct a synthetic coral $\delta^{18}O$. The equation derived from Galapagos *Porites* corals (McConnaughey, 1989) was selected, because the seasonal amplitudes calculated from this equation were closest to our measured seasonal amplitudes (differ on average by about 0.2‰) and most of the features in the synthetic and measured $\delta^{18}O$ were well matched (Figure 3.8). The relation was expressed as:

$$\delta_c - \delta_w = 0.594 - 0.209 * T$$

where δ_c: is the oxygen isotopic composition of coral skeleton in ‰ relative to VPDB, δ_w: oxygen isotopic composition of seawater in ‰ relative to VPDB, T: recorded sea water temperature in °C

Seawater temperature and $\delta^{18}O$ were averaged to the same resolution as they correspond to the coral $\delta^{18}O$ resolution. Biweekly values were used for corals Aq7 and Aq42, while for Aq19 and Aq29 weekly values were used. The predicted $\delta^{18}O$ records derived were compared with the measured values over the interval 1999-2000. Both records were in a good fit, as seen in the small excursions that appear in both records (Figure 3.8). These excursions are also present in the temperature record.

The seasonal amplitudes predicted from this equation were 1.41‰, 1.38‰, 1.34‰ and 1.19‰ for corals Aq7, Aq19, Aq29 and Aq42, respectively (Table 3.3). The measured seasonal amplitudes are lower by about 0.2‰ with the predicted values using McConnaughey equation.

Table 3.3. Measured and predicted coral $\delta^{18}O$ seasonal amplitude using the paleotemperature equation from McConnaughey (1989), and the equation obtained from this study

Coral sample	Measured seasonal amplitude (‰)	Predicted seasonal amplitude (‰) (McConnaughey 1989)	Predicted seasonal amplitude (‰) (This study)
Aq7	1.10	1.41	1.21
Aq19a	1.15	1.38	1.19
Aq19b	1.10	1.38	1.19
Aq29	0.85	1.34	1.15
Aq42	1.26	1.19	1.04
Average	1.10	1.33	1.15

Instrumental temperature records indicate that the seasonal amplitude at 42m is 1.2°C smaller compared with 7m depth. Accordingly, the predicted amplitude in coral $\delta^{18}O$ decreases by about 0.2‰ from 7 to 42m (Table 3.3). Unfortunately we are not able to detect this decrease in the seasonal amplitude in our corals $\delta^{18}O$.

Using the available data from our sites, we have calculated the relations between temperature and the isotopic difference between coral and seawater for each coral (Figure 3.9). The relations can be expressed as follows:

$T = -5.65 * (\delta_c - \delta_w) - 3.11 \quad r^2=0.95$ *for coral Aq7*

$T = -5.33 * (\delta_c - \delta_w) - 0.93 \quad r^2=0.93$ *for coral Aq19a*

$T = -5.24 * (\delta_c - \delta_w) - 0.14 \quad r^2=0.92$ *for coral Aq19b*

$T = -6.62 * (\delta_c - \delta_w) - 6.76 \quad r^2=0.94$ *for coral Aq29*

$T = -3.82 * (\delta_c - \delta_w) - 0.83 \quad r^2=0.83$ *for coral Aq42*

where δ_c is the oxygen isotopic composition of coral skeleton in ‰ relative to VPDB and δ_w is the oxygen isotopic composition of seawater in ‰ relative to VPDB, values of seawater $\delta^{18}O$ were converted to VPDB using the correction of –0.27‰ (Hut, 1987). T is the recorded seawater temperature.

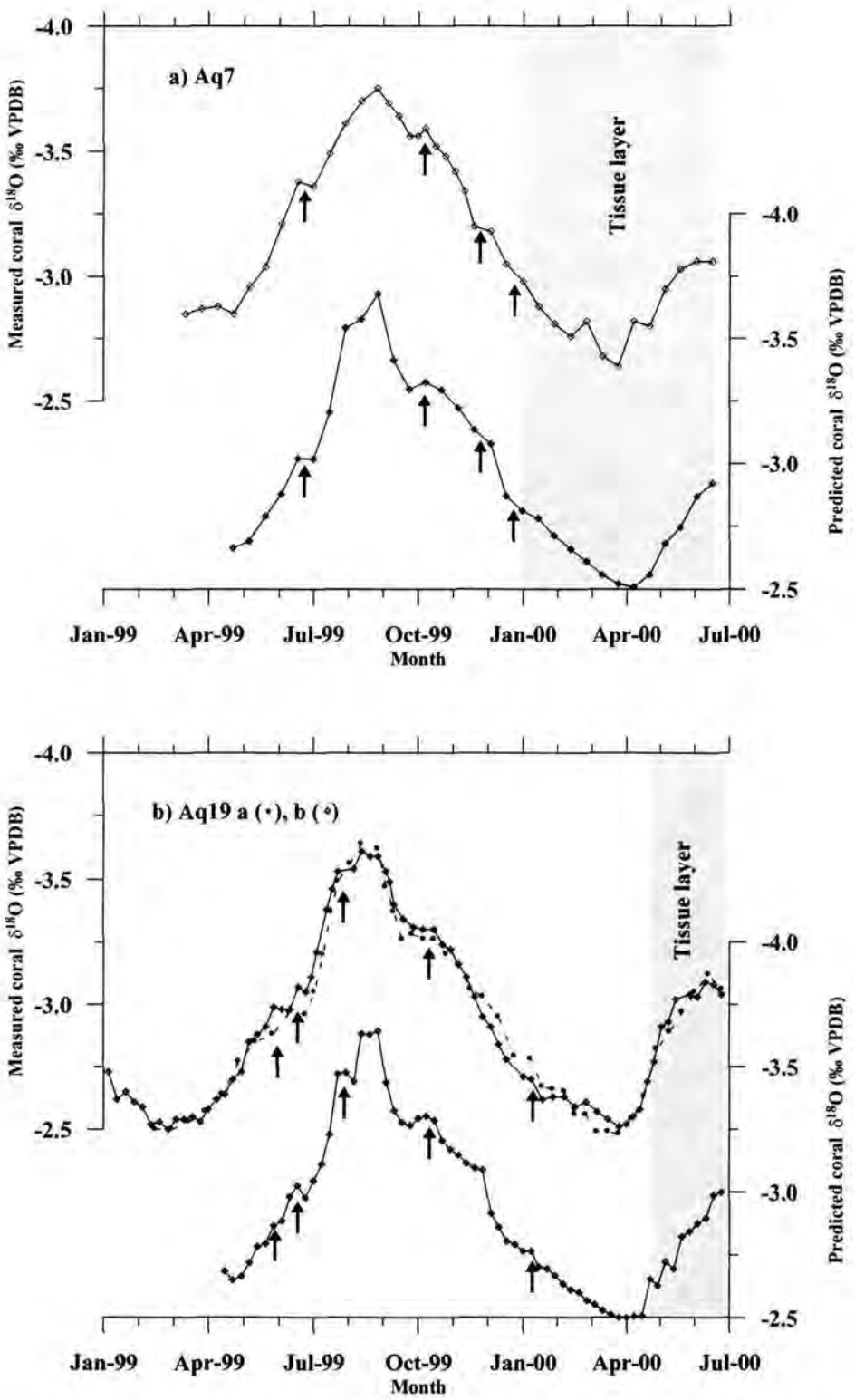

Figure 3.8. Comparison between measured and predicted coral $\delta^{18}O$ values for corals: a) Aq7, b) Aq19a, b, c) Aq29 and d) Aq42. The predicted values are based on continuous *in situ* sea temperature and $\delta^{18}O$ of seawater measurements between April 1999-June 2000 from the northern Gulf of Aqaba. The arrows indicate common peaks between both records, and the dotted bars indicate the parts occupied by tissue layer.

Continued figure 3.8

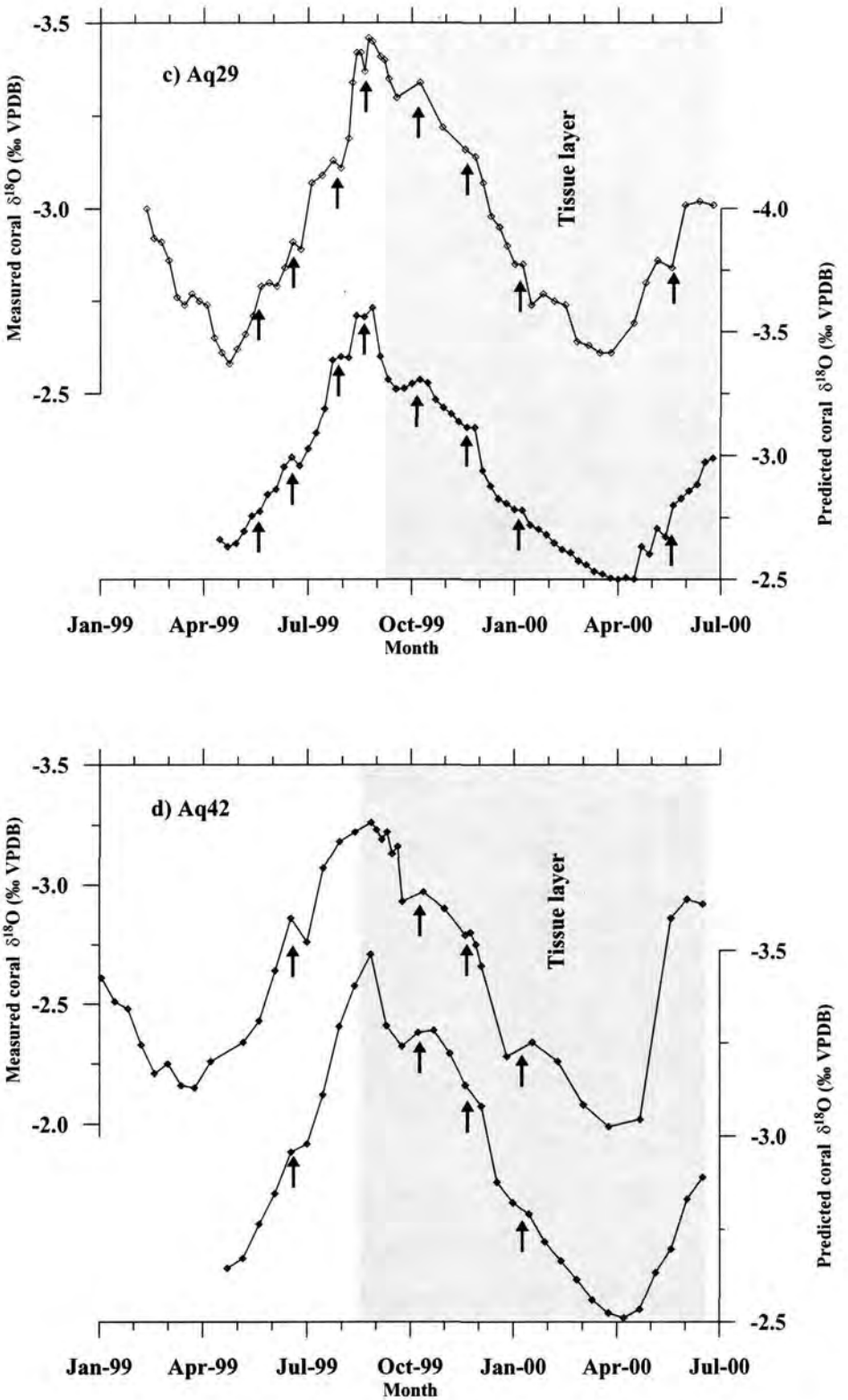

The slopes of the equations does not differ significantly from one another indicating the robustness of the relation; they change from 5.65°C/‰ to 5.33°C/‰ and 5.24°C/‰ to 6.62°C/‰ for corals Aq7, Aq19a, Aq19b, and Aq29 respectively. The difference of the slope in coral Aq42 (3.82°C/‰) was probably caused by the difference in $\delta^{18}O$ values in winter skeletal portion (Figure 3.9); this might be attributed to difference in seasonal extension rates (Morimoto et al., 1997; Suzuki et al., 1999) that will be discussed later. Therefore, we calculated an average temperature/$\delta^{18}O$ equation from all corals, but excluded coral Aq42 to calculate synthetic coral $\delta^{18}O$.

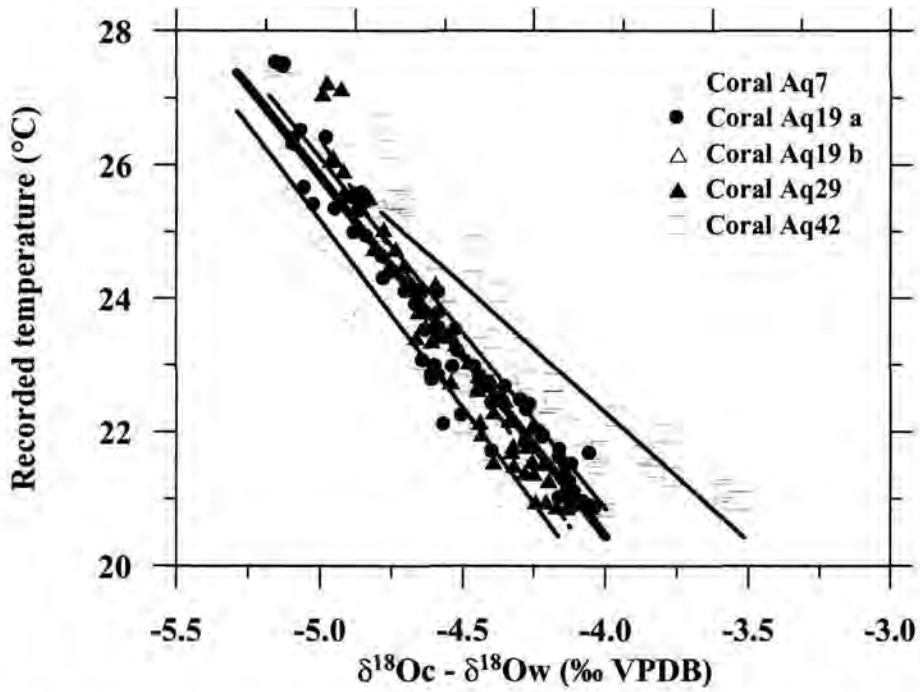

Figure 3.9. Relationship between $\delta^{18}O_c$ - $\delta^{18}O_w$ and recorded *in situ* temperatures for corals Aq7, Aq19a, b, Aq29 and Aq42. The overall obtained equation is represented by the thick line and it is as follows: $T = -5.38 * (\delta_c - \delta_w) - 1.08$ in which δ_c is the oxygen isotopic composition of coral skeleton in ‰ relative to VPDB, δ_w is the oxygen isotopic composition of seawater in ‰ relative to VSMOW and T is the recorded seawater temperature.

The slope of the equation was 5.38°C/‰ (0.186‰/°C) which is less than the widely recognized value of 0.22‰/°C (Epstein et al., 1953; Grossman and Ku, 1986), but similar to that determined by Gagan et al. (1994) for *Porites* corals from the Great Barrier Reef and Qunn et al. (1996) from New Caledonia corals.

3.6.4. Corals seasonal amplitude

By using our equation we are able to predict the seasonal coral $\delta^{18}O$ amplitudes (Table 3.3) for the shallow corals, which is close to the measured ones. However the equation fails to capture the measured seasonal amplitude in deeper corals (Aq29 and Aq42) although the predicted and measured curves were well matched (Figure 3.8).

The expected seasonal amplitude calculated from temperature and seawater $\delta^{18}O$ variation at 29m depth is 1.15‰, which is considerably larger (0.3‰) than the measured value of 0.85‰, this difference is equivalent to a difference in temperature of 1.6°C. This attenuation of the seasonal amplitude cannot be explained by temperature which decreases in summer by about 0.7°C from 7 and 29m (equal 0.13‰), and also seawater $\delta^{18}O$ variations can be neglected. Barnes et al. (1995) explains this reduction in amplitude as a result of smoothing of environmental signals due to spine thickening and this was not the case in our corals, as we will explain later. Rather, we suggest that the attenuation is due to variations of the skeletal extension rate during the year.

Many studies have considered a constant coral extension rate during the year. However, skeletal coral $\delta^{18}O$ may be influenced by the seasonal variations in extension rate (Wellington et al., 1996; Alibert and McCulloch, 1997; Barnes et al., 1995).

Comparing the predicted and measured records from this coral (Aq29), it is obvious that the maximum $\delta^{18}O$ values (winter values) fit together, while the measured values show more positive minima of $\delta^{18}O$ values (summer values) compared to the predicted ones. Based on our age model we have reconstructed the seasonal variations in coral extension rates. The results for Aq29 coral show a sharp decrease or slow down in extension rate from July-September at/or near the annual minima (Figure 3.10), which may gives more positive oxygen isotope composition during summer according to the inverse relationship between extension rate and coral $\delta^{18}O$ (Land et al., 1975; Allison et al., 1996), or this portion of temperature record are underrepresented, or the individual sampling may include material deposited over a greater time period than is indicated by the sampling resolution and then attenuated the seasonal amplitude as suggested by Leder et al. (1996) and Morimoto et al. (1997).

On the other hand amplified or expanded seasonal amplitude in coral Aq42 was observed (Table 3.2). This amplification is due to the more positive coral $\delta^{18}O$ values recorded during winter 2000 compared to other profiles (Figure 3.10) as seen also from the regression line

equation in (Figure 3.9). This was not a result of environmental factors (temperature and/or $\delta^{18}O$ seawater, compared with instrumental records), or the effect of sampling resolution, and may result from the subannual variations in extension rate.

This coral (Figure 3.10) shows a reduction in extension rate during winter, which causes these positive values and therefore increased the seasonal amplitude. The same situation was also reported by Klein et al. (1996) and Alibert and McCulloch (1997) from corals and bivalves.

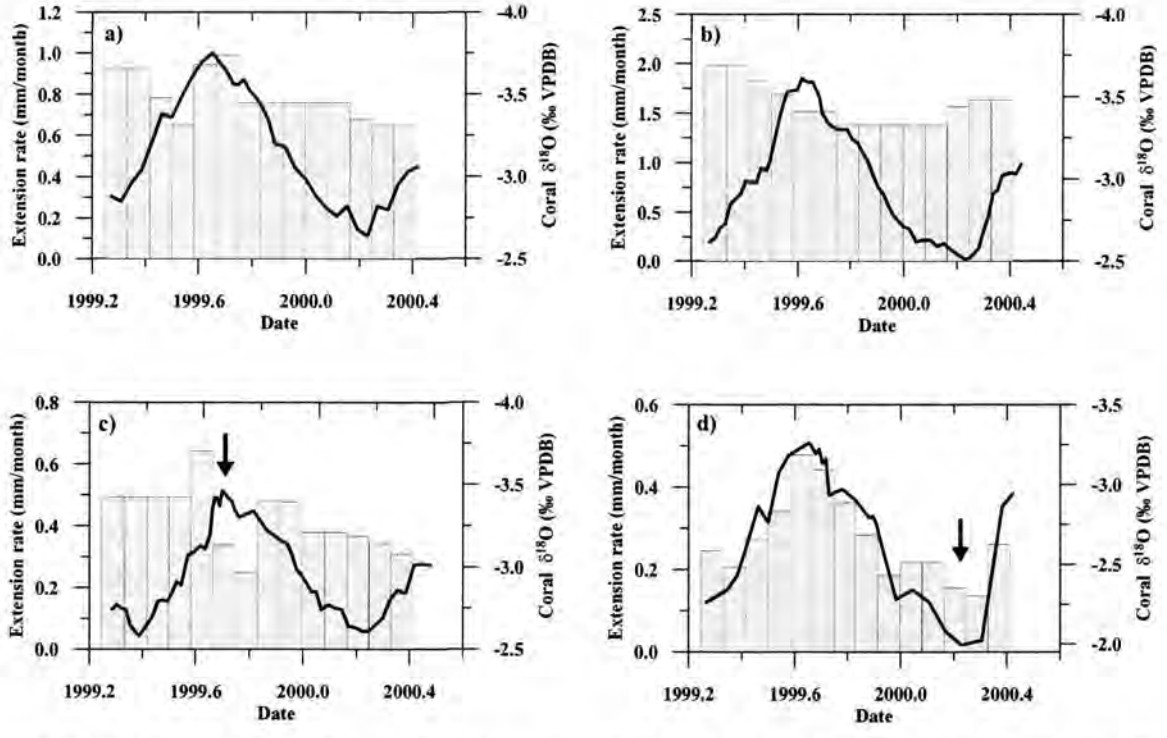

Figure 3.10. Monthly variations of growth rates in mm/month (dotted bars), and $\delta^{18}O$ record for corals: a) Aq7, b) Aq19, c) Aq29 and d) Aq42 between April1999-June 2000. The arrows indicate periods of relatively slow growth rates, which affected the measured $\delta^{18}O$ seasonal amplitudes. Values of growth rates were calculated based on the age model outlined in the method section.

Results from this study agree with those reported by Leder et al. (1996), who found that it would be impossible to record the true annual $\delta^{18}O$ maxima and minima in slower growing corals or if coral extension rate is not constant or interrupted during the year. deVilliers et al. (1995) also show a strong dependency of the skeletal chemistry on extension rate in corals from deeper depths

In the following we use the relation between temperature and coral $\delta^{18}O$ from our corals (0.18‰/°C). The average seasonal amplitude of the corals (1.10‰) is equivalent to about 6.1°C change in temperature, which is about 95% of the actually observed weekly temperature variations. The seasonal variations in seawater $\delta^{18}O$ have minor impact on coral $\delta^{18}O$ and are neglected.

The weekly sampling resolution (Aq19a) could explain 96% of the weekly temperature variations, and nearly the full range of the biweekly and monthly temperature variations. Whereas biweekly resolution (Aq7) captured 87% of the weekly temperature variations, 91% of the biweekly temperature variations and the full range of the monthly temperature variations (Table 3.4).

Table 3.4. Percent of seawater temperature variations explained by coral $\delta^{18}O$ during the period August 1999 and March 2000 from the northern Gulf of Aqaba corals

Coral Sample	Samples/year	Explained T (°C)	Weekly (%)	Biweekly (%)	Monthly (%)
Aq7	36	6.1	87	91	100
Aq19a	52	6.4	96	97	>100
Aq19b	40	6.1	91	93	>100
Aq29	42	4.7	75	75	84
Aq42	26	7.0	>100	>100	>100

These results are similar to those obtained by Leder et al. (1996) who found that weekly resolution is necessary to capture the weekly temperature range, and that biweekly resolution still accounts for more than 80% of the weekly variation. Comparing the seasonal amplitudes between corals Aq7 and Aq19a, Aq19b it seems that there is no attenuation of the isotopic signals observed between weekly and biweekly sampling resolutions.

3.6.5. The effect of tissue layer

Previous studies (Barnes and Laugh, 1992; Barnes et al., 1995; Taylor et al., 1995) suggested that coral $\delta^{18}O$ signals are subject to smoothing and distortion as a result from calcification throughout the thickness of the coral tissue layer, which may affect the geochemical record of both sudden pulse events and annual climate cycles.

The tissue layer of our corals were about 4, 4, 3.8 and 3 mm thick, equivalent to a growth period of 4.8, 2.4, 9.1 and 9.6 months for corals Aq7, Aq19, Aq29 and Aq42, respectively (Figure 3.8). Although the measured transects were partly within the tissue layer, $\delta^{18}O$ from samples within this tissue layer match closely the recorded temperature cycle, and the temperature excursions were precisely preserved in coral $\delta^{18}O$ (Figure 3.5).

The annual weekly temperature variations preserved in the $\delta^{18}O$ of corals Aq7 and Aq19a, b are in excellent agreement with the predicted values (Table 3.3). The reduced and expanded seasonal amplitude of Aq29 and Aq42 coral $\delta^{18}O$ are due to variable interannual coral extension.

All these provide evidences against Barnes' model and allow us to conclude that our corals accurately record changes in their ambient seawater, and the effect of tissue layer is minimal and negligible as found by Gagan et al. (1994), Wellington et al. (1996) and Alibert and McCulloch (1997).

3.7. Conclusions

High sampling resolution from this study confirms the ability of Red Sea corals to accurately preserve short period and magnitude temperature variations. Weekly/biweekly sampling resolution of coral $\delta^{18}O$ was able to resolve more than 95% of the weekly/biweekly temperature variations.

In contrast to instrumental temperature records, which show strong seasonal variations (7°C) and change with depth, seawater $\delta^{18}O$ exhibits a weak seasonal pattern with variations less than 0.25‰ (VSMOW). Positive correlations between seawater $\delta^{18}O$ and salinity were also obtained, and despite the data represent a limited area from the Red Sea with narrow ranges in salinity and seawater $\delta^{18}O$ variations, it shows a relation similar to that reported from the Red Sea proper, and can be expressed by the equation:

$$\delta^{18}O_{Seawater\ (VSMOW)} = 0.281 * SSS\ (‰) - 9.14$$

Coral $\delta^{18}O$ from the four colonies were calibrated against *in situ* measurements of temperature and seawater $\delta^{18}O$, all corals show similar $\delta^{18}O$/SST slopes and the equation was expressed as:

$$T = -5.38 * (\delta_c - \delta_w) - 1.08$$

where δ_c is the oxygen isotopic composition of coral skeleton in ‰ relative to VPDB, δ_w is the oxygen isotopic composition of seawater in ‰ relative to VSMOW and T is the recorded seawater temperature.

The attenuation and amplification of the measured coral seasonal amplitudes in deep and slow growing corals were due to seasonal variations in extension rate and not a result of environmental factors, different sampling resolutions or secondary thickening of skeletal elements within the tissue layer. No evidence of smoothing or distortions of the isotopic signals within the tissue layer as suggested by earlier studies were present in our corals.

In conclusion our results demonstrate that Red Sea *Porites* corals are real recorders of their environment, and the coral $\delta^{18}O$ reflecting temperature variations and seawater $\delta^{18}O$ seems to have negligible effect.

3.8. Acknowledgments

This study was carried out as part of the first author's PhD thesis at Bremen University. We are grateful to the Marine Science Station divers staff in Aqaba for their assistant with fieldwork and water samples collection. Special thanks are also due to R. Manasreh for providing salinity records from Aqaba. T. Felis and H. Kuhnert are deeply thanked for their constructive comments on the manuscript. All isotopic measurements were carried out at Bremen University. We are grateful to M. Segl for stable isotope analysis. This work is part of the Red Sea Program (RSP II), funded by the German Federal Ministry of Education, Science, Research, and Technology (BMBF).

CHAPTER FOUR

4. Invasion of anthropogenic CO_2 recorded in planktonic foraminifera from the northern Gulf of Aqaba

(To be submitted to "Earth and Planetary Science Letters ")

Saber Al-Rousan [1, 2,*], Jürgen Pätzold [1], Salim Al-Moghrabi [2] and Gerold Wefer [1]

[1] Fachbereich Geowissenschaften, Universität Bremen, D-28359 Bremen, Germany

[2] Marine Science Station, P.O. Box 195, Aqaba, Jordan

* email: alrousan@uni-bremen.de

4.1. Abstract

The stable carbon isotopic composition of the planktonic foraminifera (*Globigerinoides sacculifer*) and sedimentary organic matter from the northern Gulf of Aqaba have been investigated to estimate changes in $\delta^{13}C_{DIC}$ in surface waters during the last 1000 years. The high sedimentation rates at the core sites (about 50cm/kyr) provide high temporal resolution (10 years). Recent sediments in the uppermost top of the cores reflect present day conditions.

The $\delta^{13}C$ record of the planktonic foraminifera from three multicores display similar trends, showing a uniform and consistent $\delta^{13}C$ pattern before the 1750s, and a gradual decrease of approximately 0.63‰ over the last two centuries. This decrease seems to track the decrease of $\delta^{13}C_{DIC}$ in surface waters, which is mainly caused by the increase of anthropogenic input of ^{13}C-depleted CO_2 into the atmosphere. Similarly, a trend toward lighter values of the carbon isotopic composition of sedimentary organic matter ($\delta^{13}C_{org}$) during the last 200 years support the interpretation obtained from the planktonic foraminifera $\delta^{13}C$.

Furthermore, direct measurements of seawater show that $\delta^{13}C$ of the dissolved inorganic carbon (DIC) at the northern Gulf of Aqaba has decreased by about 0.44‰ during the period 1979-2000. The average annual decrease is 0.021‰ which is similar to that recorded in the Pacific Ocean.

The $\delta^{13}C$ values of planktonic foraminifera combined with organic matter $\delta^{13}C$ from marine sediments allow good indicators to reconstruct past changes in atmospheric CO_2 concentrations from the northern Gulf of Aqaba.

4.2. Introduction

Over the past 100,000 year, the CO_2 concentration varied naturally by less than 80 ppm as indicated by ice cores records (Barnola et al., 1987). In the last 1000 years, before the industrial revolution the concentration was relatively stable, fluctuated by about ±10 ppm around 280 ppm (Friedli et al., 1986; IPCC, 1996). During the industrial period, the increased use of fossil fuel and deforestation lead to raise this concentration to more than 369 ppm in 2000 (Keeling and Whorf, 2001).

Since anthropogenic CO_2 has a highly negative carbon isotope composition, the $\delta^{13}C$ of the atmosphere has decreased in the last two centuries by about 1.14‰ deduced from the air

bubbles trapped in ice cores (e.g. Friedli et al., 1986; Francey et al., 1999). Records of the carbon isotopic signals from tree rings showed a decline of approximately 1-2‰ from the beginning of the industrial revolution to the present (Leavitt, 1994; February and Stock, 1999; Feng, 1999).

This decrease is imprinted on the $\delta^{13}C$ of the dissolved inorganic carbon ($\delta^{13}C_{DIC}$) in the ocean, although it may have been modified locally by the degree of isotopic equilibration with the atmosphere and the extent of dilution with deeper waters. The rate of oceanic CO_2 uptake has been determined for the last 25 years from direct measurement of the $\delta^{13}C_{DIC}$ (Keeling et al., 1989; Quay et al., 1992; Bacastow et al., 1996). Long-term variations in seawater $\delta^{13}C_{DIC}$ have been estimated from shallow-dwelling corals and sponges to be in the range of 0.5 to 0.9‰ since the start of the industrial revolution. Nozaki et al. (1978) found a reduction in $\delta^{13}C$ of 0.5‰ over the past 200 years in a banded coral from Bermuda. Similarly a 0.5‰ decrease were observed in sclerosponge $\delta^{13}C$ record from Jamaica (Druffel and Benavides, 1986) between 1820 and 1972. Böhm et al. (1996) deduced a 0.7 and 0.9‰ declines in $\delta^{13}C$ from Caribbean and Coral Sea demosponges. Differences between the carbon isotope compositions of surface dwelling planktonic foraminifera from the water column and from sediment core tops were also used to determine the $\delta^{13}C$ decrease caused by the addition of anthropogenic CO_2 to the ocean. Beveridge and Shackleton (1994) estimated the change in the Eastern Atlantic surface waters of about 0.5-0.6‰ during the last two centuries, while Bauch et al. (2000) found this effect to be about 0.9‰ within the Arctic Ocean and about 0.6‰ in the Atlantic derived waters of the southern Nansen Basin.

An alternative approach to reconstruct surface water CO_2 variability is the analysis of carbon isotopes of organic matter. Significant correlations have been established between the stable isotopic composition of particulate organic matter ($\delta^{13}C_{org}$) and the concentration of dissolved molecular CO_2 in surface ocean which may allow for the reconstruction of past seawater $\delta^{13}C_{DIC}$ from the sediment record (e.g. Rau et al., 1989; Popp et al., 1989; Freeman and Hayes, 1992; Francois et al., 1993; Rau, 1994).

In the present study, three multicores have been investigated to study the variations in the stable carbon isotope composition of seawater as recorded by the planktonic foraminifera *G. sacculifer* in the northern Gulf of Aqaba during the last 1000 years. Sedimentation rates in the area are high (40-65 cm/kyr) providing a temporal sampling resolution of about 10 years. Comparison of $\delta^{13}C$ data of the *G. sacculifer* and sedimentary organic matter from the core top

samples (younger than 1950 A.D.) and the underlying sediments older than 200 years, yield information on the invasion of anthropogenic CO_2 into the surface water during the industrial revolution. Results from this study were also compared to other data deduced from other proxies.

4.3. Study area

The Gulf of Aqaba is the eastern segment of the V-shaped northern extension of the Red Sea and is located in the subtropical arid belt between 28°–29°30' North and 34°30'– 35° East (Figure 4.1). It extends over a length of 170 km and a width of 14-26 km, and reaches almost 1800 m depth. The Gulf is considered as a partially enclosed water body, connected with the Red Sea proper through the Straits of Tiran, which have a maximum depth of about 250 m.

The Gulf of Aqaba is situated between the Sinai desert and the western Arabian Desert. The area is extremely arid with high evaporation (400 cm/year) and negligible precipitation (2.2 cm/year) and runoff. Mean sea surface temperature in the Gulf is 23.5°C, while the salinity is relatively high and ranges between 40-40.5‰ (Manasreh, 1998).

Surface circulation in the northern Gulf is primarily driven by prevailing northerly winds and the inflow from the Red Sea, which compensate for the evaporative loss of water (Reiss and Hottinger, 1984). The surface inflow water becomes cooler and more saline, hence denser. Towards the northern end of the Gulf, these dense water masses sink and return flow developed above sill depth. The resulting outflow forms part of the deep saline water in the northern Red Sea (Cember, 1988).

The carbonate chemistry system within the Gulf is influenced by CO_2 penetrating from the atmosphere to the seawater, by chemical process in the water column, and by the water body formation mechanism. There is almost no input from land derived DIC due to the fact that the Gulf has no water input from the surrounding land (Krumgalz et al., 1990).

4.4. Material and Methods

Sediment samples were collected in 1999 during the METEOR cruises M44/3 in the Gulf of Aqaba and the Red Sea (Pätzold et al., 2000). In this study we focus on three multicores, sampled at different water depths (Table 4.1) from the northern end of the Gulf of Aqaba (Figure 4.1).

Table 4.1. Positions and water depths of the analysed sediment cores from the northern end of the Gulf of Aqaba.

GeoB Number	Latitude N	Longitude E	Water Depth (m)	Sediment recovery (cm)
GeoB 5801-3	29°24.90′	34°54.70′	826	40
GeoB 5807-2	29°28.81′	34°56.78′	646	39
GeoB 5810-3	29°30.21′	34°57.73′	441	35

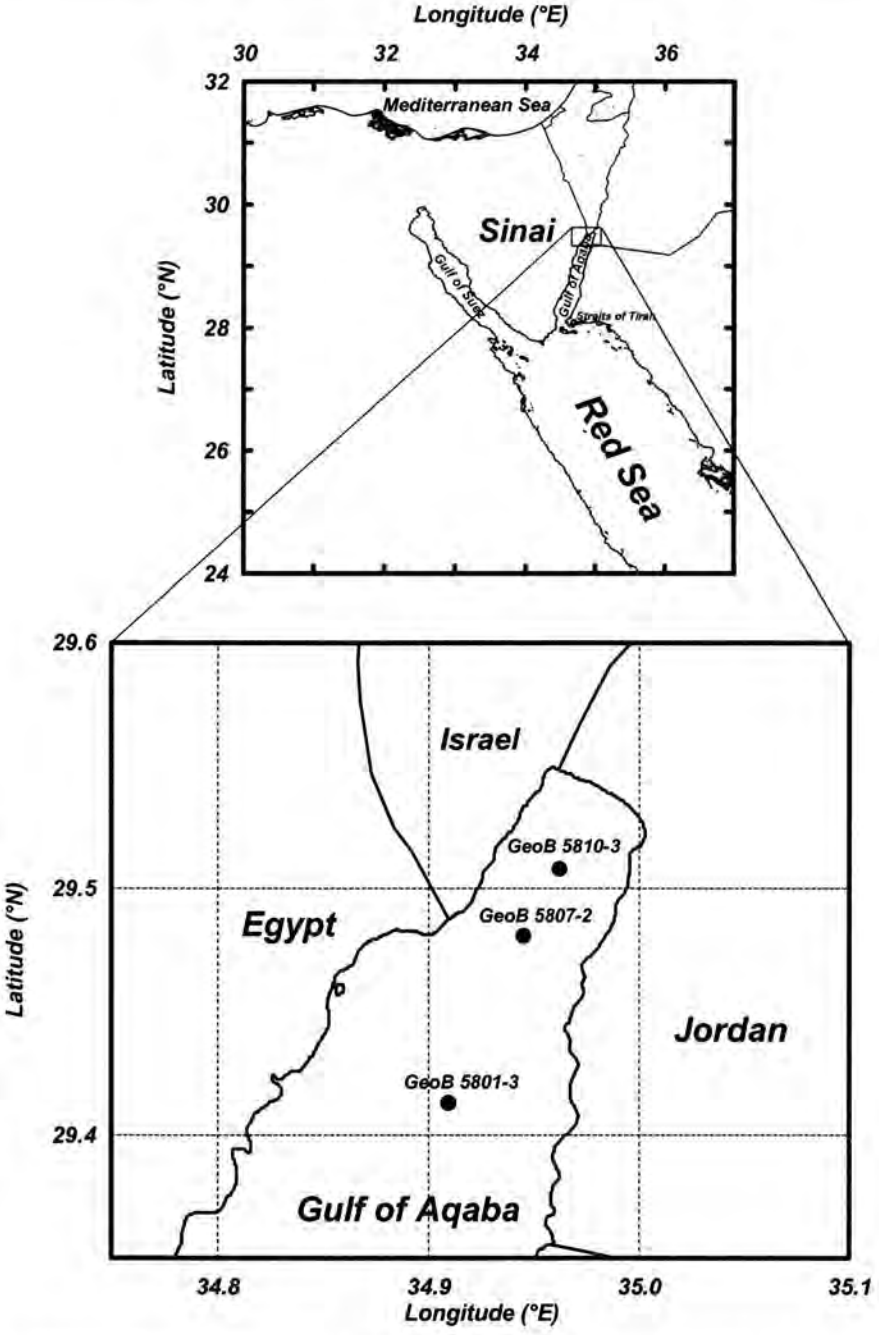

Figure 4.1. Map of the northern Gulf of Aqaba, Red Sea, showing the location of the multicores (GeoB 5810-3, GeoB 5807-2 and GeoB 5801-3) used in this study.

Sub-samples for faunal analysis were taken at 0.5 cm intervals from each multicore.Sediments were wet sieved with sieves of 63 and 150μm mesh size and dried in an oven at 55°C. From the 150μm fraction 12-18 specimens of the planktonic foraminifera *Globigerinoides sacculifer* (without final chamber) and *Globigerinoides ruber* (white) of 350 to 400 μm diameter (maximum extension) were used for stable isotope measurements. Analyses were carried out on a Finnigan MAT 251 mass spectrometer equipped with an automated carbonate preparation device. Precision based on replicates of an internal limestone standard, was better than 0.05‰ for $\delta^{13}C$.

4.4.1. Radiocarbon dating and age model

About 700 to 1000 specimens of the *Globigerinoides sacculifer* and *Globigerinoides ruber* (250-500μm) were hand picked for ^{14}C AMS dating. While carbonate hydrolysis and CO_2 reduction were performed in Bremen, Germany, AMS measurements were carried out at the Leibniz-Laboratory of the Kiel University, Germany.

Simple age models were established for the three multicores, by using the AMS ^{14}C dating form the top, intermediate and bottom parts of the sediments cores. Ages were then interpolated for each sample by assuming uniform sedimentation rates between the ^{14}C dating points (Figure 4.2).

4.4.2. Organic carbon, total nitrogen and carbonate analysis

Sediment samples (sampling step 1 cm) were freeze-dried and ground for the determination of total carbon (C_{tot}) and nitrogen (N_{tot}), and total organic carbon (C_{org}) contents. Values were obtained by combustion at 1050°C using a Heraeus CHN-O-rapid elemental analyser (Müller et al., 1994). For the determination of organic carbon, 25 mg aliquots of the dried sediments were weighted in a silver foil crucibles, wetted with a few drops of ethanol to suppress foaming during acidification, decalcified by drop wise addition of 6 N HCL, and dried on a hot plate at about 80°C. Total carbon and nitrogen were determined on untreated sample aliquots (25 mg) using tin crucibles for weighting. The carbonate content of the samples was calculated from the difference between total and organic carbon and expressed as calcite [$CaCO_3 = 8.33 * (C_{tot} - C_{org})$]. All analyses were performed in duplicate and expressed in weight percent dry, salt-free sediment assuming a pore-water salinity of 40‰. The relative precision of the measurements,

based on duplicates and control analyses of lab-internal reference sediment sample (WS1), was better than 3%.

4.4.3. Organic matter $\delta^{13}C$

One multicore (GeoB 5810-3) was selected for the determination of stable carbon isotope composition of the sedimentary organic matter in 1 cm spatial resolution. The $\delta^{13}C_{org}$ of the sediment was measured with a Finnigan Delta E mass spectrometer. After decalcification with 6 N HCl in silver crucibles and drying on a hot plate at 60°C, the samples were combusted at 1050°C in a stream of oxygen to CO_2 using a commercial Heraeus CHN analyser which is attached to the mass spectrometer. $\delta^{13}C$ values are reported against the VPDB standard. Reproducibility for $\delta^{13}C_{org}$ measurements based on internal standards was better than 0.15‰.

4.4.4. Seawater $\delta^{13}C$ measurements

Direct measurements of the $\delta^{13}C$ of the DIC at the northern Gulf of Aqaba have been obtained during the year 1999/2000. Water samples were collected in a borosilicate glass bottles on a monthly resolution from surface down to 40 m depth. The samples were carefully poisoned with 1 ml of saturated $HgCl_2$ solution. Dissolved inorganic carbon (DIC) was extracted as CO_2 gas from the water samples by aciditification with phosphoric acid (Kroopink, 1974). The $\delta^{13}C$ data were obtained on a Finnigan Delta mass spectrometer with a precision of 0.16‰ at the Geoscience Department, Bremen University. Data were related to the VPDB carbonate isotope standard.

4.5. Results

4.5.1. Sedimentation rates

The multicores extend back almost 1000 years A.D. (Table 4.2). The age model from these multicores yield sedimentation rates of between 40 and 65 cm/kyr (Figure 4.2), which is fairly high compared to other areas in the world. Therefore the sample spacing of 0.5 cm corresponds to a temporal resolution of about 10 years on average.

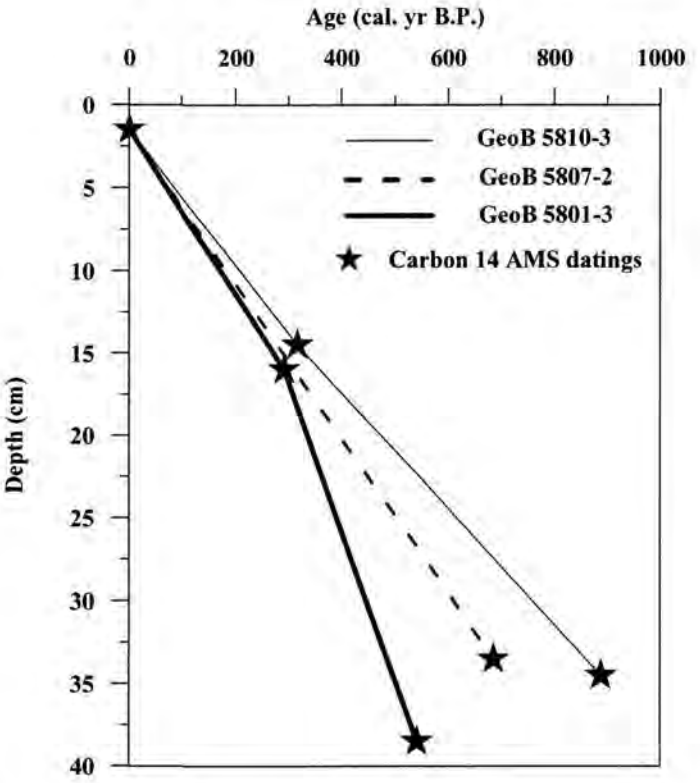

Figure 4.2. Age-depth relation of the investigated multicores from the northern Gulf of Aqaba, Stars represent the calibrated ^{14}C AMS datings positions.

Radiocarbon ^{14}C AMS dating reveal negative values from the uppermost part of the cores (Table 4.2). This means that they were formed with high initial ^{14}C levels, due to the atomic bomb testing and are younger than 1950 A.D. (Stuiver et al., 1998a; 1998b). They are considered to be representative with respect to modern plankton $\delta^{13}C$. This also ensures that our records were undisturbed, and bioturbation of the sediment is so low as core tops have this modern ^{14}C values (see also Bond et al., 2001).

Table 4.2. ^{14}C ages in the three multicores; the ages were calibrated and transformed into calendar years A.D. Samples with negative radiocarbon ages (formed since mid 1950) cannot be calibrated due to nuclear ^{14}C bomb (Stuiver and Braziunas 1993; Stuiver et al., 1998a and 1998b).

GeoB. No.	Lab. Iden.	Core depth (cm)	AMS ^{14}C age (yr BP)	Error ± (yr)	Calibrated age (cal. yr A.D.)
5801-3	KIA 11058	1.5	125	±45	-----
=	KIA 12075	16	760	±30	1658
=	KIA 11059	40	1060	±40	1409
5807-2	KIA 11060	1.5	-170	±30	-----
=	KIA 11063	39	1255	±35	1264
5810-3	KIA 11064	1.5	-145	±35	-----
=	KIA 12378	14.5	800	±35	1633
=	KIA 11064	35	1420	±40	1062

4.5.2. Carbon isotope data of planktonic foraminifera

Figure 4.3 shows the $\delta^{13}C$ record of the planktonic foraminifera *Globigerinoides sacculifer* from the three multicores. The records display similar trends. The values before the 1750s have a fairly uniform $\delta^{13}C$ pattern, ranging between 1.28 to 1.35‰ with an average of 1.31‰. An initially slow decline begins in the middle 1700s, from ca. 1.31‰ in the part older than 1750 A.D. to about 0.68‰ near the top of the cores. According to the ^{14}C AMS dating, $\delta^{13}C$ values from the upper most of the cores should reflect a mean value of present day conditions (younger than 1950). The $\delta^{13}C$ values range from 0.63 to 0.77‰ with an average of 0.68‰ (Table 4.3).

It is interesting to observe that $\delta^{13}C$ values of the planktonic foraminifera *Globigerinoides sacculifer* from the core top samples (younger than 1950 A.D.) from the three multicores are depleted by 0.63‰ on average (ranging between 0.51-0.69‰) relative to isotopic data from the bottom sediment samples older than 1750 A.D. (Table 4.3).

The same pattern was also recorded in another planktonic species *Globigerinoides ruber* (white) from the same cores (Figure 4.3). The $\delta^{13}C$ from the upper parts of the cores ranges between 0.35-0.55‰, and between 0.79-0.93‰ in the lower parts. The values of the upper multicores samples were lighter by as much as 0.38-0.47‰ (Table 4.3).

Table 4.3. Comparison between core top (younger than 1950 A.D.) and core bottom (older than 1750) $\delta^{13}C$ values of the planktonic foraminifera *Globigerinoides sacculifer* and *Globigerinoides ruber* from the three multicores.

Name of core	Average $\delta^{13}C$ (‰) (>1950 A.D.)		Average $\delta^{13}C$ (‰) (<1750 A.D.)		$\delta^{13}C$ difference (‰) (1950-1750)	
	G. sacc.	*G. ruber*	*G. sacc.*	*G. ruber*	*G. sacc.*	*G. ruber*
GeoB 5801-3	0.77	0.55	1.28	0.93	0.51	0.38
GeoB 5807-2	0.63	0.37	1.30	0.84	0.67	0.47
GeoB 5810-3	0.66	0.35	1.35	0.79	0.69	0.44
Average	0.68	0.42	1.31	0.85	0.63	0.43

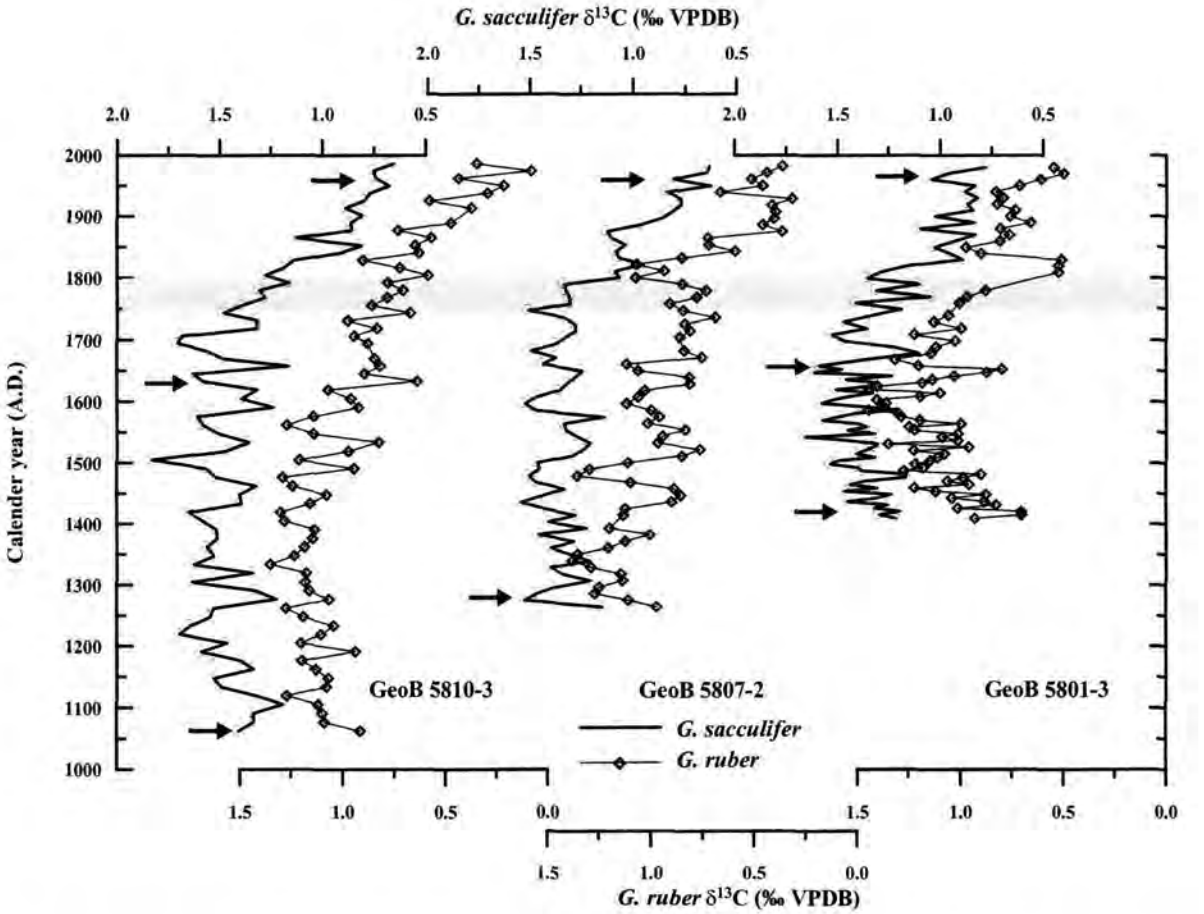

Figure 4.3. Stable carbon isotope composition ($\delta^{13}C$) of the planktonic foraminifera *G. sacculifer* and *G. ruber*, over the last 1000 years A.D. from three multicores (GeoB 5810-3, GeoB 5807-2 and GeoB 58013) collected of the northern Gulf of Aqaba, Red Sea. The arrows represent the calibrated ^{14}C radiocarbon age's positions. The grey bar indicates the transition zone between the pre-industrial and industrial periods.

4.5.3. Carbon isotopic composition of seawater

The average $\delta^{13}C$ value of seawater samples based on the monthly sampling resolution down to 30 m depth is about 1.48‰ relative to VPDB reference standard, and it ranges between 1.23-1.66‰ (Figure 4.4).

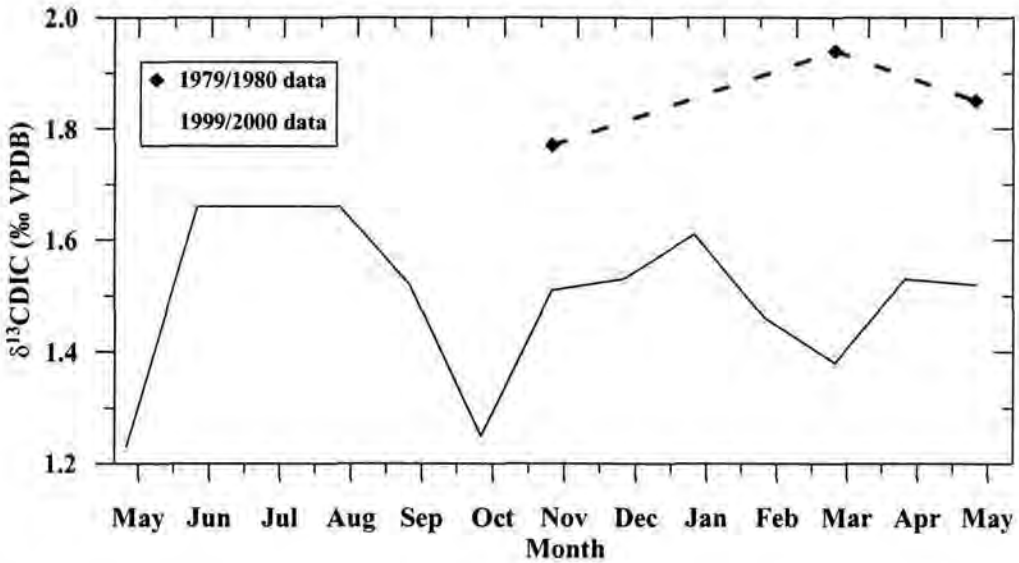

Figure 4.4. Stable carbon isotopic record of the dissolved organic carbon ($\delta^{13}C_{DIC}$) in the surface waters at the northern Gulf of Aqaba. Filled rhombs are averages of daytime samples from 0-30 m during 1979/1980 (data from Shemesh et al., 1994); open circles are averages from 0-30 during 1999/2000. The offset between both records seems to represent the decrease in $\delta^{13}C_{DIC}$ of seawater in the last 20 years due to the effect of anthropogenic CO_2 increase in the atmosphere.

Shemesh et al. (1994) have measured the carbon isotopic composition of seawater at the northern end of the Gulf of Aqaba between November 1979 and May 1980 (Figure 4.4). Values derived from this study (daytime data from surface down to 30m) have $\delta^{13}C_{DIC}$ values ranged between 1.77 to 1.94‰, and average 1.85‰.

4.5.4. Estimation of calcite $\delta^{13}C$ equilibrium

By taking the value of 1.48‰ for the surface water $\delta^{13}C_{DIC}$ at the northern end of the Gulf of Aqaba, we calculate the $\delta^{13}C$ of inorganic calcite precipitated in isotopic equilibrium with ambient seawater using the estimation of Romanek et al. (1992) for equilibrium calcification in waters warmer than 10°C as given by Mulitza et al. (1999):

$$\delta^{13}C_{equilibrium} = \delta^{13}C_{seawater} + 1.0\ ‰$$

According to this estimation, the inorganic calcite precipitated in equilibrium with DIC in seawater should have $\delta^{13}C$ value of about 2.48‰. This indicates that the planktonic foraminifera *G. sacculifer* and *G. ruber* from the northern Gulf of Aqaba does not precipitate its calcite according to equilibrium fractionation of inorganic calcite, and the $\delta^{13}C$ values from the upper parts of the three multicores have a vital effect of about -1.8‰ and -2.1‰, these values are roughly 0.8‰ and 1.1‰ lighter than that of the seawater $\delta^{13}C_{DIC}$ for *G. sacculifer* and *G. ruber* respectively.

4.5.5. Organic carbon, total nitrogen and carbonate content of the sediment

Records from the three multicores show a comparable pattern in all records (Figure 4.5). The organic carbon contents is about 0.4% (on average) in the lower parts older than 1750A.D., increasing toward 0.8% near the top of the cores (Figure 4.5). Whereas the carbonate contents show uniform pattern with minor fluctuations around 30% (Figure 4.5). Correspondingly, the C/N ratio from the multicore GeoB 5810-3 show fairly consistent values around 9.

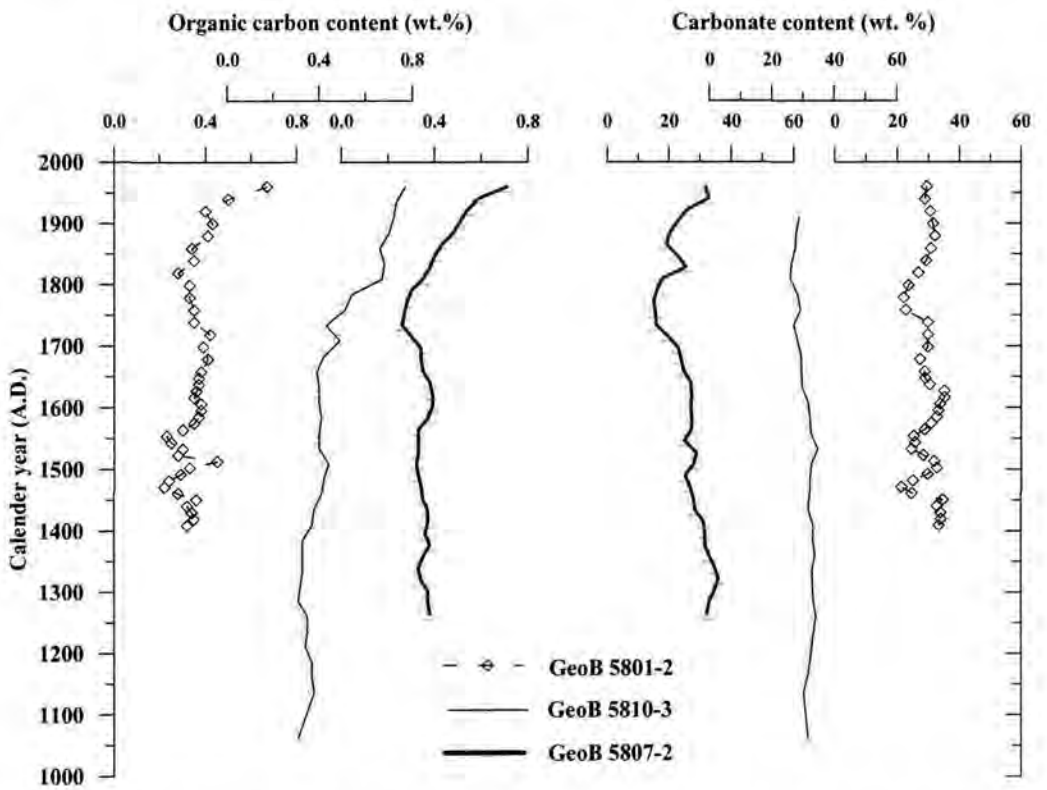

Figure 4.5. Carbonate and organic carbon contents of the multicores GeoB 5810-3, GeoB 5807-2 and GeoB 58013 investigated in this study.

4.5.6. Carbon isotopic composition of the organic matter

The $\delta^{13}C_{org}$ record from the multicore GeoB 5810-3 is shown in Figure (4.6). The results reveal significant differences of about 1.82‰ in the isotopic composition of the organic matter between upper and lower parts.

The pattern before the 1750s has a fairly consistent $\delta^{13}C_{org}$ values with average of about -19.45‰. The curve started to decrease gently in the early 1750s, from -19.45‰ in the older part to about –21.2‰ near the top (younger than 1950 A.D.).

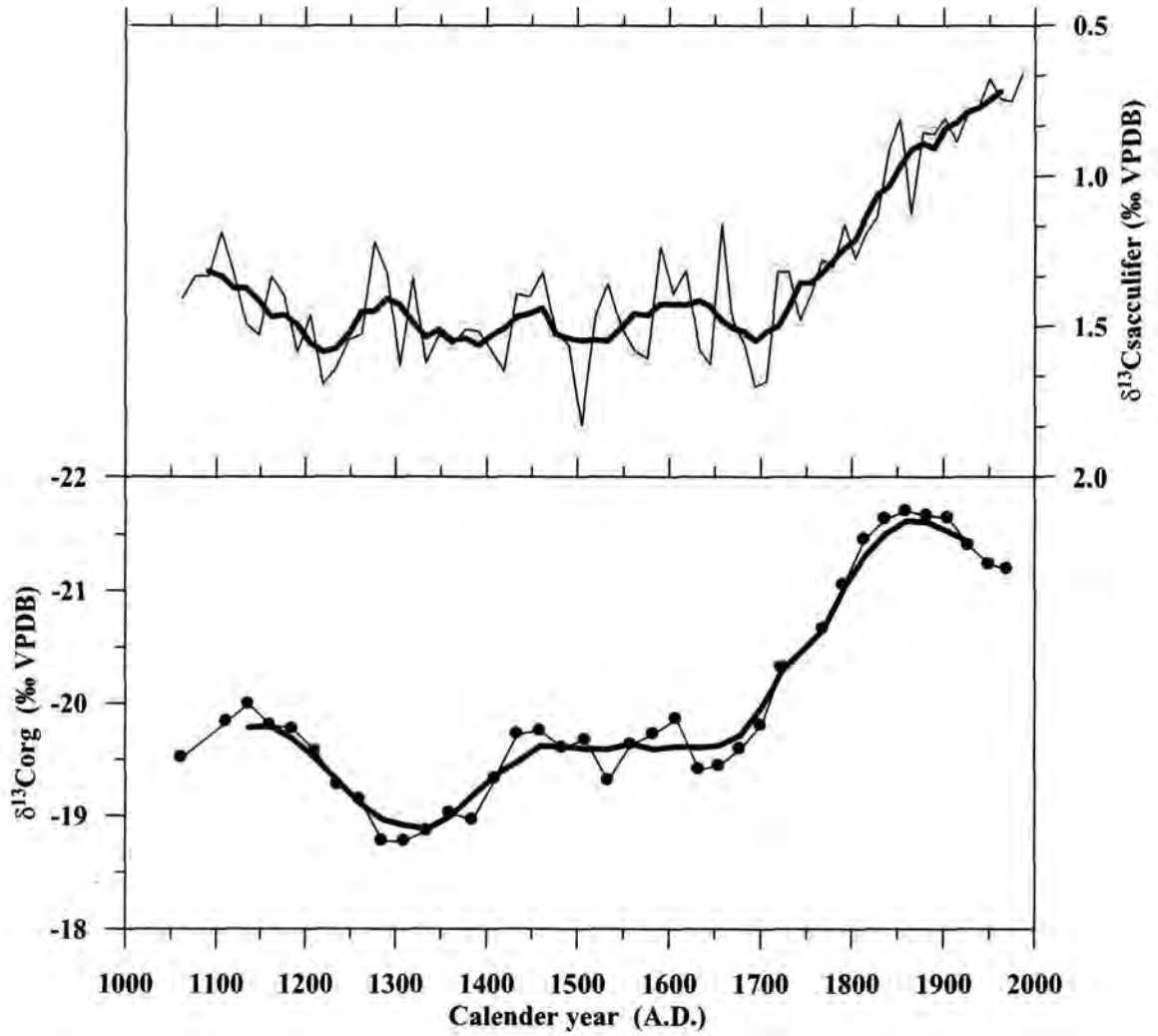

Figure 4.6. Stable carbon isotopic record of the planktonic foraminifera *G. sacculifer* and the sedimentary organic matter ($\delta^{13}C_{org}$), during the last 1000 years A.D. from the multicore GeoB 5810-3. The thick lines represent five points running average.

4.6. Discussion

4.6.1. $\delta^{13}C$ of the planktonic foraminifera G. sacculifer

Planktonic foraminifera do not precipitate their calcite shell according to the isotopic equilibrium of inorganic calcite with seawater, due to the incorporation of isotopically light CO_2 into the carbonate skeleton, vital effect from respiration, and photosynthetic activity of symbionts (Erez, 1978; Spero et al., 1991). The $\delta^{13}C$ of the planktonic foraminifera *G. sacculifer* from the northern Gulf of Aqaba revealed a vital effect of about –1.8‰, and is depleted by about 0.8‰ relative to seawater $\delta^{13}C_{DIC}$., while *G. ruber* shows larger offsets due to different physiological processes (respirations and symbiont photosynthesis) between the two species (Erez, 1978; Spero et al., 1991) These results are in a good agreement with the findings of Williams and Sommer (1977). They suggested that *G. sacculifer* could be used to infer the $\delta^{13}C$ values of the dissolved ΣCO_2 in paleoceans, because some species have $\delta^{13}C$ values, which are offset by nearly constant factor from ΣCO_2 (Shackleton and Vincent, 1978; Spero, 1992; Keir, 1995).

Additionally, it has been suggested that $\delta^{13}C$ values are size dependent especially for planktonic foraminifera (Berger, 1978; Bouvier and Duplessy, 1985; Ravelo et al., 1995). For that reason and to decrease the effect of size fraction, our forams were picked with a narrow size fraction range (350-400 µm). About 12-18 individual per sample were also analysed to an average out the intraspecific variability due to foraminiferal physiology as recommended by Spero (1992).

Results from this study show a decline in the $\delta^{13}C$ planktonic formainifera (*G. sacculifer*) of roughly 0.63‰ from approximately the beginning of the industrial revolution (1750 A.D.). The $\delta^{13}C$ record of the same species (*G. sacculifer*) in a gravity core from the same area (GeoB 5810-2; Al-Rousan unpublished data) shows a consistent $\delta^{13}C$ pattern over the last 3000 years B.P. (mid-late Holocene). The values averaged 1.39‰, which are similar to their counter bars from the lower parts of the multicores older than 1750 A.D.

If we consider that the intraspecific range of formainifera $\delta^{13}C$ values attributed to vital effect remained rather constant since the late Holocene, then changes in the $\delta^{13}C$ composition of the foraminifera shells should be still proportional to changes in the carbon isotope composition of DIC in seawater (Spero, 1992; Beveridge and Shackleton, 1994). Therefore, the 0.63‰ decrease during the last two centuries can be partly attributed to the invasion of fossil

fuel CO_2 into the surface waters, which caused a decrease in the $\delta^{13}C_{DIC}$. This value is smaller than the 1.14‰ decrease estimated for the $\delta^{13}C$ in atmospheric CO_2 during the last 200 years (Friedli et al., 1986; Francey et al., 1999), and represents about 40% of the atmospheric decrease. This is in accordance with Oeschger et al. (1975) who used a global box diffusion model, and predicted that the worldwide surface ocean response should be 40% of that in the atmosphere. This is mainly due to incomplete isotopic equilibration between $\delta^{13}C_{DIC}$ of the water and the $\delta^{13}C_{CO2}$ of the atmosphere (Lynch-Stieglitz et al., 1995). It was also concluded that varying values of $\Delta\delta^{13}C_{DIC}$ (the change in $\delta^{13}C_{DIC}$ from pre-industrial and industrial times) observed in different parts of the tropical oceans reflect the varying degree of isotopic equilibration with atmospheric CO_2, controlled by dilution of surface waters with subsurface waters (Böhm et al., 1996). In the northern Gulf of Aqaba, the reason for this small decrease is most likely due to the short exposure time of surface water to the atmosphere due to vertical mixing and dilution with water from the Red Sea, because the circulation in the northern Gulf is primarily influenced by the inflow from the Red Sea which compensate for the evaporation loss of water masses (Reiss and Hottinger, 1984).

Krumgalz et al. (1990) have studied the penetration of anthropogenic carbon dioxide in the northern Red Sea and the Gulf of Aqaba using data obtained during a cruise in winter 1982. Results demonstrate that the entire water column of the Gulf of Aqaba was saturated with an excess of anthropogenic CO_2, indicating winter overturning. In the Red Sea the upper 200m are very young with a uniform excess CO_2 signal. The old waters at 600 m are sandwiched between younger waters, the young bottom waters are formed by the overflow of younger waters from the Gulf of Aqaba over the sill in the Straits of Tiran and by the inflow of young waters from the Gulf of Suez.

4.6.2. Comparison with other paleoclimatic records

The $\delta^{13}C$ stack record of the planktonic foraminifera *G. sacculifer* from the three multicores (GeoB 5801-3; GeoB 5807-2; GeoB 5810-3) and records from tree rings, ice cores and sponges are compared in Figure (4.7).

The 0.63‰ decrease in the $\delta^{13}C$ of *G. sacculifer* from the northern Gulf of Aqaba over the past 200 years is comparable with values deduced from other marine proxies from different locations (Table 4.4). The estimated variations in seawater $\delta^{13}C$ from shallow dwelling corals,

sclerosponges and foraminifera show a decrease in the range of 0.5 to 0.9 ‰, while records from tree rings and ice cores exhibit values between 1-2‰ for the atmospheric $\delta^{13}C$ decrease due to the anthropogenic CO_2 increase (Table 4.4).

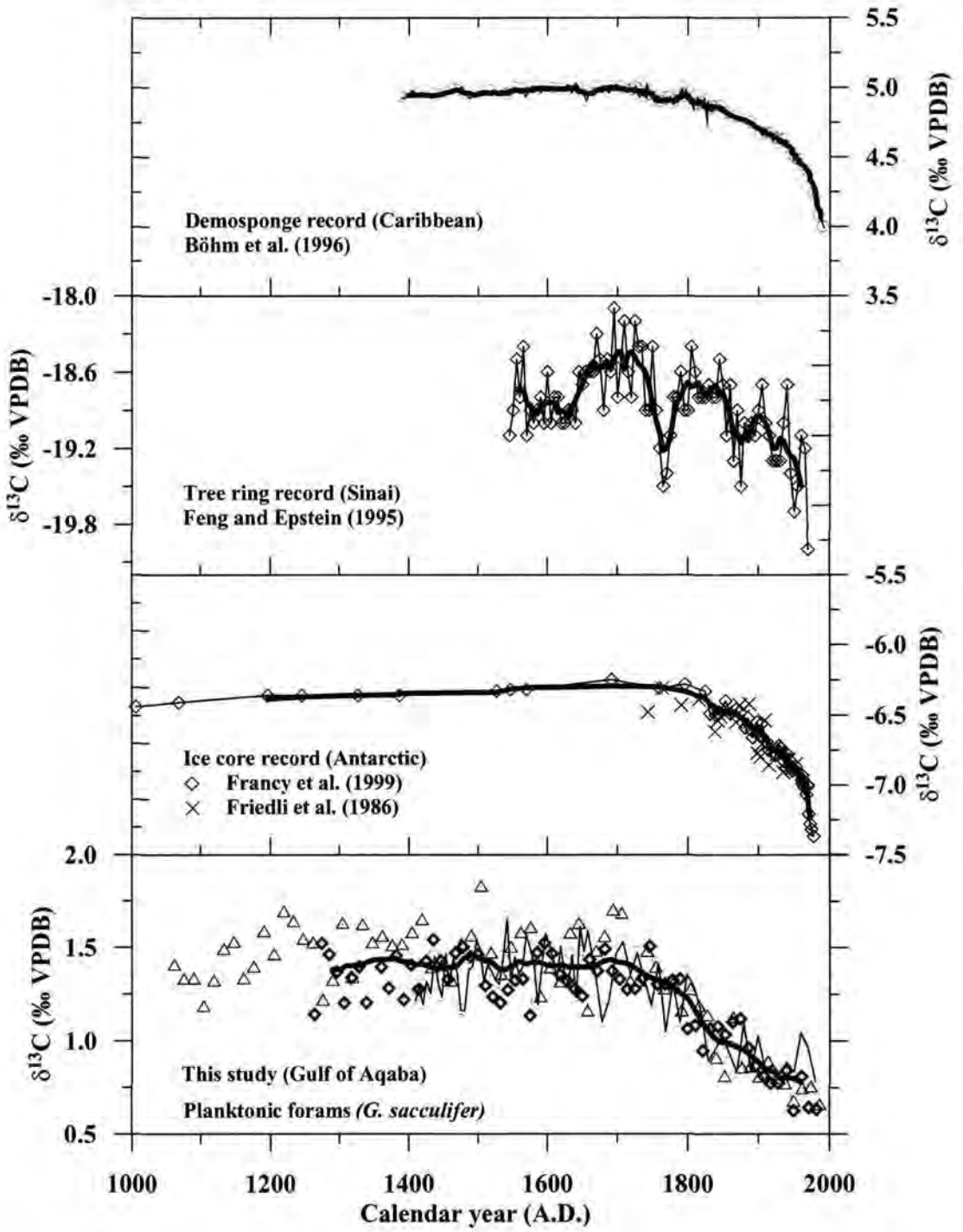

Figure 4.7. Comparison between $\delta^{13}C$ stack record (planktonic foraminifera *G. sacculifer*) from the three multicores with other published records from different proxies, showing the decrease in $\delta^{13}C$ of the atmosphere (tree ring and ice core records) and surface water $\delta^{13}C_{DIC}$ (sponge and foram records) over the last two centuries due to the increase of the anthropogenic CO_2 input in the atmosphere.

Table 4.4. Summary of some estimates of the seawater and atmosphere $\delta^{13}C$ decrease due to the anthropogenic CO_2 increase over the last 200 years, compared to results obtained from this study.

Location	Proxy	$\delta^{13}C$ decrease	Reference
Antarctic Siple	Ice core	1.14‰	Friedli et al. (1986)
South Africa	Tree Rings	1.0 –1.7‰	February and Stock (1999)
South America	Tree Rings	1.2‰	Leavitt (1994)
Bermuda	Corals *(Diploria)*	0.50‰	Nozaki et al. (1978)
Tropical ocean (Jamaica)	Sclerosponge	0.50‰	Druffel and Benavides (1986)
Caribbean Coral Sea	Sclerosponge	0.90‰ 0.70‰	Böhm et al. (1996)
Eastern Atlantic	Planktonic forams *(G. ruber; G. bulloides)*	0.50-0.60‰	Beveridge and Shackleton (1994)
Arctic Ocean Nansen Basin	Planktonic forams *(N. pachyderma (sin.))*	0.90‰ 0.60 ‰	Bauch et al. (2000)
Gulf of Aqaba	Planktonic forams *(G. sacculifer)*	0.63‰	This study

The strong $\delta^{13}C$ decline of the planktonic formainifera *G. sacculifer* since the 1750s from this study fitted to an exponential function that often follows this trend of decrease (Figure 4.7). The trend from sclerosponges, tree rings and ice core records (Böhm et al., 1996; Feng, 1999; Francey et al., 1999) show a rapid decrease in the $\delta^{13}C$ values for the most recent fifty years and much smaller change when going further back in time. The insufficient dating controls of the upper parts of the sediment records younger than A.D. 1950 from this study are most likely responsible for the normal rather than rapid $\delta^{13}C$ decrease for the most recent years.

4.6.3. Seawater $\delta^{13}C_{DIC}$ variations in the Gulf of Aqaba

Anthropogenically produced CO_2 have entered the oceans and changed the $\delta^{13}C$ of the DIC (Quay et al., 1992). This decrease has been confirmed in the northern Gulf of Aqaba from direct measurements of the $\delta^{13}C_{DIC}$ done in 1979 (Shemesh et al., 1994), and recently in 2000 in this study.

Comparison of the data shows that there is a significant offset between both records (Figure 4.4). The average $\delta^{13}C$ value of the DIC of the surface waters at the northern Gulf of Aqaba decreased by about 0.44‰ during the last 20 years, with an annual decrease of about 0.021‰.

This result is similar to that obtained by Quay et al. (1992) who found a 0.4‰ decrease of the $\delta^{13}C_{DIC}$ value in the surface waters of the Pacific ocean between 1970 and 1990. They attributed this decrease due to the uptake of the atmospheric CO_2 derived from fossil fuel combustion and deforestation. Bacastow et al. (1996) have also shown an average decrease of about 0.022‰/yr during the period 1984-1992 from direct measurements of the $\delta^{13}C_{DIC}$ near Bermuda.

4.6.4. Support from $\delta^{13}C_{org}$

Results of $\delta^{13}C_{org}$ from this study show a trend toward lighter values during the last 200 years (–19.45 to –21.2‰), and the variations of about 1.82‰ closely follow those of the $\delta^{13}C$ of the planktonic foraminifera (Figure 4.6).

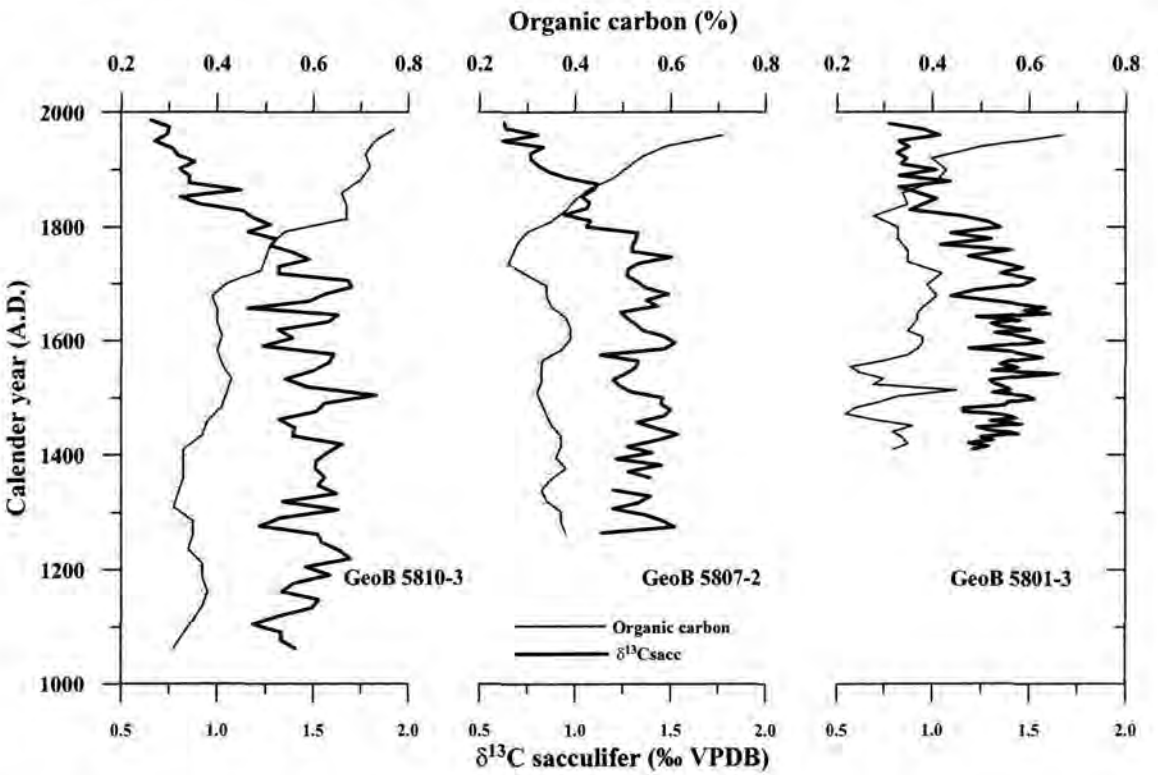

Figure 4.8. Variations of the organic carbon content and $\delta^{13}C$ of the planktonic foraminifera *G. sacculifer* in the multicore GeoB 5810-3, GeoB 5807-2 and GeoB 5801-3 from the northern Gulf of Aqaba. The organic carbon increase in the upper part of the core is most likely due to preservation effect.

The difference in stable carbon isotope composition ($\delta^{13}C_{org}$) between modern phytoplankton and underlying surface sediments older than 200 years were explained by the penetration of ocean surface waters by isotopically light carbon (Bentaleb and Fontugne, 1996; Fischer et al., 1997; 1998; Wolf-Gladrow 1999; Rosenthal et al. 2000). However, variations of $\delta^{13}C_{org}$ in marine sediments can be also ascribed to a variable mixture of carbon derived from marine and terrestrial sources, which leads to $\delta^{13}C_{org}$ contamination, and to the digenetic changes in the isotopic composition of the deposited organic matter (e.g. Fontugne and Calvert, 1992; Rau, 1994; Müller et al., 1994).

Organic carbon content in our sediments is about 0.4%; highest abundance of about 0.8% is noted in the top of the core (Figure 4.8). If we assume that this is due to increased biological productivity, then this would have a direct effect on the $\delta^{13}C_{DIC}$, because marine plankton preferentially uses ^{12}C for photosynthesis, leaving surface water enriched in ^{13}C (Broecker, 1974). By contrast $\delta^{13}C$ in the planktonic foraminifera *G. sacculifer* shows a trend in the opposite direction (Figure 4.8 and 4.9C). These results suggest that the increase of organic carbon content is not related to an increase in local productivity but can be attributed to preservation effects.

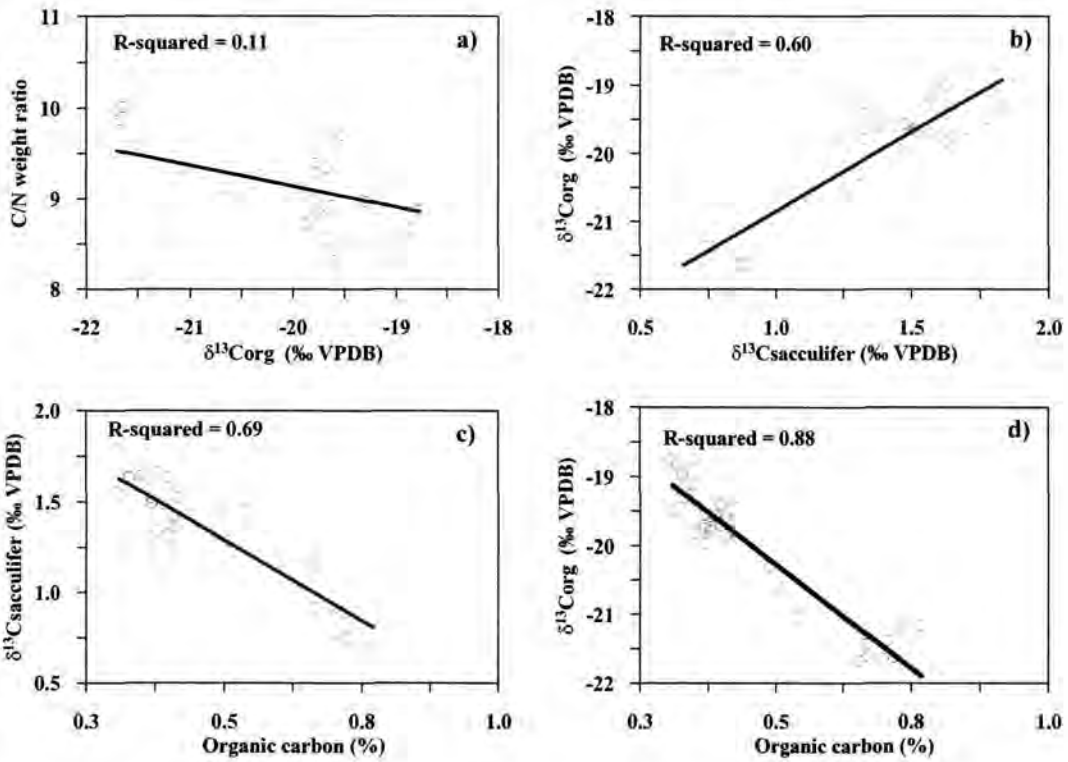

Figure 4.9. Scatter diagram of relations obtained from the chemical and isotopic analysis of the multicore GeoB 5810-3. a) C/N ratio vs. $\delta^{13}C_{org}$, b) $\delta^{13}C_{org}$ vs. $\delta^{13}C_{sacculifer}$, c) $\delta^{13}C_{sacculifer}$, vs. organic carbon content and d) $\delta^{13}C_{org}$ vs. organic carbon content. Regression lines and correlation coefficients are shown.

The $\delta^{13}C_{org}$ values in the multicore GeoB 5810-3 vary between –18.5 to –21.5‰ and are typical of the marine environment. Furthermore, the quite uniform C/N values of about 9 throughout the core, and the lack of relationship between $\delta^{13}C_{org}$ and C/N ratio (Figure 4.9A), as well as the consistent carbonate content (around 30%) which varies mainly due to the dilution effect by terrigenous sediment, all these suggest comparatively low terrigenous organic matter contribution to the sediments.

Since the magnitude of the early digenetic alteration is relatively small (Rau, 1994), and the terrestrial organic matter contributions to the sediments in the Gulf of Aqaba can be excluded, we assumed that organic carbon in our samples is driven predominantly from primary producers, and the CO_2 variations are probably the reason for isotopic variations in the $\delta^{13}C_{org}$.

The core top samples from this study exhibit $\delta^{13}C_{org}$ values close to 21‰ (Figure 4.6) similar to the value in modern plankton of the Gulf of Aqaba waters (Shemesh et al., 1994; Lorian et al., 1992). Therefore, they should represent the industrial conditions. The 1.82‰ difference between pre-industrial and industrial $\delta^{13}C_{org}$ values from this study is rather similar to the measured average differences between sinking matter and surface sediments (2‰) due to anthropogenic CO_2 increase from the tropical-subtropical Atlantic (Fischer and Wefer, 1996).

The negative relation between $CO_{2(aq)}$ and the carbon isotopic composition of marine phytoplankton has been suggested by many workers (e.g. Degens et al., 1968; Rau et al., 1989; Popp et al., 1989; Rau, 1994), and has recently been confirmed in monospecific marine phytoplankton cultures (e.g. Laws et al., 1995). Using the equation proposed by Rau (1994) and the $\delta^{13}C_{org}$ values, which represents the pre-industrial (older than 1750 A.D) and industrial (younger than 1950) conditions in the Gulf of Aqaba, we have estimated the variations in CO_2 concentration to be from 287 to 363 ppm. These results are within the range estimated for CO_2 concentrations from ice cores during the last two centuries (Friedli et al., 1986; Etheridge et al., 1996).

4.7. Conclusions

Variations in the carbon isotopic composition of the planktonic foraminifera (*G. sacculifer*) and the sedimentary organic matter ($\delta^{13}C_{org}$) revealed by this study, have been interpreted as evidence of increasing anthropogenic input of ^{13}C depleted CO_2 into the atmosphere during the last 200 years, which caused lighter $\delta^{13}C_{DIC}$.

The $\delta^{13}C$ records of the planktonic foraminifera (*G. sacculifer*) from the northern Gulf of Aqaba display similar trends from three multicores over the last 1000 years. The pattern shows little variability but no trend before 1750 A.D. Starting at the 1750s the values decrease continuously. Present values are depleted by about 0.63‰ relative to pre-1750 A.D. This decrease is similar to that estimated for surface water DIC from shallow-dwelling corals and sclerosponges from other parts of the world, and about 40% of that in the atmosphere (deduced from ice cores), due to incomplete isotopic equilibration between water and atmosphere.

Variations of the $\delta^{13}C$ of sedimentary organic matter ($\delta^{13}C_{org}$) also show a trend toward lighter values started at the beginning of the 1750 closely followed those of the $\delta^{13}C$ of the planktonic foraminifera and supporting the interpretation. Furthermore, results from direct measurements of seawaters $\delta^{13}C_{DIC}$ in the Gulf show a decrease of about 0.44‰ during the last 20 years (0.021‰/yr), which is similar to values measured in the Pacific Ocean (Quay et al., 1992).

Finally, the results of our carbon isotopic composition analysis of both organic matter and planktonic foraminifera calcite shells, allow us to conclude that $\delta^{13}C_{DIC}$ is surface waters in the northern Gulf of Aqaba has decreased due to the anthropogenic CO_2 increase in the atmosphere during the last two centuries. This decrease has left a marked imprint on the $\delta^{13}C$ of both organic matter and foraminifera shells.

4.8. Acknowledgments

We thank H. Arz for valuable comments and assistant with field and lab work during sediment cores collection and slicing. H. Kuhnert and T. Felis are also thanked for constructive comments on the manuscript. Discussions with G. Fischer, R. Schneider and P. Müller have been most helpful. We thank L. Böhme, X. Feng, and R. Francey for providing their data. Special thanks are due to M. Segl for performing stable isotope measurements and preparation of ^{14}C AMS dating samples. We are grateful to H. Buschhoff and P. Müller for CHN analysis of the sediment samples. This work is partly supported by the Red Sea program (RSP II), funded by the BMBF (German Ministry for Education, Science, Research, and Technology) and a grant from the University of Bremen.

5. Conclusions and future perspectives

5.1. General conclusions

From the high-resolution stable isotope analysis in corals (*Porites spp.*) and planktonic foraminifera (*G. sacculifer*) from the northern Gulf of Aqaba, the following conclusions have been drawn.

5.1.1. Coral records

High-resolution coral $\delta^{18}O$ records from the northern Gulf of Aqaba were investigated in order to evaluate the environmental and biological effects that may distort the signals obtained from this proxy. The study provides the first continues time series records of seawater stable isotopic composition ($\delta^{18}O$, $\delta^{13}C$) from the area and offers acceptable coral $\delta^{18}O$/temperature relation for the region.

- The high correlation between coral $\delta^{18}O$ and recorded seawater temperatures in both Aqaba and Eilat in the northern end of the Gulf of Aqaba suggests that a large majority of the seasonal variations in coral oxygen isotopes can be explained by the sea surface temperature variations. The interannual salinity variations seem to be responsible for decreasing the correlation between coral $\delta^{18}O$ and seawater temperature at the annual time scale.
- The different $\delta^{18}O$/temperature relations from the two different colonies and also from the same colonies indicates that $\delta^{18}O$ of coral skeletons is growth dependent. Significant $\delta^{18}O$ depletion is observed at high extension rates, and heavier values at low extension rates. The relation between coral $\delta^{18}O$ and extension rate can be explained by a simple exponential model, in which the inverse function extends over extension rates 1-5 mm/yr. For more rapidly growing corals and portions of coral colonies, the relation is constant and the extension rate did not appear to have any significant effect on coral $\delta^{18}O$. Thus we suggest that $\delta^{18}O$ values from *Porites* corals should be obtained from fast growing corals or portions of the colonies (>5 mm/yr), where the isotopic disequilibrium is fairly constant.

- The offset in $\delta^{18}O$ profiles cannot be always explained as a function of extension and/or calcification rate and may result from coral species differences. Skeletal extension rate and coral species should be considered when interpreting and comparing coral paleoclimatic data from various coral species with different extension rates. Moreover, these results can be used to evaluate and correct coral $\delta^{18}O$ values obtained from modern and fossil corals for extension rate effects.

- High sampling resolution from this study confirms the ability of Red Sea *Porites* corals to accurately preserve short period and magnitude temperature variations. Weekly/biweekly coral $\delta^{18}O$ records are able to capture fine details of the weekly temperature records and to resolve more than 95% of the weekly/biweekly temperature variations.

- Seawater $\delta^{18}O$ from the northern Gulf of Aqaba exhibits a weak seasonal pattern with variations less than 0.25‰ (VSMOW). These variations seem to have negligible effect on the seasonal coral $\delta^{18}O$ cycle. It shows positive correlations with seawater salinity (60%) similar to that reported from the Red Sea proper, and can be expressed by the equation $\delta^{18}O_{Seawater\ (VSMOW)} = 0.281 * salinity\ (‰) - 9.14$.

- The $\delta^{18}O$ signals from samples within the tissue layer can precisely record temperature variations and show no evidence for smoothing or distortion of these signals due to calcification throughout the thickness of the tissue layer as suggested by earlier studies.

- The interruption or inconstant extension rate in slow growing corals during the year may result in attenuation or amplification of the coral $\delta^{18}O$ seasonal amplitude and make it not possible to record the true environmental signals.

- The relation between oxygen isotopic composition of coral skeleton, seawater temperature and seawater $\delta^{18}O$ from the northern Gulf of Aqaba based on corals from different depths from this study can be expressed by the equation $T = -5.38 * (\delta_c - \delta_w) - 1.08$, where δ_c is the oxygen isotope composition of coral in ‰ relative to VPDB, δ_w is that of water in ‰ relative to VSMOW and T is temperature in °C. The slope of the equation 0.186‰/1°C is similar to that obtained from high-resolution studies in other parts of the world.

5.1.2. Sediment records

Carbon stable isotopic composition of the planktonic foraminifera (*G. sacculifer*) was used to reconstruct the variations of seawater dissolved inorganic carbon (DIC) from the northern Gulf of Aqaba. The study was conducted on three multicorers extends almost 1000 years BP with high temporal resolution up to 10 years. This chronology is the first with such resolution to show a decline in the $\delta^{13}C$ from planktonic foraminifera from sediment records which is related to anthropogenic CO_2 increase.

- High offsets (0.63‰) between the carbon isotopic values of the planktonic foraminifera *G. sacculifer* younger than 1950s and values older than 1750s from the three multicorers from the northern Gulf of Aqaba indicate the anthropogenic CO_2 uptake by the surface water which caused decrease in its $\delta^{13}C_{DIC}$.
- The decrease of the carbon isotope of sedimentary organic matter ($\delta^{13}C_{org}$) during the last 200 years by about 2‰ was not related to local productivity or terrigenous input increase and tend to support the interpretation obtained from the $\delta^{13}C$ of the planktonic foraminifera. The variations in CO_2 concentration calculated from $\delta^{13}C_{org}$ values, which represent the pre-industrial and industrial conditions in the Gulf of Aqaba are estimated to be from 287 to 363 ppm. These values are within the range estimated for CO_2 concentrations from ice cores during the last two centuries.
- A comparison of carbon isotope measurements of the northern Gulf of Aqaba seawater obtained in 1999 with measurements recorded in 1979 shows a decrease of $\delta^{13}C_{DIC}$ values of about 0.44‰ during the last 20 years (annual decrease of 0.021‰) resulting from increasing of anthropogenic CO_2 input into the atmosphere.
- The invasion of anthropogenic CO_2 into the Gulf of Aqaba waters is a real phenomenon, and has leaved a marked imprint on the carbon stable isotope composition of the planktonic foraminifera and sedimentary organic matter.
- The results from this study reveal that $\delta^{13}C$ of planktonic foraminifers combined with organic matter $\delta^{13}C$ from marine sediments allow good indicators to reconstruct past changes in atmospheric CO_2 concentrations from the northern Gulf of Aqaba.

5.2. Future perspectives

5.2.1. Fossil corals and sediment records

The Gulf of Aqaba is characterized by a high diversity of coral reef communities, which represent the northern limit (29°32'N) for reef corals in the western Indo-Pacific region (Schuhmacher et al., 1995). Living corals can be found down to 200 m. However, uplifted and submerged reef terraces are distributed along the Gulf coasts.

The applicability of corals as high-resolution climate proxies from this study and from earlier studies in the Gulf of Aqaba (e.g., Klein et al., 1992; 1993; 1997; Heiss, 1996; Heiss et al., 1999; Felis et al., 1998; 2000; Moustafa et al., 2000) encourage for further investigations to be carried out on fossil corals, this can offer a unique source of information on tropical climate variability throughout the late Quaternary (e.g., Beck et al., 1997; Guilderson et al., 1994; McCulloch et al., 1999).

Recent research indicates that some climatic phenomena such as El Niño Southern Oscillation (ENSO) and the North Atlantic Oscillation (NAO) have an impact on the Middle East climate (e.g., Charles et al., 1997). These phenomena have been recently identified from a 245-year long oxygen isotopic coral record from the northern Red Sea (Felis et al., 2000; Rimbu et al., 2001). Furthermore, Mid-Holocene corals $\delta^{18}O$ records from the northern Red Sea indicate higher seasonality in temperature and/or seasonal changes in the hydrological balance during that period in the region (Moustafa et al., 2000).

We have collected fossil corals from the Holocene and last interglacial raised reef terraces from Aqaba, at the northern end of the Gulf. A 44-year long $\delta^{18}O$ record has been already generated in bimonthly resolution from the last interglacial period (Felis et al., in preparation). Preliminary results of spectral analysis suggest that comparable climatic modes and atmospheric teleconnection were active during that period. Furthermore, results from Sr/Ca combined to stable oxygen ratios indicate cooler and fresher mean conditions during that period in the northern Gulf of Aqaba.

Sediment cores have been collected recently from the northern Gulf of Aqaba during Meteor Cruise M44/3 in 1999 (Pätzold et al., 2000). The longest core recovered from the area extends back to the last 8000 years B.P. and shows high sedimentation rates (~30cm/kyr) in the area. The stable oxygen composition record of planktonic foraminifera indicates a humid period during mid-Holocene (Arz et al., in prep.). Combining of the high-resolution paleoclimatic archives from marine sediments and coral records will provide better understanding of the

patterns and mechanisms of climate variability during the recent past and during the late Quaternary.

New construction works at Aqaba have recovered huge and well-preserved coral colonies from the raised and submerged reef terraces, which are suitable material for paleostudies. Drilling of both raised and submerged reef terraces will enable to fill the gap and to understand the full history of reef development, sea level and paleoclimatic changes in the area.

5.2.2. Calibration studies

Several elemental indicators in coral skeletons and foraminifera shells have proven to provide different environmental proxies for temperature, salinity, vertical mixing and other environmental parameters. However, the work in understanding these proxies, their controllers and sensitivity is still in progress.

The Sr/Ca ratio in corals is one of these indicators, it has been proven to provide high accuracy thermometers (e.g., Beck et al., 1992; McCulloch et al., 1994), combination of this proxy with oxygen isotope proxy can provide important information about sea surface temperatures and hydrological balance variations (McCulloch et al., 1994, Gagan et al., 1998). However it has been found that Sr/Ca ratios exhibits different temperature calibrations (Beck et al., 1992) and show growth rate dependence (de Villiers et al., 1995).

Therefore, calibration of Sr/Ca ratios in corals against *in situ* measurements of seawater temperatures and Sr/Ca ratios as well as investigation of the biological factors that may affect this ratio (e.g., growth rate, interspecific offset) from the northern Gulf of Aqaba could be focus for future studies. This will help in solving some of these problems and can provide empirical relationship for the region that can be applied to late quaternary coral records. Additionally, further indicators such as Mg/Ca, U/Ca and B/Ca can be investigated; they can offer valuable proxies from corals.

The continuation of water sampling program for stable isotope analysis and hourly seawater temperature records from different water depth that have been initiated in April 1999 in the northern Gulf of Aqaba, will provide a unique record from the Red Sea and will help in the interpretation of past and future coral stable isotope records.

Furthermore, temperature loggers fixed at depths of 0.5; 1.5; 2.5; 3.5; 4.5 and 5m above sea floor in front of the Marine Science Station at Aqaba in June 2000 will provide high resolution

long term temperature records which can be used to assess and calculate the effect of temperature on the isotopic records when corals grow into shallower and warmer waters. For example, Heiss et al. (1999) have shown different isotope records form horizontal and vertical cores from a huge *Porites* coral colony from Aqaba that is probably related to coral growth into shallower water depths. The calculated effect from the temperature records can be then used to correct this isotope chronology, and to improve the interpretations of future records.

6. References

Aharon P (1991) Recorders of reef environment histories: Stable isotopes in corals, giant calms and calcareous algae. Coral Reefs 10: 71-90

Alibert C, and McCulloch MT (1997) Strontium/calcium ratios in modern *Porites* corals from the Great Barrier Reef as a proxy for sea surface temperature: Calibration of the thermometer and monitoring of ENSO. Paleoceanography 12: 345-363

Allison NT, Tudhope AW, Fallick AE (1996) Factors influencing the stable carbon and oxygen isotopic composition of *Porites lutea* coral skeletons from Phuket, South Thailand. Coral Reefs 15: 43-57

Al-Rifaiy IA, Cherif OH (1988) The fossil coral reefs of Al-Aqaba, Jordan. Facies 18: 219-230

Andrié C, Merlivat L (1989) Contribution des données isotopique de deutérium, oxygène-18, hélium-3 et tritium, à l'étude de la circulation de la Mer Rouge. Oceanol. Acta 12: 165-174

Bacastow RB, Keeling CD, Lueker TJ, Wahlen M, Mook WG (1996) The ^{13}C Suess effect in the world surface oceans and its implications for oceanic uptake of CO_2: Analysis of observations at Bermuda. Global Biogeochem. Cycles 10: 335-346

Badran MI, Foster P (1998) Environmental quality of the Jordanian coastal waters of the Gulf of Aqaba, Red Sea. Aquatic Ecosystem Health and Mangment 1: 75-89

Barnes DJ, Lough JM (1989). The nature of skeletal density banding in scleractinian corals: fine banding and seasonal patterns J. Exp. Mar. Biol. Ecol. 126: 119-134

Barnes DJ, Lough JM (1992) Systematic variations in the depth of skeleton occupied by coral tissue in massive colonies of *Porites* from the Great Barier Reef. J. Exp. Mar. Biol. Ecol. 159: 113-128

Barnes DJ, Lough JM (1993) On the nature and causes of density banding in massive coral skeletons. J. Exp. Mar. Biol. Ecol. 167: 91-108

Barnes DJ, Taylor RB, Lough JM (1995) On the inclusion of trace materials into massive coral skeletons. Part II: distortions in skeletal records of annual climate cycles due to growth processes. J. Exp. Mar. Bio. Ecol. 194: 251-275

Barnola JM, Raynaud D, Korotkevich YS, Lorius C (1987) Vostok ice core provides 160 000-year record of atmosphere CO_2. Nature 329: 408-414

Bauch D, Carstens J, Wefer G, Thiede J (2000) The imprint of anthropogenic CO_2 in the Arctic Ocean: Evidence from planktic ^{13}C data from water column and sediment surfaces. Deep-Sea Res. 47 (9-11): 1791-1808

Beck JW, Récy J, Taylor F, Edwards RL, Cabioch G (1997) Abrupt changes in early Holocene tropical sea surface temperature derived from coral records. Nature 385: 705-707

Beck JW, Edwards RL, Ito E, Taylor FW, Recy J, Rougerie F, Joannot P, Henin C (1992) Sea surface temperature from coral skeleton strontium/calcium ratios. Science 257: 644-647

Bentaleb I, Fontugne M, Descolas-Gros C, Girardin C, Mariotti A, Pierre C, Brunet C, Poisson A (1996) Organic carbon isotopic composition of phytoplankton and sea-surface PCO_2 reconstructions in the Southern Indian Ocean during the last 50.000 yr. Org. Geochem. 24 (4): 399-410

Berger WH (1975) Deep-sea carbonates: dissolution profiles from foraminiferal preservation. In: Dissolution of Deep-Sea Carbonates (W.V. Sliter, AWH Be, WH Berger eds). Special Publication No. 13, Cushman Foundation for Foraminifera Research, Washington, Dc 82-84

Berger WH, Killingley JS, Vincent E (1978) Stable isotope in deep-sea carbonates: Box core ERDC-92, West Equatorial Pacific, Oceanol. Acta 1: 203-216

Beveridge NAS, Shackleton NJ (1994) Carbon isotopes in recent foraminifera: A record of anthropogenic CO_2 invasion of the surface ocean. Earth Planet. Sci. Lett. 126: 259-273

Bond G, Kromer B, Beer J, Muscheler R, Evans M, Showers W, Hoffmann S, Lotti-Bond R, Hajdas I, Bonani G (2001) Persistent solar influence on North Atlantic climate during the Holocene. Science 294: 2130-2136

Bouvier-Soumagnac, Y, Duplessy J-C (1985) Carbon and oxygen isotopic composition of planktonic foraminifera from laboratory culture, plankton tows and recent sediment: Implications for the reconstruction of paleoclimatic conditions and of the global carbon cycle. J. Foraminiferal Res. 15: 302-320

Böhm F, Joachimski MM, Lehnert H, Morgenroth G, Kretschmer W, Vacelet J, Dullo W-Chr (1996) Carbon isotope records from extant Caribbean and South Pacific sponges: Evolution of $\delta^{13}C$ in surface water DIC. Earth Planet. Sci. Lett. 139: 291-303

Bradley RS (1999) Paleoclimatology: Reconstructing climates of the Quaternary. Second edition. International Geophysics Series, volume 68. Academic Press, San Diego, CA, 613 pp

Broecker WS (1974) Chemical Oceanography. New York, Harcourt Brace Jovanovich, 214pp.

Brocker WS, Peng TH (1982) Tracers in the Sea. Lamont Doherty Geol. Obs. Publication, Columbia University, New Yorlk 689 pp

Carriquiry JC (1994) ^{18}O fractionation in the coralline aragonite of *Porites lobata*: implications in oceanic paleothermometry studies, Ciencias Marinas 20: 585-606

Carriquiry JC, Risk MJ, Schwarcz HP (1994) Stable isotope geochemistry of corals from Costa Rica as a proxy indicator of the El Niño/Southern Oscillation (ENSO). Geochim. Cosmochim. Acta 58: 335-351

Carriquiry JC, Soto-Castro JF, Charles CD, Moore M (1998) Stable isotope records and trace element records in coral growth bands and tracers of ENSO activity in the Mexican Pacific, Proc. Am. Quat. Assoc., 12-13

Cember RP (1988) On the sources, formation and circulation of Red Sea deep water. J. Geophys. Res. 93 (C7): 8175-8191

Chalker BE, Barnes DJ (1990) Gamma densitometry for the measurement of coral skeleton density. Coral Reefs 9: 11-23

Chalker BE, Barnes DJ, Isdale PJ (1985) Calibration of X-ray densitometry for measurement of coral skeletal density. Coral Reefs 4: 95-100

Charles CD, Hunter DE, Fairbanks RG (1997) Interaction between the ENSO and the Asian monsoon in a coral record of tropical climate. Science 277: 925-928

Cohen AL, Hart SR (1997) The effect of colony topography on climate signals in coral skeleton. Geochim. Cosmochim. Acta 61: 3905-3912

Cole JE, Fairbanks RG (1990) The southern oscillation recorded in the $\delta^{18}O$ of corals from Tarawa Atoll. Paleoceanography 5: 669-683

Cook ER (1995) Temperature histories from tree rings and corals. Climate Dynamics (11): 211-22

Craig H (1957) Isotopic standards for carbon and oxygen and correction factors for mass-spectrometer analysis of carbon dioxide. Geochim. Cosmochim. Acta 12: 133-149

Craig H (1961) Standard for reporting concentrations of deuterium and oxygen-18 in natural waters. Science 133: 1833-1834

Craig H (1966) Isotopic composition and origin of the Red Sea and Salton Sea geothermal brines. Science 154: 1544-1548

Craig H, Gordon LI (1965) Deuterium and Oxygen 18 variations in the ocean and marine atmosphere. In: Stable isotope in oceanography studies and paleotemperatures. Spaleo. Cons. Noz. Ric. Les Geol. Nucl., Pisa, pp. 9-130

Crowley TJ, Quinn TM, Taylor FW, Henin C, Joannot P (1997) Evidence for a volcanic cooling signal in a 335-year coral record from New Caledonia; Paleoceanography 12: 633-639

Degens ET, Guillard RRL, Sackett WM, Hellebust JA (1968) Metabolic fractionation of carbon isotope in marine plankton. I-Temperature and resperation experiments. Deep-Sea Res. 15: 1-9

Delaygue G, Bard E, Rollion C, Jouzel J, Stievenard M, Duplessy J-C, Ganssen G (2001) Oxygen isotope/salinity relationship in the northern Indian Ocean. J. Geophys. Res. 106(C3): 4565-4574

de Villiers S, Nelson BK, Chivas AR (1995) Biological controls on coral Sr/Ca and $\delta^{18}O$ reconstructions of sea surface temperatures. Science 269: 1247-1249

Dodge RE, Brass GW (1984) Skeletal extension, density and calcification of the reef coral, *Montastrea annularis*: St. Croix, U.S. Virgin Islands. Bull. Mar. Sci. 34 (2): 288-307

Druffel ERM, Benavides LM (1986) Input of excess CO_2 to the surface ocean based on $^{13}C/^{12}C$ ratios in a banded Jamaican sclerosponge. Nature 321: 58-61

Dunbar RB, Wellington GM (1981) Stable isotopes in a branching coral monitor seasonal temperature variation. Nature 293: 453-455

Dunbar RB, Wellington GM, Colgan MW, Glynn PW (1994) Eastern Pacific sea surface temperature since 1600 A.D.: The $\delta^{18}O$ record of climate variability in Galapagos corals. Paleoceanograpghy 9: 291-315

Duplessy J-C, Blanc P-L, Be AWH (1981) Oxygen-18 enrichment of planktonic foraminifera due to gametogenic calcification below the euphotic zone. Science 213: 1247-1250

Duplessy J-C, Labeyrie L, Juillet-Leclerc A, Maitre F, Duprat J, Sarnthein M (1991) Surface salinity reconstruction of the North Atlantic during the Last Glacial Maximum. Oceanologica Acta 14: 311-324

Emiliani C (1954) Depth habitats of some species of pelagic foraminifera as indicated by oxygen ratios. American J. Science 252: 149-158

Emiliani C (1955) Pleistocene temperatures. J. Geol. 63: 538-578

Emiliani C (1966) Paleotemperature analysis of Caribbean cores, P6304-8 and P6304-9 and a generalized temperature curve for the past 425.000 years. J. Geol. 74: 109-124

Emiliani C (1971) Depth habitats of growth stages of pelagic foraminifera. Science 173: 1122-1124

Epstein S, Mayeda TK (1953) Variations of $^{18}O/^{16}O$ ratio in natural waters. Geochim. Cosmochim. Acta 4: 213-224

Epstein S, Buchsbaum R, Lowenstam HA, Urey HC (1953) Revised carbonate-water isotopic temperature scale. Geol. Soc. America Bull. 64: 1315-1322

Erez J (1978) Vital effect on stable-isotope composition seen in foraminifera and coral skeletons. Nature 273: 199-202

Erez J, Honjo S (1981) Comparison of isotopic composition of planktonic foraminifera in plankton tows, sediment traps and sediments. Palaeogeography, Palaeoclimatology, Palaeoecology 33: 129-156

Etheridge DM, Steele LP, Langenfelds RL, Francey RJ, Barnola J-M, Morgan VI (1996) Natural and anthropogenic changes in atmospheric CO_2 over the last 1000 years from air in Antarctic ice and firn. J. Geophys. Res. 101(D2): 4115–4128,

Fairbanks RG, Dodge RE (1979) Annual periodicity of the $^{18}O/^{16}O$ and $^{13}C/^{12}C$ ratios in the coral *Montastrea annularis*. Geochim. Cosmochim. Acta 43: 1009-1020

February EC, Stock WD (1999) Declining trend in the 13C/12C ratio of atmospheric carbon dioxide from tree rings of South Africa *Widdringtonia cedarbergensis*. Quat. Res. 52: 229-236

Felis T, Pätzold J, Wefer G, Fine M, Loya Y, Nawar AH (1998) First results of a coral-based history of recent climate in the northern Red Sea. Zbl Geol Paläont, I, H 1/2: 197-209

Felis T, Pätzold J, Loya Y, Moaz F, Nawar AH, and Wefer G (2000) A coral oxygen isotope record from the northern Red Sea documenting NAO, ENSO, and North Pacific teleconnection on Middle East climate variability since the year 1750. Paleoceanography 15: 679-694

Feng X (1999) Trends in intrinsic water-use efficiency of natural trees for the past 100-200 years: A response to atmospheric CO_2 concentration. Geochim. Cosmochim. Acta 63: 1891-1903

Fischer G, Wefer G (1996) Long-term observation of particle fluxes in the eastern Atlantic: seasonality, changes in flux with depth and comparison with the sediment record. In: Wefer G, Berger WH, Siedler G, Webb D (Eds.), The South Atlantic: Present and Past Circulation, Springer, Berlin, pp. 325-344

Fischer G, Schneider R, Müller PJ, Wefer G (1997) Anthropogenic CO_2 in southern ocean surface waters: evidence from stable organic carbon isotopes. Terra Nova 9: 153-157

Fischer G, Müller PJ, Wefer G (1998) Latitudinal δ^{13}Corg variations in sinking matter and sediments from the South Atlantic: effects of anthropogenic CO_2 and implications for palaeo-pCO_2 reconstructions. J. Mar. Sys. 17: 471-495

Fontugne MR, Calvert SE (1992) Late Pleistocene variability of the carbon isotopic composition of organic matter in eastern Mediterranean: Monitor of changes in carbon sources and atmospheric CO_2 concentrations. Paleoceanography 7: 1-20

Francey RJ, Allison CE, Etheridge DM, Trudinger CM, Enting IG, Leuenberger M, Langenfelds RL, Michel E, Steele LP (1999) A 1000-year high precision record of $\delta^{13}C$ in atmospheric CO_2. Tellus 51B: 170-193

Francois R, Altabet MA, Goericke R (1993) Changes in the $\delta^{13}C$ of surface water particulate organic matter across the subtropical convergence in the SW Indian Ocean. Global Biogeochem. Cycles 7: 627-644

Freeman KH, Hayes JM (1992) Fractionation of carbon isotope by phytoplankton and estimates of ancient CO_2 levels. Global Biogeochem. Cycles 6: 185-198

Friedli H, Lötscher H, Oeschger H, Siegenthaler U, Stauffer B (1986) Ice core record of the $^{13}C/^{12}C$ ratio of atmosphere CO_2 in the past two centuries. Nature 324: 237-238

Friedman GM (1968) Geology and geochmistry of reefs, carbonate sediments, and waters, Gulf of Aqaba (Elat), Red Sea. J. Sed. Petr. 38 (3): 895-919

Gagan MK, Chivas AR, Isdale PJ (1994) High-resolution isotopic records from corals using ocean temperature and mass-spawning chronometers. Earth Planet. Sci. Lett. 121: 249-258

Gagan MK, Chivas AR, Isdale PJ (1996) Timing coral-based climatic histories using ^{13}C enrichments driven by synchronized spawning. Geol. 24: 1009-1012

Gagan MK, Ayliffe LK, Hopley D, Cali JA, Mortimer GE, Chappell J, McCulloch MT, Head MJ (1998) Temperature and surface-ocean water balance of the Mid-Holocene tropical western Pacific. Science 279: 1014-1018

Gagan MK, Ayliffe LK, Beck JW, Cole JE, Druffel ERM, Dunbar RB, Schrag DB (2000) New views of tropical paleoclimates from corals. Quat. Sci. Rev. 19: 45-64

Ganssen G, Kroom D (1991) Evidence for Red Sea surface circulation from oxygen isotopes of modern surface waters and planktonic foraminiferal tests. Paleoceanography 6: 73-82

Genin A, Lazar B, Brenner S (1995) Vertical mixing and coral death in the Red Sea following the eruption of Mount Pinatubo. Nature 377: 507-510

Goreau TJ (1977) Coral skeletal chemistry: physiological and environmental regulation of stable isotopes and trace metals in *Montastrea annularis*. Proc. Roy. Soc. Lond B. 196: 291-315

Grossman EL, (1987) Stable isotopes in modern benthic foraminifera: A study of vital effect: J. Foram. Res. 17: 48-61

Grossman EL, Ku TL, (1986) Oxygen and carbon isotope fractionation in biogenic aragonite: Temperature effects. Chem. Geol. 59: 59-74

Grottoli AG, Wellington GM (1999) Effect of light and zooplankton on skeletal $\delta^{13}C$ values in the eastern Pacific corals *Pavona clavus* and *Pavona gigantea*. Coral Reefs 18: 29-41

GuildersonTP, Fairbanks RG, Rubenstone JL (1994) Tropical temperature variations since 20,000 years ago: modulating interhemispheric climate change. Science 236: 663-665

Gvirtzman G (1994) Fluctuations of sea level during the past 400 000 years: the record of Sinai, Egypt (northern Red Sea). Coral Reefs 13: 203-214

Gvirtzman G, Buchbinder B (1978) Recent and Pleistocene coral reefs and coastal sediments of the Gulf of Aqaba. Tenth International Congress on Sedimentology, Jerusalem, Excursion Guidebook, Part II, pp 161-191, International Association of Sedimentology, Jerusalem, Israel

Heiss GA (1996) Annual band width variation in *Porites* sp. from Aqaba, Gulf of Aqaba, Red Sea. Bull. Mar. Sci. 59: 393-403

Heiss GA, Dullo W-Chr, Joachimski M, Reijmer J, Schuhmacher H (1999) Increased seasonality in the Gulf of Aqaba, Red Sea recorded in the oxygen isotope record of a *Porites lutea* coral. Senckenbergiana Maritima 30: 17-26

Hemleben Ch, Spindler M, Anderson OR (1989) Modern planktonic foraminifera. Springer, New York, 363 pp

Hughen KA, Overpeck JT, Peterson LC, Trumbore S (1996) Abrupt deglacial climatic changes in the tropical Atlantic. Nature 380: 51-54

Hulings NC (1979) Currents in the Jordan Gulf of Aqaba. Dirasat 6: 21-33

Hulings NC (1989) A Review of Marine Science Research in the Gulf of Aqaba. Puplications of the Marine Science Station, Jordan, 267 pp

Hut G. (1987) Stable isotope reference samples for geochemical and hydrological investigations, Consultants' Group Meeting IAEA, Vienna, 16.-18.04.1985. In: Report to the Director General I (eds), Vienna, pp1-42

IPCC (1996) Climate Change 1995. The Science of Climate Change. Houghton JT, Meira Filho LG, Callander BA, Harris N, Kattenberg A, Maskall K (eds.). Cambridge University Press, Cambridge, 572 pp

Isdale P (1984) Fluorescent bands in massive corals record centuries of coastal rainfall. Nature 310: 578-579

Keeling CD, Whorf TP (2001) Atmospheric CO_2 records from sites in the SIO air sampling network. In Trends: A Compendium of Data on Global Change. Carbon Dioxide Information Analysis Center, Oak Ridge National Laboratory, U.S. Department of Energy, Oak Ridge, Tenn., U.S.A.

Keeling C, Bacastow R, Carter A, Piper S, Whorf T, Heimann M, Mook W, Roeloffzen H (1989) A three-dimensional model of atmospheric CO_2 transport based on observed winds 1. analysis of observational data. In Aspects Of Climate Variability In: The Pacific and the Western American pp. 165-236, DH, Petersen, Washington DC.

Keir R (1995) Is there a component of Pleistocene CO_2 change associated with carbonate dissolution cycles? Paleoceanography 10: 871-880

Klein R, Pätzold J, Wefer G, Loya Y (1992) Seasonal variations in the stable isotopic composition and the skeletal density pattern of the coral *Porites lobata* (Gulf of Eilat, Red Sea). Mar. Biol. 112: 259-263

Klein R, Pätzold J, Wefer G, Loya Y (1993) Depth-related timing of density band formation in *Porites* spp. corals from the Red Sea inferred from X-ray chronology and stable isotope composition. Mar. Ecol. Prog. Ser. 97: 99-104

Klein R, Tudhope AW, Chilcott CP, Pätzold J, Abdulkarim Z, Fine M, Fallick AE, Loya Y (1997) Evaluating southern Red Sea corals as a proxy record from the Asian monsoon. Earth Planet. Sci. Lett. 148: 381-394

Klein RT, Lohmann KC, Thayer CW (1996) Bivalve skeletons record sea-surface temperature and $\delta^{18}O$ via Mg/Ca and $^{18}O/^{16}O$ ratios. Geol. 24: 415-418

Klinker J, Reiss Z (1976) Observation on the circulation pattern in the Gulf of Elat (Aqaba), Red Sea. Israel J. Earth Sci. 25: 85-103

Klinker J, Reiss Z (1978) Nutrients and biomass distribution in the Gulf of Aqaba, (Elat) Red Sea, pp 53-64.

Knutson DW, Buddemeier RW, Smith SV (1972) Coral chronometers: seasonal growth bands in reefs corals. Science 177: 270-272

Kroopnick PM (1974) The dissolved O_2-CO_2-^{13}C system in the eastern equatorial Pacific. Deep-Sea Res. 21: 211-227

Kroopnick PM (1985) The distribution of ^{13}C of $\sum CO_2$ in the world oceans. Deep-Sea Res. 32: 57-84

Krumgalz BS, Erez J, Chen CTA (1990) Anthropogenic CO_2 penetration in the northern Red Sea and in the Gulf of Aqaba. Oceanologica Acta 13 (3): 283-290

Kuhnert H, Pätzold J, Wyrwoll KH. (2000) Monitoring climate variability over the past 116 years in coral oxygen isotope from Ningaloo Reef, Western Australia. Int. J. Earth Sci. 88: 725-732

Land LS, Lang J, Barnes D (1975) Extension rate: A primary control on the isotopic composition form West India (Jamaica) scleractinian reef coral skeleton. Mar. Biol. 33: 221-233

Laws E, Popp B, Bidigare R, Kennicutt M, Macko S (1995) Dependence of phytoplankton carbon isotopic composition on growth rate and $[CO_2]$aq: Theoretical considerations and experimental results. Geochim. Cosmochim. Acta 59 (6): 1131-1138

Lea DW, Shen GT, Boyle EA (1989) Coralline barium records temporal variability in equatorial Pacific upwelling. Nature 340: 373-376

Leavitt SW (1994) South America tree rings show declining $\delta^{13}C$ trend. Tellus 46B: 152-157

Leder JJ, Swart PK, Szmant AM, Dodge RE (1996) The origin of variations in the isotopic record of scleractinian corals: I. Oxygen; Geochim. Cosmochim. Acta 60: 2857-2870

Leger G, Millot C, Mahasneh D, Vaugelas J, Abu-Hilal A, Joabert J (1986) Measurement of currents in near shore area of the Jordanian coast of the Gulf of Aqaba. Univ. de Nice. Internal report. pp18

Levanon-Spanier I, Padan E, and Reiss Z (1979) Primary production in a desert-enclosed sea the Gulf of Aqaba, Red Sea. Deep-Sea Res. 26: 673-685

Linsely BK, Dunbar RB, Wellington GM, and Mucciarone DA (1994) A coral-based reconstruction of Inter Tropical Convergence Zone variability over Central America since 1707. J. Geophys. Res. 99: 9977-9994

Lorian D, Erez J, Lazar B (1992) Stable carbon isotope in the reef ecosystem of the Gulf of Eilat-Red Sea. In: Richmond RH (ed) Proc 7th Int Coral Reef Symp. University of Guam, Mangilao, Guam, p 364

Lough JM, Barnes DJ (2000) Environmental controls on growth of the massive coral *Porites*. J. Exp. Mar. Biol. Ecol. 245: 225-243

Lynch-Stieglitz J, Stocker TF, Broecker WS, Fairbanks RG (1995) The influence of air-sea exchange on ^{13}C of CO_2 on the in the surface ocean: Observations and Modeling, Global Biogeochem. Cycles 9: 653-665

Manasreh RS (1998) Water circulation in the Gulf of Aqaba, Red Sea. M.sc. thesis, Yarmouk University, Irbid, Jordan, 112 pp

McConnaughey T (1989) ^{13}C and ^{18}O isotopic disequilibrium in biological carbonates: I. Patterns. Geochim. Cosmochim. Acta 53: 151-162

McCulloch MT, Gagan MK, Mortimer GE, Chivas AR, Isdale PJ (1994) A high resolution Sr/Ca and $\delta^{18}O$ coral record from the Great Barrier Reef, Australia, and the 1982-1983 El Nino. Geochim. Cosmochim. Acta 58: 2747-2754

McCulloch MT, Tudhope AW, Esat TM, Mortimer GE, Chappell J, Pillans B, Chivas AR, Omura A (1999) Coral record of equatorial sea-surface temperature during the penultimate deglaciation at Huon peninsula. Science 283: 202-204

Morimoto M, Kayanne H, Yonekura N, Abe O, Matsumoto E (1997) Effect of seasonal difference in growth rate of coral skeletons on oxygen isotope records. Coral Climatology by Annual Bands. Proceeding of Third International Marine Science Symposium (Matsumoto, E., ed) 30-34, Japan, Marine Science Foundation, Tokyo

Moustafa YA (2000) Paleoclimatic reconstructions of the northern Red Sea during the Holocene inferred from stable isotope records of modern and fossil corals and molluscs, Berichte Fachbereich Geowissenschaften Universität Bremen 153, 102 pp., Universität Bremen, Bremen, Germany

Moustafa YA, Pätzold J, Loya Y and Wefer G (2000) Mid-Holocene stable isotope record of corals from the Northern Red Sea. Int. J. Earth Sci. 88: 742-751

Mulitza S, Arz H, Kemle-von Mücke S, Moos C, Niebler H-S, Pätzold J, Segl M (1999) The South Atlantic carbon isotope record of planktic foraminifera. In: Fischer G, Wefer G (eds.), Use of Proxies in Paleoceanography: Examples from the South Atlantic. Springer-Verlag, Berlin, New York, pp 427-445

Müller PJ, Schneider RR, Ruhland G (1994) Late Quaternary pCO_2 variations in the Angola current: evidence from organic carbon $\delta^{13}C$ and alkenon temperatures. In Carbon Cycling in the Glacial Ocean: Constraints on the Ocean's Role in Global Climate Change (Zahn, R., Kaminski, M. & Pedersen, T.F., eds.) NATO ASI Series, I 17, Springer, Berlin, 343-366 pp

NOAA (1993) Coral records of ocean atomsphere variability: report from the workshop on coral paleoclimate reconstruction. (NOAA Climate and Global Change Program)

Nozaki Y, Rye DM, Turekian KK, Dodge RE (1978) A 200-year record of carbon-13 ad carbon-14 variations in a Bermuda coral. Geophys. Res. Lett. 5: 825-828

Oeschger H, Siegenthaler U, Schotterer U, Gugelmann A (1975) A box diffusion model to study the carbon dioxide in nature. Tellus 27: 168-192

Paillard D, Labeyrie L, Yiou P (1996) Macintosh Program Performs time-series analysis. Eos. Trans. AGU, 77 (39), 379

Paldor N, Anati DA (1979) Seasonal variations of temperature and salinity in the Gulf of Elat (Aqaba). Deep-Sea Res. 26 (6A): 661-672

Pätzold J (1984) Growth rhythms recorded in stable isotope and density bands in reef coral *Porites lobata* (Cebu, Philippines). Coral Reefs 3: 87-90

Pätzold J (1986) Temperature and CO_2 changes in tropical surface waters of the Philippines during the past 120 years: record in the stable isotopes of hermatypic corals; Berichte-Reports, Geol Paläont Inst Univ Kiel (in German), Nr. 12, 92p., 29 Figs., 5 Tab., 1 Taf., Kiel

Pätzold J, Halbach PE, Hempel G, Weikert H (2000), Östliches Mittelmeer- Nördliches Rotes Meer 1999. Cruise No. 44 22 January-16 May 1999, Universität Hamburg 240 pp

Popp BN, Takigiku R, Hayes JM, Louda JW, Baker EW (1989) The post Paleozoic chronology and mechanism of $\delta^{13}C$ depletion in primary marine organic matter. Am. J. Sci. 289: 436-454

Quay PD, Tilbrook B, Wong CS (1992) Oceanic uptake of fossil fuel CO_2: Carbon-13 evidence. Science 256: 74-79

Quinn TM, Taylor FW, Crowley TJ, Link SM (1996) Evaluation of sampling resolution in coral stable isotope records: A case study using records from New Caledonia and Tarawa. Paleoceanography 11: 529-542

Quinn TM, Crowely TJ, Taylor FW, Henin C, Joannot P, Join Y (1998) A multicentury stable isotope record from a New Caledonia coral: interannual and decadal sea surface temperature variability in the southwest Pacific since 1657 A. D. Paleoceanography 13(4): 412-426

Rau GH (1994) Variations in sedimentary organic $\delta^{13}C$ as a proxy for past changes in ocean and atmospheric CO_2 concentrations: In Carbon Cycling in the Glacial Ocean:

Constraints on the Ocean's Role in Global Climate Change (Zahn, R., Kaminski, M. and Pedersen, T.F., eds.) NATO ASI Series, I 17, Springer, Berlin, 307-321

Rau GH, Takahashi T, Des Marais DJ (1989) Latitudinal variations in plankton $\delta^{13}C$: Implications for CO_2 and productivity in past oceans. Nature 341: 516-518

Ravelo AC, Fairbanks RG (1995) Carbon isotopic fractionation in multiple species of planktonic foraminifera from core tops in the tropical Atlantic. J. Foram. Res. 25 (1): 53-74

Reiss Z, Hottinger L (1984) The Gulf of Aqaba: Ecological Micropaleontology. Springer-Verlag, Berlin, 345 pp

Rimbu N, Lohmann G, Felis T, Pätzold J (2001) Arctic oscillation signature in a Red Sea coral. Geophys. Res. Lett. 28 (15): 2959-2962

Romanek CS, Grossman EL, Morse JW (1992) Carbon isotope fractionation in synthetic aragonite and calcite: effects of temperature and precipitation rate: Geochim. Cosmochim. Acta 56: 419-430

Rosenthal Y, Dahan M, Shemesh A (2000) Southern ocean contributions to glacial-interglacial changes of atmospheric pCO_2: An assessment of carbon isotope records in diatoms. Paleoceanography 15: 65-75

Rostek F, Ruhland G, Bassinot FC, Müller PJ, Labeyrie LD, Lancelot Y, Bard E (1993) Reconstructing Indian Ocean surface temperature and salinity using ^{18}O and alkenone records. Nature 364: 319-321

Schneider RC, Smith SV (1982) Skeletal Sr content and density in *Porites* spp. In relation to environmental factors. Mar. Biol. 66: 121-131

Schuhmacher H, Kiene W, Dullo W (1995) Factors controlling Holocene reef growth: An interdisciplinary approach. Facies 32: 145-188

Scoffin TP, Tudhope AW, Brown BE, Chansang H, Cheeney RF (1992) Patterns and possible environmental controls of skeletogenesis of *Porites lutea*, South Thailand. Coral Reefs 11: 1-11

Seibold E, Berger W (1993) The Sea Floor, An Introduction to Marine Geology. Springer-Verlag, Berlin 356 pp.

Shackleton NJ (1967) Oxygen isotope analysis and Pleistocene temperatures re-assessed. Nature 215: 15-17

Shackleton NJ (1974) Attainment of isotopic equilibrium between ocean water and benthonic foraminifera genus *Uvigerina*: Isotopic changes in the ocean during the last glacial. In:

Les Methodes quantitatives d'etude des variation du climat au cours du Pleistocene. Coll. Int. CNRS Paris 119: 203-210

Shackleton NJ, Vincent E (1978) Oxygen and carbon isotope studies in recent foraminifera from southwest Indian Ocean. Mar. Micropaleontol. 3: 1-13

Shackleton NJ, Hall MA, Shuxi C (1983) Carbon isotope data in core V19-30 confirm reduced carbon-dioxide concentration in the ice age atmosphere. Nature 306: 319-322

Shemesh A, Luz B, Erez J (1994) Carbon isotopes, dissolved oxygen, and the carbonate system in the northern Gulf of Aqaba. Isr. J. Earth. Sci. 43: 145-155

Shen GT, Boyle EA (1987) Lead in corals: reconstruction of historical industrial fluxes to the surface ocean. Earth Planet. Sci. Lett. 82: 289-304

Shen, GT, Boyle EA (1988) Determination of lead, cadmium, and other trace metals in annually-banded corals. Chem. Geol. 67: 47-62

Shen GT, Cole JE, Lea DW, Linn LJ, McConnaughey TA, Fairbanks RG (1992) Surface ocean variability at Galapagos from 1936-1982: Calibration of geochemical tracers in corals. Paleoceanography 7: 563-583

Shulmeister, J. & Lees, B.G. (1995) Pollen evidence from tropical Australia for the onset of an ENSO dominated climate at circa 4000 yrs BP. Holocene 5: 10-18

Spero HJ (1992) Do planktic foraminifera accurately record changes in the carbon isotopic composition of seawater ∑CO2? Mar. Micropaleontol. 19: 275-285

Spero HJ, Lerche I, Williams DF (1991) Opening the carbon isotope 'vital effect' black box. 2: Quantitave model for interpreting foraminiferal carbon isotope data. Paleoceanography 6: 639-655

Strasser A, Strohmenger C, Davaud E, Bach A (1992) Sequential evolution and diagenesis of Pleistocene coral reefs (South Sinai, Egypt). Sed. Geol. 78: 59-79

Stuiver M, Braziunas TF (1993) Modelling atmospheric ^{14}C influences and ^{14}C ages of marine samples to 10,000 BC. Radiocarbon 35: 137-189

Stuiver M, Reimer PJ, Bard E, Beck WE, Burr GS, Hughen KA, Kromer B, McCormac FG, v. d. Plicht J, Spurk M (1998a) INTCAL98 radiocarbon age calibration 0-24,000 BP. Radiocarbon 40: 1041-1083

Stuiver M, Reimer PJ, Braziunas TF (1998b) High-precision radiocarbon age calibration for terrestrial and marine samples. Radiocarbon 40: 1127-1151

Suzuki A, Yukino I, Kawahata H (1999) Temperature- skeletal $\delta^{18}O$ relationship of Porites australiensis from Ishigaki Island, the Ryukyus, Japan. Geochem. J. 33(6): 419-428.

Swart PK (1983) Carbon and oxygen isotope fractionation in Scleractinian corals: A review. Earth Sci. Rev. (19): 51-80

Taylor RB, Barnes DJ, Lough JM (1993) Simple models of density band formation in massive corals. J. Exp. Mar. Biol. Ecol. 167: 109-125

Taylor RB, Barnes DJ, Lough JM (1995) On the inclusion of trace materials into massive coral skeletons.1. Material occurring in the environment in short pulses. J. Exp. Mar. Biol. Ecol. 85: 255-278

Urey HC (1947) The thermodynamic properties of isotopic substances. J. Chem. Soc.: 562-581

Veron JEN (1993) A biogeographic database of hermatypic corals: species of the Central Indo-Pacific genera of the world. Australian Institute of Marine Science, Townsville, 433pp

Vincent E, Berger WH (1981) Planktonic foraminifera and their use in paleoceanography. In: Emiliani C (ed) The Sea, Vol. 7. Wiley-Interscience, New York, pp 1025-1119

Von Rad U, Schaaf M, Michels KH, Schulz H, Berger WH, Sirocko F (1999) A 5000-yr record of climate change in varved sediments from the oxygen minimum zone off Pakistan, Northeastern Arabian Sea. Quat. Res. 51: 39-53

Weber JN, Woodhead PMJ (1972) Temperature dependence of oxygen-18 concentration in reef coral carbonates. J. Geophys. Res. 77: 463-473

Wefer G, Berger WH (1991) Isotope paleontology: growth and composition of extant calcareous species. Mar. Geol. 100: 207-248

Wefer G, Berger WH, Bijma J, Fischer G (1999) Clues to Ocean History: a Brief Overview of Proxies. In: Fischer G, Wefer G (eds.), Use of Proxies in Paleoceanography: Examples from the South Atlantic. Springer-Verlag, Berlin, New York, pp 1-68

Weil S, Buddemeier R, Smith S, Kroopnick P (1981) The stable isotopic composition of coral skeletons: controlled by environmental variables. Geochim. Cosmochim. Acta 45: 1174-1153

Wellington G, Glynn P (1983) Environmental influences on skeletal banding in Eastern Pacific (Panama) corals. Coral Reefs 1: 215-222

Wellington GM, Dunbar RB (1995) stable isotopic signiture of ENSO in eastern tropical Pacific reef corals. Coral Reefs 14: 5-25

Wellington GM, Dunbar RB, Merlen G (1996) Calibration of stable isotope signature in Galapagos corals. Paleoceanography 11: 467-480

Williams DF, Sommer MA (1977) Carbon isotopic compositions of recent planktonic foraminifera of the Indian Ocean. Earth Plan. Sci. Lett. 36: 391-403

Winter A, Goenaga C, Maul GA (1991) Carbon and Oxygen isotope time series from an 18-year Caribbean reef coral. J. Geophys. Res. 96 (C9): 16673-16678

Wolff T, Grieger B, Hale W, Dürkoop A, Mulitza S, Pätzold J, Wefer G (1999) On the reconstruction of paleosalinities. In: Fischer G, Wefer G (eds), Use of Proxies in Paleoceanography: Examples from the South Atlantic. Springer, Berline, New York, pp. 207-228

Wolf-Gladrow DA, Riebesell U, Burkhardt S, Bijma J (1999) Direct effects of CO_2 concentration on growth and isotopic composition of marine plankton. Tellus 51B: 461-476

Wolf-Vecht A, Paldor N, Brenner S (1992) Hydrographic indicators of advection/convection effects in the Gulf of Eilat. Deep-Sea Res. 39: 1393-1401

7. Appendix: Data tables

7.1. Coral records

7.1.1. Stable isotope data

7.1.1.1. Coarse resolution records

Profile Aq-19A		
Age (years)	$\delta^{18}O$ ‰ (VPDB)	$\delta^{13}C$ ‰ (VPDB)
1999.208	-2.860	-3.090
1999.125	-3.076	-3.401
1999.042	-3.308	-3.625
1998.958	-3.627	-3.138
1998.875	-3.594	-3.126
1998.792	-3.503	-3.439
1998.708	-3.609	-3.314
1998.625	-3.630	-3.079
1998.542	-3.369	-3.004
1998.458	-3.249	-3.046
1998.375	-3.154	-2.991
1998.292	-3.091	-2.804
1998.208	-2.850	-2.960
1998.125	-2.909	-3.036
1998.042	-3.086	-3.695
1997.958	-3.335	-3.792
1997.875	-3.436	-3.667
1997.792	-3.412	-3.445
1997.708	-3.464	-3.324
1997.625	-3.515	-3.213
1997.542	-3.477	-3.140
1997.458	-3.352	-3.178
1997.375	-3.227	-3.095
1997.292	-3.089	-3.022
1997.208	-2.950	-2.950
1997.125	-3.050	-3.250
1997.042	-3.080	-3.393
1996.958	-3.166	-3.414
1996.875	-3.388	-3.347
1996.792	-3.525	-3.302
1996.708	-3.467	-3.502
1996.625	-3.344	-3.755
1996.542	-3.238	-3.513
1996.458	-3.115	-3.383
1996.375	-2.976	-3.027
1996.292	-2.831	-2.440
1996.208	-2.740	-3.040
1996.125	-2.808	-3.583
1996.042	-2.859	-3.739
1995.958	-3.130	-3.470
1995.875	-3.333	-3.286
1995.792	-3.439	-3.225
1995.708	-3.467	-3.192
1995.625	-3.421	-3.149
1995.542	-3.204	-3.366
1995.458	-2.979	-3.354
1995.375	-2.891	-3.363
1995.292	-2.775	-3.238
1995.208	-2.610	-3.010
1995.125	-2.850	-3.270
1995.042	-3.148	-3.138
1994.958	-3.411	-2.953
1994.875	-3.537	-2.817
1994.792	-3.481	-2.761
1994.708	-3.555	-2.821
1994.625	-3.519	-2.827
1994.542	-3.387	-2.787
1994.458	-3.255	-2.759
1994.375	-2.999	-2.589
1994.292	-2.745	-2.433
1994.208	-2.720	-2.580
1994.125	-2.850	-3.268
1994.042	-3.118	-3.589
1993.958	-3.244	-3.209
1993.875	-3.268	-2.836
1993.792	-3.313	-2.926
1993.708	-3.366	-2.865
1993.625	-3.420	-2.718
1993.542	-3.427	-2.693
1993.458	-3.284	-2.715
1993.375	-3.145	-2.845
1993.292	-2.985	-2.823
1993.208	-2.600	-2.200
1993.125	-2.600	-2.596
1993.042	-2.600	-2.992
1992.958	-2.927	-3.163
1992.875	-3.133	-3.228
1992.792	-3.166	-3.151
1992.708	-3.297	-2.862
1992.625	-3.444	-2.538
1992.542	-3.402	-2.433
1992.458	-3.205	-2.410
1992.375	-2.686	-2.487
1992.292	-2.497	-2.737
1992.208	-2.450	-3.060
1992.125	-2.723	-3.287
1992.042	-2.953	-3.298
1991.958	-3.132	-3.054
1991.875	-3.237	-3.093
1991.792	-3.337	-3.092
1991.708	-3.446	-2.951
1991.625	-3.455	-2.820
1991.542	-3.383	-2.716
1991.458	-3.127	-2.697
1991.375	-2.946	-2.616
1991.292	-2.803	-2.503
1991.208	-2.660	-2.390
1991.125	-2.711	-2.831
1991.042	-2.802	-3.354
1990.958	-2.840	-3.534
1990.875	-2.865	-3.450
1990.792	-3.020	-3.244
1990.708	-3.241	-3.158
1990.625	-3.263	-3.177
1990.542	-3.259	-3.089
1990.458	-3.294	-3.115
1990.375	-3.091	-2.799
1990.292	-2.992	-2.965
1990.208	-2.730	-3.080

Profile El-15A		
Age (years)	$\delta^{18}O$ ‰ (VPDB)	$\delta^{13}C$ ‰ (VPDB)
1996.208	-2.570	-3.360
1996.125	-2.670	-3.597
1996.042	-2.771	-3.806
1995.958	-2.876	-3.769
1995.875	-2.978	-3.661
1995.792	-3.062	-3.281
1995.708	-3.115	-3.027
1995.625	-3.096	-3.032
1995.542	-3.022	-2.684
1995.458	-2.859	-2.466
1995.375	-2.503	-2.752
1995.292	-2.411	-2.851
1995.208	-2.320	-2.950
1995.125	-2.341	-3.110
1995.042	-2.566	-3.256
1994.958	-2.939	-3.329
1994.875	-3.217	-2.973
1994.792	-3.283	-2.847
1994.708	-3.254	-2.694
1994.625	-3.217	-2.449
1994.542	-3.010	-2.217
1994.458	-2.725	-2.110
1994.375	-2.575	-2.196
1994.292	-2.445	-2.306
1994.208	-2.410	-2.340
1994.125	-2.443	-3.090
1994.042	-2.530	-3.340
1993.958	-2.630	-3.465
1993.875	-2.767	-3.493
1993.792	-2.933	-3.380
1993.708	-3.000	-3.280
1993.625	-3.067	-3.180
1993.542	-3.047	-3.100
1993.458	-3.030	-3.047
1993.375	-3.030	-3.008
1993.292	-2.907	-2.697
1993.208	-2.090	-2.280
1993.125	-2.301	-2.324
1993.042	-2.541	-3.381
1992.958	-2.715	-3.514
1992.875	-2.847	-3.631
1992.792	-2.940	-3.725
1992.708	-2.982	-3.066
1992.625	-3.149	-2.773
1992.542	-2.968	-2.401
1992.458	-2.775	-2.494
1992.375	-2.496	-2.673
1992.292	-2.317	-2.864
1992.208	-2.310	-2.990
1992.125	-2.521	-3.201
1992.042	-2.727	-3.428
1991.958	-2.972	-3.413
1991.875	-3.100	-3.185
1991.792	-3.081	-2.978
1991.708	-3.260	-2.754
1991.625	-3.214	-3.113
1991.542	-2.870	-2.665
1991.458	-2.870	-2.425
1991.375	-2.739	-1.934
1991.292	-2.606	-1.875
1991.208	-2.580	-2.420
1991.125	-2.656	-2.979
1991.042	-2.738	-3.400
1990.958	-2.837	-3.470
1990.875	-2.925	-3.440
1990.792	-3.003	-3.336
1990.708	-3.082	-3.231
1990.625	-3.125	-3.046
1990.542	-2.938	-2.352
1990.458	-2.722	-2.094
1990.375	-2.466	-2.438
1990.292	-2.369	-2.602
1990.208	-2.340	-2.690
1990.125	-2.560	-3.197
1990.042	-2.750	-3.490
1989.958	-2.910	-3.570
1989.875	-2.920	-3.490
1989.792	-2.930	-3.410
1989.708	-3.050	-3.340
1989.625	-2.970	-2.860
1989.542	-2.930	-2.920
1989.458	-2.890	-2.980
1989.375	-2.710	-2.379
1989.292	-2.482	-2.527
1989.208	-2.380	-2.460
1989.125	-2.619	-3.098
1989.042	-2.773	-3.205
1988.958	-2.897	-3.010
1988.875	-3.092	-2.886
1988.792	-3.252	-2.802
1988.708	-3.277	-2.874
1988.625	-3.207	-3.052
1988.542	-3.120	-3.080
1988.458	-2.917	-2.924
1988.375	-2.770	-2.768
1988.292	-2.604	-2.548
1988.208	-2.360	-2.210
1988.125	-2.491	-2.823
1988.042	-2.640	-3.305
1987.958	-2.807	-3.311
1987.875	-2.883	-3.230
1987.792	-3.012	-3.098
1987.708	-3.189	-2.965
1987.625	-3.169	-3.019
1987.542	-3.018	-3.149
1987.458	-2.870	-2.846
1987.375	-2.724	-2.343
1987.292	-2.555	-2.106
1987.208	-2.450	-2.600

Profile El-15B		
Age (years)	$\delta^{18}O$ ‰ (VPDB)	$\delta^{13}C$ ‰ (VPDB)
1996.208	-2.240	-2.640
1996.083	-2.597	-2.694
1995.917	-3.075	-2.766
1995.750	-3.058	-2.296
1995.583	-2.981	-1.806
1995.417	-2.714	-1.377
1995.250	-2.447	-0.948
1995.083	-3.074	-2.445
1994.917	-3.300	-2.652
1994.750	-3.140	-1.892
1994.583	-2.848	-1.707
1994.417	-2.512	-1.717
1994.250	-2.175	-1.727
1994.083	-2.377	-2.418
1993.917	-2.726	-1.041
1993.750	-3.060	-2.390
1993.583	-3.060	-2.450
1993.417	-2.554	-2.494
1993.250	-2.048	-2.539
1993.083	-2.182	-2.670
1992.917	-2.532	-2.830
1992.750	-2.882	-2.990
1992.583	-2.808	-2.671
1992.417	-2.591	-2.191
1992.250	-2.375	-1.711
1992.083	-2.532	-2.276
1991.917	-2.820	-2.717
1991.750	-2.914	-2.559
1991.583	-2.675	-2.086
1991.417	-2.642	-2.061
1991.250	-2.166	-2.676
1991.083	-2.406	-3.184
1990.917	-2.875	-3.618
1990.750	-2.708	-3.245
1990.583	-2.541	-2.872
1990.417	-2.388	-2.796
1990.250	-2.254	-3.071

Profile El-15C		
Age (years)	$\delta^{18}O$ ‰ (VPDB)	$\delta^{13}C$ ‰ (VPDB)
1996.083	-1.972	-2.686
1995.917	-2.207	-2.758
1995.750	-2.353	-2.631
1995.583	-2.293	-2.514
1995.417	-2.176	-2.206
1995.250	-1.933	-2.301
1995.083	-1.995	-2.654
1994.917	-2.454	-2.969
1994.750	-2.878	-3.023
1994.583	-2.769	-2.777
1994.417	-2.561	-2.552
1994.250	-1.847	-2.311
1994.083	-2.291	-2.903
1993.917	-2.703	-2.955
1993.750	-2.313	-2.211
1993.583	-2.107	-2.603
1993.417	-2.037	-2.382
1993.250	-1.751	-2.247
1993.083	-1.997	-2.475
1992.917	-2.447	-2.775
1992.750	-2.489	-2.797
1992.583	-2.394	-2.727
1992.417	-2.145	-2.657
1992.250	-1.845	-2.588
1992.083	-1.855	-2.590
1991.917	-1.935	-2.602
1991.750	-1.915	-2.568
1991.583	-2.099	-2.680
1991.417	-2.217	-2.719
1991.250	-1.924	-2.392
1991.083	-2.185	-2.475
1990.917	-2.506	-2.770
1990.750	-2.673	-2.970
1990.583	-2.701	-2.856
1990.417	-2.471	-2.626
1990.250	-1.993	-2.716

Profile Aq-19C		
Age (years)	$\delta^{18}O$ ‰ (VPDB)	$\delta^{13}C$ ‰ (VPDB)
1999.083	-1.939	-2.616
1998.917	-2.187	-2.616
1998.750	-2.435	-2.616
1998.583	-2.323	-2.500
1998.417	-2.089	-2.346
1998.250	-1.855	-2.191
1998.083	-1.890	-2.021
1997.917	-1.902	-1.637
1997.750	-1.961	-1.418
1997.583	-2.265	-1.766
1997.417	-2.467	-1.731
1997.250	-2.064	-1.664
1997.083	-2.059	-1.905
1996.917	-2.259	-2.178
1996.750	-2.641	-2.231
1996.583	-2.500	-2.217
1996.417	-2.202	-2.110
1996.250	-1.959	-1.786
1996.083	-2.170	-1.902
1995.917	-2.534	-2.165
1995.750	-2.608	-2.433
1995.583	-2.585	-2.703
1995.417	-2.367	-2.612
1995.250	-2.084	-2.401
1995.083	-2.294	-2.526
1994.917	-2.726	-2.953
1994.750	-2.981	-3.404
1994.583	-2.795	-3.525
1994.417	-2.469	-3.182
1994.250	-2.154	-2.878

7.1.1.2. Fine-resolution records

Profile Aq7	
Age (years)	$\delta^{18}O$ (‰) VPDB
2000.459	-3.06
2000.421	-3.06
2000.382	-3.03
2000.344	-2.95
2000.306	-2.8
2000.267	-2.82
2000.229	-2.64
2000.191	-2.68
2000.152	-2.82
2000.114	-2.76
2000.075	-2.81
2000.037	-2.88

1999.999	-2.98
1999.96	-3.05
1999.922	-3.18
1999.883	-3.2
1999.86	-3.34
1999.837	-3.42
1999.814	-3.48
1999.791	-3.52
1999.768	-3.59
1999.749	-3.56
1999.73	-3.56
1999.704	-3.64
1999.679	-3.69
1999.653	-3.75

1999.615	-3.7
1999.576	-3.61
1999.538	-3.49
1999.499	-3.36
1999.461	-3.38
1999.423	-3.21
1999.385	-3.04
1999.347	-2.96
1999.309	-2.85
1999.271	-2.88
1999.233	-2.87
1999.195	-2.85

Profile Aq19/3	
Age (years)	$\delta^{18}O$ (‰) VPDB
2000.481	-3.04
2000.462	-3.08
2000.442	-3.09
2000.423	-3.03
2000.405	-3.04
2000.371	-3.02
2000.353	-2.93
2000.336	-2.91
2000.318	-2.77
2000.301	-2.69
2000.283	-2.58
2000.266	-2.55
2000.249	-2.52
2000.231	-2.51
2000.204	-2.54
2000.178	-2.57
2000.151	-2.61
2000.125	-2.59
2000.099	-2.63
2000.072	-2.63
2000.046	-2.62
2000.019	-2.70
2000.000	-2.71

1999.961	-2.78
1999.942	-2.84
1999.923	-2.91
1999.904	-2.95
1999.884	-3.03
1999.865	-3.11
1999.846	-3.16
1999.827	-3.22
1999.807	-3.24
1999.788	-3.30
1999.762	-3.30
1999.739	-3.31
1999.715	-3.34
1999.692	-3.40
1999.682	-3.49
1999.673	-3.53
1999.654	-3.59
1999.635	-3.59
1999.615	-3.61
1999.596	-3.54
1999.558	-3.53
1999.545	-3.46
1999.532	-3.38
1999.507	-3.21
1999.494	-3.11
1999.481	-3.05

1999.462	-3.07
1999.443	-2.98
1999.423	-2.98
1999.404	-2.99
1999.385	-2.91
1999.365	-2.88
1999.346	-2.85
1999.327	-2.73
1999.307	-2.70
1999.288	-2.64
1999.269	-2.62
1999.249	-2.58
1999.230	-2.53
1999.211	-2.55
1999.191	-2.54
1999.172	-2.54
1999.153	-2.50
1999.132	-2.53
1999.112	-2.52
1999.092	-2.59
1999.072	-2.61
1999.052	-2.65
1999.031	-2.62
1999.011	-2.73

Profile Aq19/4	
Age (years)	$\delta^{18}O$ ‰ (VPDB)
2000.481	-3.06
2000.450	-3.12
2000.418	-3.05
2000.387	-2.97
2000.356	-2.89
2000.325	-2.82
2000.293	-2.63
2000.262	-2.54
2000.231	-2.48
2000.204	-2.49
2000.178	-2.49
2000.151	-2.56
2000.125	-2.56
2000.099	-2.65
2000.072	-2.66
2000.046	-2.67
2000.019	-2.78
1999.981	-2.79
1999.942	-2.95
1999.904	-3.03
1999.875	-3.06
1999.846	-3.16
1999.817	-3.20
1999.788	-3.26
1999.763	-3.26
1999.737	-3.28
1999.712	-3.26
1999.693	-3.37
1999.673	-3.47
1999.654	-3.62
1999.615	-3.64
1999.587	-3.56
1999.558	-3.49
1999.543	-3.37
1999.522	-3.20
1999.502	-3.05
1999.481	-2.96
1999.442	-2.97
1999.402	-2.88
1999.362	-2.85
1999.322	-2.77
1999.282	-2.64
1999.242	-2.57
1999.202	-2.53
1999.162	-2.50
1999.122	-2.50
1999.082	-2.49
1999.042	-2.49
1999.002	-2.45
1998.961	-2.55
1998.920	-2.56
1998.879	-2.59
1998.838	-2.71
1998.797	-2.82
1998.756	-2.83
1998.715	-2.85
1998.674	-2.94
1998.633	-3.01
1998.593	-3.09
1998.551	-3.13

Profile Aq29	
Age (years)	$\delta^{18}O$ ‰ (VPDB)
2000.481	-3.01
2000.447	-3.02
2000.413	-3.01
2000.380	-2.84
2000.346	-2.86
2000.317	-2.80
2000.288	-2.69
2000.231	-2.61
2000.204	-2.61
2000.177	-2.63
2000.149	-2.64
2000.122	-2.74
2000.095	-2.75
2000.068	-2.77
2000.040	-2.74
2000.019	-2.85
2000.000	-2.85
1999.981	-2.90
1999.962	-2.95
1999.942	-2.98
1999.923	-3.07
1999.904	-3.14
1999.879	-3.16
1999.824	-3.22
1999.769	-3.34
1999.712	-3.30
1999.693	-3.35
1999.683	-3.40
1999.673	-3.41
1999.654	-3.45
1999.644	-3.46
1999.635	-3.37
1999.625	-3.42
1999.615	-3.42
1999.605	-3.34
1999.596	-3.19
1999.577	-3.11
1999.558	-3.13
1999.532	-3.09
1999.507	-3.07
1999.481	-2.89
1999.462	-2.91
1999.443	-2.84
1999.424	-2.79
1999.405	-2.80
1999.386	-2.79
1999.367	-2.71
1999.348	-2.66
1999.329	-2.62
1999.310	-2.58
1999.292	-2.61
1999.274	-2.65
1999.256	-2.74
1999.238	-2.75
1999.220	-2.77
1999.202	-2.74
1999.184	-2.76
1999.165	-2.86
1999.147	-2.91
1999.129	-2.92
1999.111	-3.00

Profile Aq42	
Age (years)	$\delta^{18}O$ ‰ (VPDB)
2000.459	-2.92
2000.421	-2.94
2000.382	-2.86
2000.306	-2.02
2000.229	-1.99
2000.168	-2.08
2000.106	-2.26
2000.045	-2.34
1999.983	-2.28
1999.922	-2.66
1999.909	-2.75
1999.896	-2.80
1999.883	-2.79
1999.832	-2.90
1999.781	-2.97
1999.730	-2.93
1999.717	-3.16
1999.704	-3.13
1999.692	-3.22
1999.679	-3.19
1999.666	-3.23
1999.653	-3.26
1999.614	-3.22
1999.576	-3.18
1999.538	-3.07
1999.499	-2.76
1999.461	-2.86
1999.423	-2.64
1999.384	-2.43
1999.346	-2.34
1999.268	-2.26
1999.229	-2.15
1999.197	-2.16
1999.165	-2.25
1999.133	-2.21
1999.101	-2.33
1999.069	-2.48
1999.037	-2.51
1999.005	-2.61

7.1.2. Annual coral growth data

Profile	Year	Extension rate (cm/year)	Bulk density ($g.cm^{-3}$)	Calcification rate ($g.cm^{-2}.year^{-1}$)	$\delta^{18}O$ ‰ (VPDB)
El-15A	1995	0.95	1.21	1.149	-2.76
	1994	1.25	1.23	1.537	-2.83
	1993	1.00	1.21	1.210	-2.77
El-15B	1995	0.40	1.58	0.632	-2.89
	1994	0.50	1.66	0.830	-2.85
	1993	0.40	1.56	0.624	-2.60
El-15C	1995	0.25	1.72	0.430	-2.15
	1994	0.30	1.66	0.498	-2.48
	1993	0.15	1.55	0.232	-2.10
	1992	0.20	1.54	0.308	-2.23
	1991	0.25	1.46	0.365	-2.07
Aq-19A	1998	1.25	0.99	1.237	-3.30
	1997	1.45	1.03	1.493	-3.28
	1996	1.40	1.07	1.498	-3.12
	1995	1.50	1.01	1.515	-3.10
	1994	1.70	1.06	1.802	-3.21
	1993	1.60	1.07	1.712	-3.10
Aq-19C	1998	0.10	1.57	0.157	-2.08
	1997	0.25	1.52	0.380	-2.12
	1996	0.20	1.47	0.294	-2.26
	1995	0.15	1.47	0.220	-2.42
	1994	0.25	1.47	0.368	-2.60
Aq193	1998	2.00	1.10	2.200	-2.98
Aq193	1997	1.90	1.08	2.052	-2.98
Aq29	1998	0.54	1.37	0.735	-3.00
Aq42	1998	0.35	1.45	0.506	-2.74
Aq42	1997	0.40	1.43	0.572	-2.72
Aq7	1998	0.99	1.09	1.079	-3.19
Aq7	1997	1.02	1.09	1.112	-3.17

7.2. Environmental data

7.2.1. Weekly average seawater temperature records

Date	Age (years)	Temperature (°C) 7 m depth	Temperature (°C) 19 m depth	Temperature (°C) 29 m depth	Temperature (°C) 42 m depth
04/13/99	1999.288	21.6865	21.6608	21.5243	21.5320
04/20/99	1999.308	21.4914	21.4888	21.3901	21.4130
04/27/99	1999.327	21.5896	21.5938	21.4973	21.5224
05.04.99	1999.346	21.9435	21.9305	21.7930	21.7901
05.11.99	1999.365	22.3292	22.3082	22.1690	22.1346
05/18/99	1999.385	22.4127	22.4039	22.2933	22.3087
05/25/99	1999.404	22.8637	22.8195	22.6916	22.6671
06.01.99	1999.423	22.9689	22.9488	22.8298	22.7887
06.08.99	1999.442	23.5579	23.5098	23.3592	23.3032
06/15/99	1999.462	23.9089	23.7655	23.5882	23.4661
06/22/99	1999.481	23.5294	23.5118	23.4108	23.3557
06/29/99	1999.5	23.9696	23.8940	23.8036	23.7050
07.06.99	1999.519	24.3568	24.2814	24.1679	24.0463
07/13/99	1999.538	25.3121	24.9702	24.7498	24.5692
07/20/99	1999.558	26.7324	26.3880	25.9138	25.3167
07/27/99	1999.577	26.9982	26.4952	26.0651	25.6421
08.03.99	1999.596	26.5668	26.3727	26.1161	25.7711
08.10.99	1999.615	27.8544	27.5074	27.1420	26.6997
08/17/99	1999.635	27.7302	27.4498	27.0688	26.4909
08/24/99	1999.654	27.6467	27.4867	27.2330	26.7748
08/31/99	1999.673	26.4924	26.2922	26.0834	25.6907
09.07.99	1999.692	25.7924	25.6401	25.5426	25.2798
09/14/99	1999.712	25.5697	25.3901	25.3356	25.1380
09/21/99	1999.731	25.4527	25.3283	25.3623	25.2522
09/28/99	1999.75	25.6777	25.4991	25.4768	25.3471
10.05.99	1999.769	25.6914	25.5641	25.5749	25.4966
10.12.99	1999.788	25.5836	25.4738	25.5169	25.4935
10/22/99	1999.808	25.0605	24.9161	25.0391	25.0565
10/29/99	1999.827	24.7506	24.6114	24.7451	24.7675
11.05.99	1999.846	24.5226	24.3795	24.4946	24.5223
11.12.99	1999.865	24.2226	24.0816	24.2090	24.2461
11/19/99	1999.885	24.1883	24.0449	24.1456	24.1720
11/26/99	1999.904	24.2080	24.0749	24.2145	24.2215
12.03.99	1999.923	23.3091	23.1886	23.3167	23.3527
12.10.99	1999.942	23.0517	22.9516	23.0425	23.0774
12/17/99	1999.962	22.8469	22.7159	22.8270	22.8927
12/24/99	1999.981	22.7500	22.6542	22.7442	22.7996
12/31/99	2000	22.5441	22.4513	22.5496	22.5977
01.07.00	2000.019	22.4691	22.3867	22.4690	22.5119
01/14/00	2000.038	22.0751	21.9864	22.0774	22.1077
01/21/00	2000.058	21.9902	21.9000	21.9436	21.9816

Table 7.2.1. continued

01/28/00	2000.077	21.7814	21.7133	21.7826	21.8188
02.04.00	2000.096	21.5761	21.4932	21.5594	21.6127
02.11.00	2000.115	21.4052	21.3320	21.3789	21.4270
02/18/00	2000.135	21.3174	21.2373	21.2728	21.3242
02/25/00	2000.154	21.1502	21.0876	21.1148	21.1585
03.03.00	2000.173	21.0919	21.0283	21.0623	21.0928
03.10.00	2000.192	20.9891	20.9335	20.9437	21.0042
03/17/00	2000.212	20.9486	20.8751	20.9201	20.9724
03/24/00	2000.231	20.9257	20.8510	20.8673	20.9352
03/31/00	2000.25	20.9575	20.8849	20.8822	20.9648
04.07.00	2000.269	21.0491	20.9600	20.9546	21.0057
04/14/00	2000.288	21.1291	20.9946	20.9558	21.0082
04/21/00	2000.308	22.0245	21.8173	21.7046	21.7013
04/28/00	2000.327	21.7855	21.6861	21.5430	21.5186
05.05.00	2000.346	22.3143	22.2298	22.1391	22.0751
05.12.00	2000.365	22.1713	22.0881	21.9601	21.9099
05/19/00	2000.385	22.8891	22.7558	22.6290	22.5945
05/26/00	2000.404	22.8970	22.8324	22.7391	22.7469
06.02.00	2000.423	23.0528	22.9659	22.8691	22.8576
06.09.00	2000.442	23.1513	23.0487	22.9667	22.9256
06/16/00	2000.461	23.5803	23.5035	23.4270	23.3741
06/25/00	2000.481	23.6050	23.5371	23.4736	23.4407

7.2.2. Seawater stable isotope data

	Surface		7 m depth		19 m depth		29 m depth		42 m depth	
Date	$\delta^{18}O$ ‰ (SMOW)	$\delta^{13}C$ ‰ (VPDB)	$\delta^{18}O$ ‰ (SMOW)	$\delta^{13}C$ ‰ (VPDB)	$\delta^{18}O$ ‰ (SMOW)	$\delta^{13}C$ ‰ (VPDB)	$\delta^{18}O$ ‰ (SMOW)	$\delta^{13}C$ ‰ (VPDB)	$\delta^{18}O$ ‰ (SMOW)	$\delta^{13}C$ ‰ (VPDB)
04/13/99	-----	-----	-----	1.24	1.78	1.23	-----	1.33	1.83	1.14
05/11/99	-----	-----	1.89	1.12	1.81	1.16	1.85	1.40	1.77	1.30
06/12/99	-----	-----	1.88	1.64	1.76	1.69	1.91	1.65	1.87	1.66
07/13/99	-----	-----	1.93	1.66	1.83	1.65	1.87	1.67	1.79	1.69
08/14/99	1.99	-----	1.94	-----	1.96	-----	1.89	-----	1.84	-----
09/08/99	1.85	1.66	1.96	-----	1.86	-----	1.85	-----	1.91	1.56
10/16/99	1.79	-----	1.91	-----	1.95	-----	2.03	-----	1.84	1.28
11/13/99	1.69	1.19	-----	1.30	1.92	1.27	1.80	1.26	1.85	1.52
12/22/99	1.82		1.88	-----	1.91	1.51	1.94	-----	1.88	-----
01/17/00	1.89	1.51	1.90	1.52	1.83	1.55	1.79	-----	1.86	-----
02/20/00	1.75	1.60	1.73	1.79	1.88	-----	1.94	1.44	1.78	1.42
03/14/00	1.90	-----	1.83	1.44	1.85	1.50	1.78	1.43	1.82	-----
04/13/00	1.88	-----	1.92	1.39	1.83	1.37	1.88	-----	1.82	1.29
05/14/00	1.85	1.42	1.94	1.60	1.88	1.57	1.82	-----	1.92	1.53
06/21/00	1.73	1.30	1.82	1.60	1.91	1.58	1.93	1.60	1.81	-----

7.3. Sediment records

7.3.1. Carbon stable isotope composition of planktonic foraminifera G. sacculifer and G. ruber

GeoB 5801-3		
Calib. Age (A.D.)	*G. sacc* $\delta^{13}C$ ‰ (VPDB)	*G. ruber* $\delta^{13}C$ ‰ (VPDB)
>1950	0.778	0.548
>1950	0.960	0.500
>1950	1.040	0.610
1950.000	0.830	0.714
1939.931	0.882	0.830
1929.862	0.820	0.794
1919.793	0.869	0.824
1909.724	0.842	0.736
1899.655	1.024	0.760
1889.586	0.831	0.660
1879.517	1.094	0.806
1869.448	0.829	0.762
1859.379	0.931	0.808
1849.310	1.025	0.975
1839.241	0.953	0.900
1829.172	0.889	0.510
1819.103	1.150	0.525
1809.034	1.287	0.525
1798.966	1.352	-------
1788.897	1.096	-------
1778.828	1.306	0.880
1768.759	1.045	0.970
1758.690	1.409	1.007
1748.621	1.186	-------
1738.552	1.329	1.060
1728.483	1.467	1.128
1718.414	1.354	0.999
1708.345	1.528	1.224
1698.276	1.467	1.027
1688.207	1.215	1.118
1678.138	1.098	1.141
1668.069	1.360	1.315
1658.000	1.588	1.202
1652.467	1.475	0.800
1646.933	1.610	0.872
1641.400	1.230	1.030
1635.867	1.456	1.136
1630.333	1.303	1.184
1624.800	1.351	1.401
1619.267	1.504	1.440
1613.733	1.324	1.099
1608.200	1.440	1.194
1602.667	1.521	1.403
1597.133	1.575	1.359
1591.600	1.380	1.370
1586.067	1.191	1.444
1580.533	1.408	1.301
1575.000	1.492	1.286
1569.467	1.570	1.194
1563.933	1.392	0.999
1558.400	1.351	1.247
1552.867	1.447	1.221
1547.333	1.313	1.013
1541.800	1.654	1.089
1536.267	1.444	1.015
1530.733	1.300	1.348
1525.200	1.320	0.962
1519.667	1.365	1.225
1514.133	1.405	1.079
1508.600	1.314	1.110
1503.067	1.492	1.145
1497.533	1.530	1.215
1492.000	1.396	1.176
1486.467	1.377	1.269
1480.933	1.158	0.900
1475.400	1.162	0.986
1469.867	1.361	1.061
1464.333	1.435	0.958
1458.800	1.302	1.221
1453.267	1.464	1.118
1447.733	1.232	0.876
1442.200	1.301	1.042
1436.667	1.448	0.885
1431.133	1.250	0.827
1425.600	1.316	1.014
1420.067	1.189	0.704
1414.533	1.291	0.703
1409.000	1.211	0.930

GeoB 5807-2		
Calib. Age (A.D.)	***G. sacc* $\delta^{13}C$ ‰ (VPDB)**	***G. ruber* $\delta^{13}C$ ‰ (VPDB)**
>1950	0.630	0.367
>1950	0.640	0.440
>1950	0.806	0.516
1950.000	0.622	0.462
1939.281	0.836	0.668
1928.563	0.770	0.321
1917.844	0.769	0.417
1907.125	0.809	0.400
1896.406	0.863	0.407
1885.688	0.960	0.459
1874.969	1.117	0.367
1864.250	1.098	0.726
1853.531	1.032	0.722
1842.813	1.076	0.595
1832.094	1.062	0.852
1821.375	0.946	1.071
1810.656	1.081	0.939
1799.938	1.061	1.074
1789.219	1.328	0.852
1778.500	1.321	0.735
1767.781	1.301	0.783
1757.063	1.299	0.912
1746.344	1.503	0.848
1735.625	1.330	0.692
1724.906	1.277	0.841
1714.188	1.272	0.815
1703.469	1.326	0.865
1692.750	1.370	-------
1682.031	1.489	0.842
1671.313	1.371	0.755
1660.594	1.432	1.118
1649.875	1.236	1.063
1639.156	1.275	0.816
1628.438	1.317	0.815
1617.719	1.353	1.031
1607.000	1.465	1.062
1596.281	1.522	1.117
1585.563	1.468	0.999
1574.844	1.134	0.962
1564.125	1.328	1.017
1553.406	1.321	0.837
1542.688	1.269	0.945
1531.969	1.201	0.969
1521.250	1.234	0.766
1510.531	1.293	0.854
1499.813	1.459	1.111
1489.094	1.449	1.294
1478.375	1.500	1.353
1467.656	1.468	1.098
1456.938	1.327	0.890
1446.219	1.426	0.859
1435.500	1.539	0.903
1424.781	1.423	1.124
1414.063	1.274	1.133
1403.344	1.403	-------
1392.625	1.218	1.198
1381.906	1.454	1.009
1371.188	1.279	1.124
1360.469	1.392	1.205
1349.750	-------	1.354
1339.031	1.202	1.380
1328.313	1.394	1.288
1317.594	1.336	1.145
1306.875	1.200	1.137
1296.156	1.366	1.247
1285.438	1.460	1.268
1274.719	1.520	1.107
1264.000	1.140	0.973

GeoB 5810-3		
Calib. Age (A.D.)	***G. sacc* $\delta^{13}C$ ‰ (VPDB)**	***G. ruber* $\delta^{13}C$ ‰ (VPDB)**
>1950	0.658	0.347
>1950	0.752	0.084
>1950	0.743	0.438
1950.000	0.677	0.218
1937.808	0.770	0.297
1925.615	0.798	0.582
1913.423	0.888	0.376
1901.231	0.807	
1889.038	0.861	0.473
1876.846	0.856	0.733
1864.654	1.126	0.570
1852.462	0.810	0.650
1840.269	0.908	0.633

GeoB 5810-3 continued

1828.077	1.136	0.903
1815.885	1.186	0.726
1803.692	1.274	0.588
1791.500	1.450	0.784
1779.308	1.304	0.710
1767.115	1.278	0.787
1754.923	1.393	0.860
1742.731	1.479	0.676
1730.538	1.318	0.977
1718.346	1.318	0.836
1706.154	1.685	0.946
1693.962	1.702	0.879
1681.769	1.558	------
1669.577	1.479	0.846
1657.385	1.160	0.820
1645.192	1.629	0.895
1633.000	1.578	0.641
1618.725	1.314	1.070
1604.450	1.391	0.961
1590.175	1.235	0.925
1575.900	1.608	1.141
1561.625	1.580	1.270
1547.350	1.502	1.142
1533.075	1.356	0.828
1518.800	1.470	0.974
1504.525	1.830	1.210
1490.250	1.564	0.944
1475.975	1.517	1.288
1461.700	1.320	1.241
1447.425	1.402	1.078
1433.150	1.392	1.158
1418.875	1.651	1.301
1404.600	1.580	1.282
1390.325	1.516	1.136
1376.050	1.511	1.145
1361.775	1.561	1.185
1347.500	1.526	1.234
1333.225	1.623	1.351
1318.950	1.338	1.176
1304.675	1.631	1.180
1290.400	1.325	1.160
1276.125	1.219	1.066
1261.850	1.526	1.274
1247.575	1.545	1.189
1233.300	1.640	1.043
1219.025	1.694	1.105
1204.750	1.462	1.200
1190.475	1.587	0.938
1176.200	1.396	1.198
1161.925	1.334	1.130
1147.650	1.529	1.070
1133.375	1.491	1.079
1119.100	1.321	1.272
1104.825	1.186	1.118
1090.550	1.332	1.097
1076.275	1.332	1.088
1062.000	1.406	0.914

7.3.2. Sediment organic carbon and carbonate contents

GeoB 5801-3			
Calib. Age (A.D.)	**TC (%)**	**OC (%)**	**$CaCO_3$ (%)**
>1950	4.20	0.67	29.40
1939.867	3.96	0.50	28.80
1919.733	4.06	0.40	30.50
1899.600	4.20	0.43	31.40
1879.467	4.25	0.41	32.00
1859.333	4.03	0.34	30.70
1839.200	3.85	0.35	29.20
1819.067	3.48	0.28	26.70
1798.933	3.15	0.33	23.50
1778.800	2.97	0.33	22.00
1758.667	3.08	0.35	22.70
1738.533	3.92	0.35	29.70
1718.400	3.98	0.42	29.70
1698.267	3.95	0.39	29.70
1678.133	3.67	0.41	27.20
1658.000	3.83	0.38	28.70
1647.625	3.84	0.37	28.90
1637.250	4.01	0.37	30.30
1626.875	4.56	0.36	35.00
1616.500	4.56	0.35	35.10
1606.125	4.41	0.38	33.60
1595.750	4.35	0.38	33.10
1585.375	4.28	0.37	32.60

GeoB 5801-3 continued

1575.000	4.03	0.35	30.70
1564.625	3.74	0.30	28.70
1554.250	3.26	0.23	25.20
1543.875	3.32	0.25	25.60
1533.500	3.24	0.30	24.50
1523.125	3.66	0.28	28.20
1512.750	4.26	0.45	31.70
1502.375	4.24	0.33	32.60
1492.000	3.84	0.29	29.60
1481.625	3.23	0.24	24.90
1471.250	2.77	0.22	21.20
1460.875	3.23	0.28	24.60
1450.500	4.51	0.36	34.60
1440.125	4.24	0.32	32.70
1429.750	4.41	0.34	33.90
1419.375	4.43	0.35	34.00
1409.000	4.32	0.32	33.30

GeoB 5807-2

Calib. Age (A.D.)	TC (%)	OC (%)	$CaCO_3$ (%)
>1950	4.51	0.71	31.70
1941.189	4.53	0.59	32.80
1922.378	3.62	0.54	25.70
1903.568	3.25	0.51	22.80
1884.757	2.90	0.48	20.20
1865.946	2.73	0.43	19.20
1847.135	3.13	0.40	22.70
1828.324	3.43	0.38	25.40
1809.514	2.49	0.35	17.80
1790.703	2.22	0.30	16.00
1771.892	2.08	0.28	15.00
1753.081	2.14	0.27	15.60
1734.270	2.16	0.26	15.80
1715.459	2.67	0.30	19.70
1696.649	3.09	0.34	22.90
1677.838	3.20	0.34	23.80
1659.027	3.32	0.35	24.70
1640.216	3.61	0.38	26.90
1621.405	3.66	0.39	27.20
1602.595	3.63	0.39	27.00
1583.784	3.63	0.37	27.20
1564.973	3.58	0.33	27.10
1546.162	3.32	0.33	24.90
1527.351	3.78	0.33	28.70
1508.541	3.67	0.32	27.90
1489.730	3.34	0.33	25.10
1470.919	3.53	0.34	26.60
1452.108	3.70	0.35	27.90
1433.297	3.78	0.37	28.40
1414.486	4.10	0.37	31.10
1395.676	4.15	0.36	31.60
1376.865	4.17	0.38	31.60
1358.054	4.31	0.35	33.00
1339.243	4.51	0.33	34.80
1320.432	4.64	0.34	35.80
1301.622	4.51	0.37	34.50
1282.811	4.31	0.37	32.80
1264.000	4.24	0.38	32.20

GeoB 5810-3

Calib. Age (A.D.)	TC (%)	OC (%)	$CaCO_3$ (%)	Tot N (%)	C/N	$\delta^{13}C_{org}$ ‰ (VPDB)
>1950	4.55	0.77	31.5	0.091	8.46	-21.19
>1950	4.39	0.73	30.5	0.083	8.8	-21.23
1927.357	4.21	0.71	29.2	0.087	8.18	-21.4
1904.714	4.16	0.72	28.7	0.072	10	-21.64
1882.071	4.03	0.7	27.7	0.071	9.86	-21.66
1859.429	3.95	0.66	27.4	0.067	9.85	-21.7
1836.786	3.82	0.67	26.2	0.067	10	-21.63
1814.143	3.78	0.67	25.9	0.07	9.57	-21.45
1791.5	3.93	0.54	28.2	0.058	9.31	-21.05
1768.857	4	0.51	29.1	0.056	9.11	-20.66
1746.214	3.97	0.5	28.9	0.058	8.62	-----
1723.571	3.87	0.49	28.2	0.053	9.25	-20.32
1700.929	3.95	0.42	29.4	0.048	8.75	-19.8
1678.286	3.93	0.39	29.5	0.047	8.3	-19.59
1655.643	3.97	0.4	29.7	0.047	8.51	-19.44
1633	4.2	0.4	31.7	0.045	8.89	-19.41
1608.174	4.26	0.41	32.1	0.047	8.72	-19.86
1583.348	4.3	0.4	32.5	0.045	8.89	-19.72
1558.522	4.57	0.41	34.7	0.048	8.54	-19.63
1533.696	4.36	0.43	32.7	0.048	8.96	-19.31
1508.87	4.29	0.42	32.2	0.045	9.33	-19.67
1484.043	4.27	0.41	32.2	0.046	8.91	-19.6
1459.217	4.2	0.38	31.8	0.041	9.27	-19.75
1434.391	4.37	0.37	33.3	0.042	8.81	-19.72
1409.565	4.3	0.33	33.1	0.039	8.46	-19.33

GeoB 5810-3 continued

1384.739	4.4	0.33	33.9	0.04	8.25	-18.96
1359.913	4.28	0.33	32.9	0.039	8.46	-19.02
1335.087	4.28	0.32	33	0.037	8.65	-18.86
1310.261	4.31	0.31	33.3	0.035	8.86	-18.77
1285.435	4.45	0.35	34.2	0.039	8.97	-18.77
1260.609	4.37	0.35	33.5	0.037	9.46	-19.14
1235.783	4.28	0.34	32.8	0.038	8.95	-19.27
1210.957	4.25	0.37	32.3	0.038	9.74	-19.57
1186.13	4.15	0.37	31.5	0.039	9.49	-19.77
1161.304	4	0.38	30.2	0.039	9.74	-19.8
1136.478	3.91	0.37	29.5	0.036	10.28	-19.99
1111.652	3.93	0.35	29.8	0.032	10.94	-19.83
1062	4.12	0.31	31.7	0.032	9.69	-19.51